ISSN 1408-7073

# RMZ – MATERIALS AND GEOENVIRONMENT

PERIODICAL FOR MINING, METALLURGY AND GEOLOGY

# RMZ – MATERIALI IN GEOOKOLJE

REVIJA ZA RUDARSTVO, METALURGIJO IN GEOLOGIJO

RMZ-M&G, Vol. 57, No. 2 pp. 159–294 (2010)
Ljubljana, June 2010

*Historical Rewiev*

More than 80 years have passed since in 1919 the University Ljubljana in Slovenia was founded. Technical fields were joint in the School of Engineering that included the Geologic and Mining Division while the Metallurgy Division was established in 1939 only. Today the Departments of Geology, Mining and Geotechnology, Materials and Metallurgy are part of the Faculty of Natural Sciences and Engineering, University of Ljubljana.

Before War II the members of the Mining Section together with the Association of Yugoslav Mining and Metallurgy Engineers began to publish the summaries of their research and studies in their technical periodical Rudarski zbornik (Mining Proceedings). Three volumes of Rudarski zbornik (1937, 1938 and 1939) were published. The War interrupted the publication and not untill 1952 the first number of the new journal Rudarsko-metalurški zbornik - RMZ (Mining and Metallurgy Quarterly) has been published by the Division of Mining and Metallurgy, University of Ljubljana. Later the journal has been regularly published quarterly by the Departments of Geology, Mining and Geotechnology, Materials and Metallurgy, and the Institute for Mining, Geotechnology and Environment.

On the meeting of the Advisory and the Editorial Board on May 22nd 1998 Rudarsko-metalurški zbornik has been renamed into "RMZ - Materials and Geoenvironment (RMZ -Materiali in Geookolje)" or shortly RMZ - M&G.

RMZ - M&G is managed by an international advisory and editorial board and is exchanged with other world-known periodicals. All the papers are reviewed by the corresponding professionals and experts.

RMZ - M&G is the only scientific and professional periodical in Slovenia, which is published in the same form nearly 50 years. It incorporates the scientific and professional topics in geology, mining, and geotechnology, in materials and in metallurgy.

The wide range of topics inside the geosciences are wellcome to be published in the RMZ -Materials and Geoenvironment. Research results in geology, hydrogeology, mining, geotechnology, materials, metallurgy, natural and antropogenic pollution of environment, biogeochemistry are proposed fields of work which the journal will handle. RMZ - M&G is co-issued and co-financed by the Faculty of Natural Sciences and Engineering Ljubljana, and the Institute for Mining, Geotechnology and Environment Ljubljana. In addition it is financially supported also by the Ministry of Higher Education, Science and Technology of Republic of Slovenia.

Editor in chief

# Table of Contents – Kazalo

### *Original Scientific Papers – Izvirni znanstveni članki*

**Flow stresses and activation energy of BRCMO tool steel** 159
Krivulje tečenja in aktivacijska energija za orodno jeklo BRCMO
Fajfar, P., Bombač, D., Markoli, B.

**Adsorption of Ni (II) ions from aqueous solution on anode dust: Effect of pH value** 165
Adsorbcija Ni(II) ionov iz vodne raztopine anodnega prahu: učinek pH vrednosti
Štrkalj, A., Rađenović, A., Malina, J.

**Hardenability modeling** 173
Modeliranje prekaljivosti
Kovačič, M.

**Estimation of Groundwater Recharge under various land covers in parts of Western ghat, Karnataka, India** 181
Ocena napajanja podzemne vode na območjih z različno pokrovnostjo tal v delih zahodnega Gathsa, Karnataka, Indija
Purandara, B. K., Venkatesh, B., Choubey, V. K.

**Jurassic and Cretaceous neptunian dikes in drowning successions of the Julian High (Julian Alps, NW Slovenia)** 195
Neptunski dajki v potopitvenih zaporedjih Julijskega platoja (Julijske Alpe, SZ Slovenija)
Šmuc, A.

**Revision of coal reserves and placement of exploitation fields in exploitation of the lignite deposit in Premogovnik Velenje** 215
Revizija rezerv premoga in umeščanje odkopnih polj pri eksploataciji ležišča lignita v Premogovniku Velenje
Medved, M., Lajlar, B., Malenković, V., Dervarič, E.

**3D analysis of the influence of primary support stiffness on the surface movements during tunnel construction** 237
3D-analize vpliva togosti primarnega podporja na razvoj pomikov površine med gradnjo predora
Likar, J.

*Professional Papers – Strokovni članki*

**Multi-objective methods for welding flux performance optimization** 251
Več namenske metode za optimizacijo uspešnosti varilnega praška
Adeyeye, A. D., Oyawale, F. A.

**The drilling and casing program for $CO_2$ storage** 271
Načrtovanje in izvedba globokih vrtin pri skladiščenju $CO_2$
Vukelić, Ž.

**Author`s Index, Vol. 57, No. 2** 279

**Instructions to Authors** 281

**Template** 289

# Flow stresses and activation energy of BRCMO tool steel

# Krivulje tečenja in aktivacijska energija za orodno jeklo BRCMO

Peter Fajfar[1,] *, David Bombač[1], Boštjan Markoli[1]

[1]University of Ljubljana, Faculty of Natural Sciences and Engineering, Aškerčeva cesta 12, SI-1000 Ljubljana

*Corresponding author. E-mail: peter.fajfar@ntf.uni-lj.si

**Received:** March 16, 2010 **Accepted:** May 20, 2010

**Abstract:** Flow stresses and activation energy of BRCMO high-speed steel has been investigated. Hot compression tests in the temperature range of 900–1050 °C at strain rates of 0.001–10 $s^{-1}$ and true strain of 0–0.9 were applied on Gleeble 1500D thermo-mechanical simulator. For entire hot working range the constants of the hyperbolic sine function and activation energy were calculated. The value of activation energy is 607 kJ $mol^{-1}$. The microstructures of the samples after deformation were analysed by means of light microscopy.

**Izvleček:** Preiskovali smo krivulje tečenja in izračunavali aktivacijsko energijo hitroreznega jekla BRCMO. Na termo-mehanskem simulatorju Gleeble 1500D smo izvedli tlačne preizkuse do stopnje deformacije 0,9 v temperaturnem območju 900–1050 °C in v območju hitrosti deformacije 0,001–10 $s^{-1}$. Za celotno temperaturno območje smo izračunali konstante hiperbolične funkcije in aktivacijsko energijo, ki je 606 kJ $mol^{-1}$. Mikrostrukture preoblikovanih vzorcev smo analizirali s svetlobno mikroskopijo.

**Key words:** high-speed tool steel, flow curves, activation energy
**Ključne besede:** hitrorezna jekla, krivulje tečenja, aktivacijska energija

*Original scientific paper*

## INTRODUCTION

For modern industrial mass production, machining is one of the most important shaping and forming processes. Almost all tools employed for this purpose are made from high speed steels, or HSS. The term `high speed steel' was derived from the fact that high-speed steel is capable of cutting metal at a much higher rate than carbon tool steel. It retains its hardness even when the point of the tool is heated to a low red temperature. HSS is a type of steel that is used in high speed applications, such as manufacturing of taps, dies, twist drills, reamers, saw blades and other cutting tools. HSS steel contains many alloying elements. Alloying elements are added to HSS to improve hardenability, control grain growth, improve strength, hardness and wear resistance. [1, 2, 3, 4] Main alloying elements are chromium, tungsten, molybdenum, vanadium and cobalt. When steels contain a combination of more than 7 % of molybdenum, tungsten and vanadium, and more than 0.60 % carbon, they are referred to as high speed steels or HSS. Carbon forms carbides, which increases wear resistance and it is responsible for the basic matrix hardness. Chromium promotes deep hardening and produces readily soluble carbides. Molybdenum in tool steels increases their hardness and wear resistance. Molybdenum also acts in conjunction with elements like chromium to produce substantial volumes of extremely hard and abrasion resistant carbides. Cobalt improves red hardness and peovides retention of hardness for the matrix. Depending on the steel composition several types of carbides are precipitated in HSS: mainly MC, $M_2C$ and $M_6C$. A distinguishing feature of HSS is the uniform distribution and small size of the primary carbides. The primary carbides and their distribution have a major influence on the wear resistance and toughness of the material.

In the present paper the flow curves and activation energy for deformation of the BRMCO HSS were examined with respect to the dependence on temperature and strain rate.

## MATERIAL AND METHODS

A BRCMO type high-speed tool steel with the following chemical composition: C 0.91 %, Cr 4.15 %, Mo 4.7 %, W 6.3 %, V 2.1 %, Co 4.75 %, and Fe balance was used as samples for hot compression tests on Gleeble 1500D thermal-mechanical simulator. The initial cylindrical specimen was 10 mm in diameter and 15 mm in height and was machined from the rolled bar. The heat treatment condition for hot compression test is shown in Figure 1. Specimens were heated (cf. Figure 1) with rate of 3 °C $s^{-1}$ (1) then held on soaking temperature 1160 °C for 10 min (2). After that they were cooled with rate of 2 °C $s^{-1}$ on deformation temperature (3), held for 10 min at deformation temperature (4) and then deformed with prescribed strain rate (5) followed by water quenching (6) to retain the recrystallized microstructures. For reduction of friction between specimens and the tool anvil Ni-based lubricant, carbon and tantalum foils were used. The hot temperature compression tests were performed at six different temperatures: 900 °C, 950 °C, 1000 °C, 1050 C, 1100 °C and 1150 °C and five different strain rates: 0.001 $s^{-1}$, 0.01 $s^{-1}$, 0.1 $s^{-1}$, 1 $s^{-1}$ and 10 $s^{-1}$. The maximum strain for all tests was 0.9. The temperature of the test specimen was measured by means of the thermocouple at the centre of the specimen.

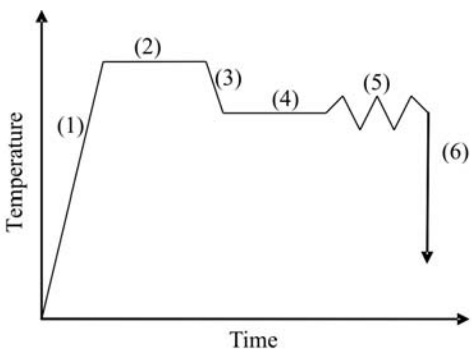


**Figure 1.** Heat treatment condition of compression test

The specimens were sectioned along the longitudinal compression axis and prepared for the light-optical microscopy. The microstructures in the centre of the section plane were examined using Zeiss Axio Imager A1m.

## Results and discussion

The flow curves of BRCMO high-speed steel were evaluated in the temperature range of 900–1150 °C and in the strain rate range of 0.001–10 $s^{-1}$. The effect of temperature on the flow curves is shown in Figure 2. It shows that strain corresponding to the peak flow stress increases as the temperature decreases. The value of the peak strain is 0.11 for the 900 °C temperature. It decreases in the temperature range of 950–1150 °C and remains at constant value of 0.05. The increase of strain rate leads to the peak flow stress increase. The value of the peak strain at the 1100 °C is 0.45 for the strain rate 0.001, 0.21 for strain rates 1 and 0.1 and 0.05 for strain rates 0.01 and 0.001. The steady state flows are not fully reached at temperatures lower than 1000 °C.

The effect of the strain rate on the flow curves is shown in Figure 3. It can be seen that the peak flow stresses increase with the increasing strain rate. These curves are typical of a dynamic recrystallization (DRX) process. At the stress peak the strain hardening is balanced with softening and afterwards with the increase of strain the softening mechanism prevails over the work hardening. At higher temperatures (>1000 °C) a strain independent steady state stress is attained except for the higher strain rate (Figure 3).

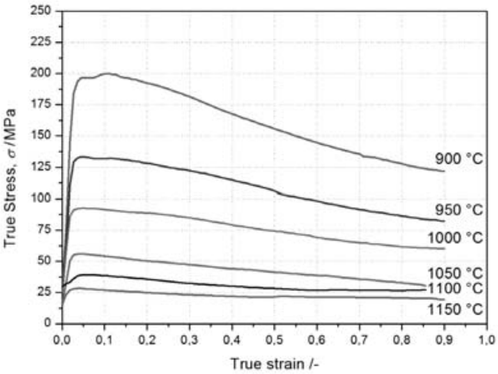


**Figure 2.** True stress / true strain curves of BRCMO at 0.001 $s^{-1}$ strain rate

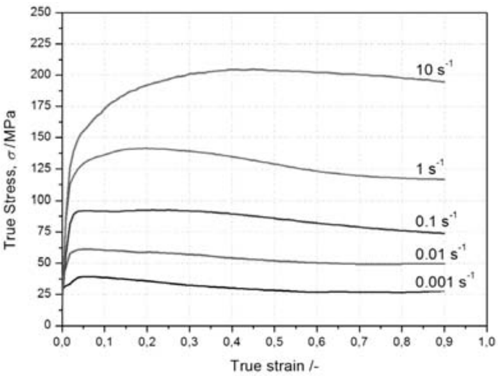


**Figure 3.** True stress / true strain curves of BRCMO at the temperature of 1100 °C

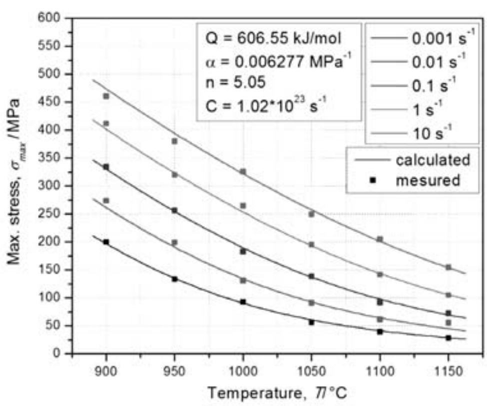


**Figure 4.** Dependence of the peak flow stress on temperature

With the Arrhenius equation the relationship between the strain rate, flow stress and temperature was described. Activation energy $Q$ was determined with the following equation:

$$\dot{\varepsilon} = A[sin\boldsymbol{h}(\alpha\sigma)]^n exp\left(-\frac{Q}{RT}\right)$$

where $A$, $\alpha$ are material constants, $n$ is stress exponent $\dot{\varepsilon}$ is strain rate, $\sigma$ is flow stress, $T$ is the absolute temperature and $R$ is the universal gas constant. The comparison between measured and calculated dependence of peak stresses on temperature for different strain rates is shown in Figure 4. A very good fit of data was obtained by taking $\alpha = 0.006$ MPa$^{-1}$ and $n = 5$. The value of the activation energy was 607 kJ mol$^{-1}$. This value for the activation energy was compared with other investigations as summarized in the Table 1.

The microstructures of BRCMO HSS before and after the hot compression test are shown in Figure 5. Fine precipitated carbide particles can be seen in the initial billet microstructure (Figure 5a). Carbides are mostly distributed within the grains. In micrograph (Figure 5b) of the hot deformed specimen at temperature 1000 °C and strain rate of 0.001 $s^{-1}$ the amount and the shape of carbides hasn't changed.

**Table 1.** Values of the activation energy for hot working of tool steel

| Steel | $Q$/kJ mol$^{-1}$ | Temperature $T$/°C | Ref. |
|---|---|---|---|
| M32 | 607 | 900–1105 | Current work |
| M2 | 610 | 900–1100 | [5] |
| T1 | 654 | <1000 | [1] |
| | 467 | >1000 | |

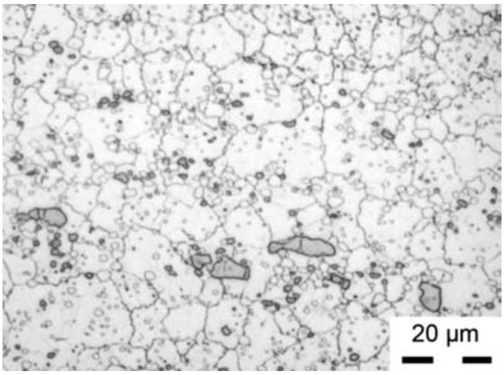


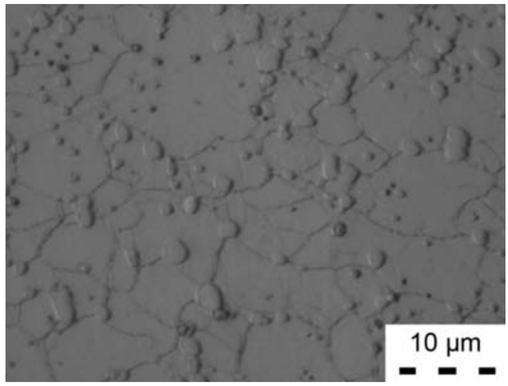


**Figure 5.** Light-optical micrographs of BRCMO at: (a) initial state, (b) 1000 °C, $\dot{\varepsilon}$ = 0.001 s$^{-1}$

## Conclusions

For hot compression test of BRCMO high-speed steel Gleeble 1500D thermo-mechanical simulator was applied. The true stress – true strain curves and activation energy has been determined in the temperature range of 900–1050 °C at strain rates of 0.001–10 s$^{-1}$ and true strain of 0–0.9.

The presence of stress peaks in flow curves is an indication of the initiation of DRX. A strain independent steady state stress is attained at the temperatures above 1000 °C (Figure 2). The comparison between measured and calculated dependence of peak stresses on temperature for different strain rates shows good agreement.

The activation energy $Q$ for deformation was evaluated by fitting the hyperbolic sine function to the stress corresponding to the peak. A value of 607 J mol$^{-1}$ was obtained for this steel which is close to the value reported for other tool steels, Table 1.

## REFERENCES

[1] LIU J., CHANG H., WU R., HSU T.Y.,RUAN X. (2000) : Materials Characterization Vol. 45, pp. 175–186.

[2] VEČKO PIRTOVŠEK T., PERUŠ I., KUGLER G., TURK R., TERČELJ M. (2008) : Metalurgija Vol. 47., No. 4, pp. 307–311.

[3] RODENBURG C. KRZYZANOWSKI M, BEYNON J. H., RAINFORTH W. M. (2004) : Mater. Sci. and Eng. A 386, pp. 420–427.

[4] PIPPEL E., WOLTERSDORF J., PÖCKL. (1999), Mater. Charact., Vol. 43, pp. 41–55.

[5] IMBERT C., RYAN N. D, MCQUEEN H. J. (1984), Metall Trans A, Vol. 15, pp. 1855–1864.

# Adsorption of Ni (II) ions from aqueous solution on anode dust: Effect of pH value

# Adsorbcija Ni(II) ionov iz vodne raztopine anodnega prahu: učinek pH vrednosti

Anita Štrkalj[1,]*, Ankica Rađenović[1], Jadranka Malina[1]

[1]University of Zagreb, Faculty of Metallurgy, Aleja narodnih heroja 3, 44 000 Sisak, Croatia

*Corresponding author. E-mail: strkalj@simet.hr

**Received:** November 20, 2009 **Accepted:** January 28, 2010

**Abstract:** In this study, the anode dust, a solid residue of aluminium production, was examined as a non-conventional and low-cost sorbent for the removal of Ni (II) from aqueous solution. The adsorption capacity was found to be pH dependent and decreased along with an increase pH. The maximum adsorption was obtained at pH 4.5. The results were analyzed by the Langmuir and Freundlich isotherm at the best pH value.

**Izvleček:** V članku je opisan poskus z anodnim prahom, ki je trdna usedlina pri pridobivanju aluminija, za neobičajno in cenovno odstranjevanje Ni(II) iz vodne raztopine. Dokazano je bilo, da je adsorbcijska kapaciteta odvisna od pH in se zmanjšuje z naraščajočo vrednostjo pH. Največja adsorbcija je bila pri pH 0.5. Rezultati so bili analizirani z Langmuirovo in Freundlichovo izotermo pri najboljši vrednosti pH.

**Key words**: anode dust, adsorption, Ni (II) ions, aqueous solution, pH value
**Ključne besede:** anodni prah, adsorbcija, Ni (II) ioni, vodna raztopina, vrednost pH

## Introduction

The removal of toxic heavy metals such as cadmium, copper, lead, nickel, mercury, and zinc from aqueous environment has received considerable attention in recent years due to their toxicity and carcinogenicity which may cause damage to various systems of the human body. [1]

Nickel is metal frequently encountered in raw wastewater streams from industries

*Original scientific paper*

such as mining, electroplating, metallurgy, electroplating, pigment and ceramics industries. [2] This metal is non-biodegradable toxic heavy metal and may cause dermatitis, allergic sensitization and cancer. [3, 4]

It is essential to remove Ni (II) ions from industrial wastewater before being discharged. For this reason, generally are used the advanced treatment processes such as chemical reduction, ion exchange, reverse osmosis, electro dialysis, and adsorption. Since the cost of these processes is rather expensive, the use of agricultural residues or industrial by-product was received with considerable attention [5] In recent years, a number of industrial by-product as waste mould sand,[6] blast furnace sludge, [7] steel slag, [8] red mud[9] were used for the removal of toxic metals from aqueous solutions.

For reduction of alumina in aluminium production by the electrolytic process, carbon anodes are used. The remaining parts of the anodes after use for aluminium production are called anode butts. The cleaned anode butts are crushed and reused for the production of new anodes (about 20 % of the anode is recycled). Anode dust originates from the baking process and during the transport of anodes. Owing to its granulometry and chemical composition, the anode dust is considered as a waste material. [10, 11] In this study, the anode dust, a solid residue of aluminium production, was investigated as a non-conventional and low-cost adsorbent for the removal of Ni (II) ions from aqueous solution. The influence of pH value on adsorption capacity of anode dust is examined.

## Materials and methods

### Preparation and characterization of anode dust

Anode dust, which is a solid residue of aluminium production, was used as the adsorbent. For analysis, a representative sample of anode dust was obtained using a quartering technique. The sample was dried at 105 °C for 4 h and sieved to particle size 0.125–0.2 mm. The chemical composition of the sample was determined by atomic absorption spectroscopy (the AAS method). The mineralogical composition of the anode dust sample was determined by the X-ray diffraction method (XRD method). The chemical composition of the examined anode dust is presented in Table 1. It was found that the anode dust was dominated by C ($w$(C) = 94.49 %), followed by Si ($w$(Si) = 1.73 %), Al ($w$(Al) = 1.69 %), S ($w$(S) = 1.50 %), and Fe ($w$(Fe) = 0.34 %). The mineralogical composition (XRD analysis) of anode dust is shown in Figure 1.

### Batch experiment

A stock solution of Ni (II) ions was prepared by dissolving $NiCl_2\cdot 6H_2O$ in 1000 mL deionized water. This solution was diluted as required to obtain the standard solutions. The initial concentrations of the solutions contained 50–500 mg $L^{-1}$ of Ni (II) ions. The batch experiments were carried out in 100 mL conical flasks by agitating 0.375 mg anode dust with 25 mL of the aqueous Ni (II) ions solution for a period of 30 min (equilibrium time) at 20 °C on a mechanical shaker. The adsorption of nickel ions by anode dust was studied in a pH range of

**Table 1**. Chemical composition of anode dust sample in mass fractions (*w*/%)

| Components | C | Si | Al | S | Fe | Na | V | Ca | Ni |
|---|---|---|---|---|---|---|---|---|---|
| *w*/% | 94.49 | 1.73 | 1.69 | 1.50 | 0.34 | 0.089 | 0.072 | 0.044 | 0.043 |

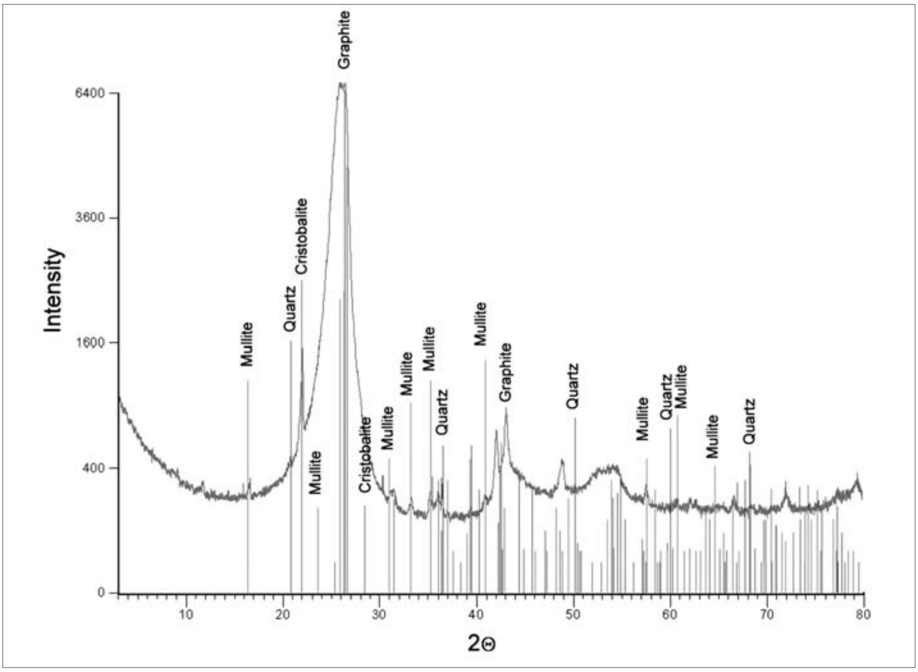


**Figure 1.** XRD pattern of the anode dust sample

4.5–7. Solutions of 0.5 M HCl and 0.5 M NaOH were used for pH adjustments.

The concentration of Ni (II) ions before and after the adsorption was determined spectrophotometrically with standard method.[12]

The amount of Ni (II) ions adsorbed at equilibrium i. e. the adsorption capacity, $q_e$/(mg/g), was calculated according to the formula:

$$q_e = \frac{c_0 - c_e}{m} \cdot V \qquad (1)$$

where,

$q_e$ – adsorption capacity, mg/g
$c_0$ – initial concentration of nickel ions, mg/L
$c_e$ –equilibrium concentration of nickel ions, mg/L
$V$ – volume of solution, L
$m$ – adsorbent mass, g

## Results and discussion

One of the most critical parameter in the adsorption process of metal ions from aqueous solution is the pH of medium. [1] The capacity of Ni (II) ions removed is shown in Figure 2.

The effect of pH on the adsorption capacity of anode dust may be attributed to the combination of the nature of the surface and amount of Ni (II) ions. Change of pH value causes the ionization of the acid groups (hydroxyl, carboxyl, phenol etc.) present in anode dust surface.[13]This suggest that electrostatic interaction between divalent Ni (II) ions and anode dust negatives sites could be the most prevalent mechanism of metal-binding. It is evident from Figure 2 that the capacity is higher at lower pH. The best adsorption of Ni (II) ions was obtained at the pH value of 4.5. For higher pH values, Ni (II) ions precipitate in the form of metallic hydroxides and adsorption capacity was decreased. [14]

Adsorption equilibrium data were fitted to the Langmuir and Freundlich isotherms at pH value of 4.5–7 with linear regression analysis.

The linear equations of Langmuir and Freundlich are represented as follows (Equations (2) and (3), respectively): [8]

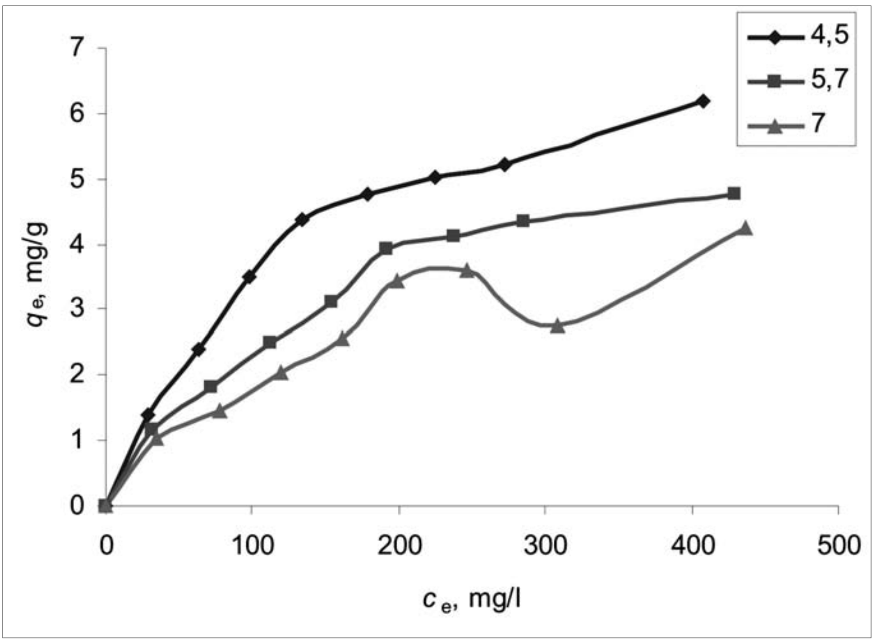


**Figure 2.** Effect of pH value on the adsorption capacity ($q_e$) of anode dust with different equilibrium concentration ($c_e$) of Ni (II) ions

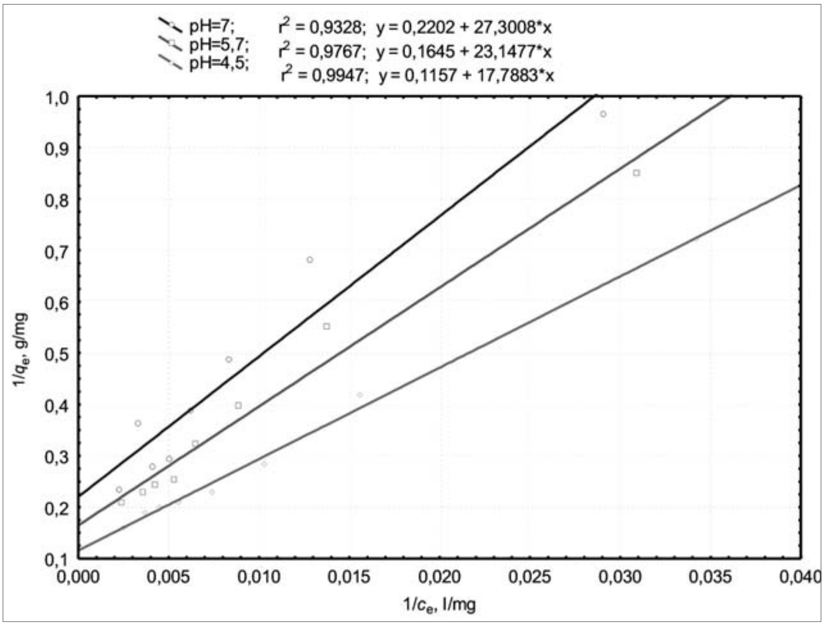


**Figure 3.** Langmuir isotherms for adsorption of Ni(II) ions on anode dust at pH value of 4.5–7

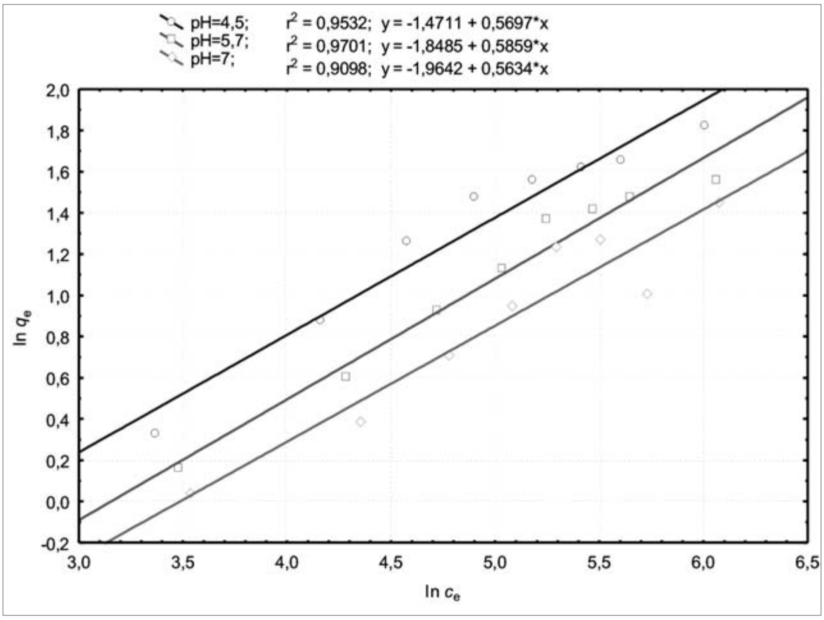


**Figure 4.** Freundlich isotherms for adsorption of Ni(II) ions on anode dust at pH value of 4.5–7

**Table 2**. Values of Langmuir/Freundlich constants and correlation coefficients

| | Langmuir isotherm | | | Freundlich isotherm | | |
|---|---|---|---|---|---|---|
| pH | $q_m$/ (mg/g) | $K_L$/ (L/mg) | $R^2$ | $n$ | $K_F$ | $R^2$ |
| 7 | 4.54 | $8.06 \cdot 10^{-3}$ | 0.9328 | 1.775 | 0.140 | 0.9098 |
| 5.7 | 6.08 | $7.11 \cdot 10^{-3}$ | 0.9767 | 1.707 | 0.157 | 0.9701 |
| 4.5 | 8.64 | $6.50 \cdot 10^{-3}$ | 0.9947 | 1.755 | 0.230 | 0.9532 |

$$\frac{1}{q_e} = \frac{1}{K_L \cdot q_m \cdot c_e} + \frac{1}{q_m} \quad (2)$$

where,
$q_e$ - adsorption capacity, mg/g
$c_e$ - equilibrium concentration of nickel ions, mg/L
$q_m$ - saturation adsorption capacity of the anode dust, mg/g
$K_L$ - Langmuir constant

$$\ln q_e = K_F + \frac{1}{n} \ln c_e \quad (3)$$

where,
$q_e$ - adsorption capacity, mg/g
$c_e$ – equilibrium concentrations of nickel ions, mg/L
$K_F$ and $n$ – the Freundlich constants
The Langmuir adsorption isotherms for Ni (II) ions adsorption on anode dust are shown in Figure 3. The Freundlich adsorption isotherms for Ni (II) ions adsorption on anode dust are shown in Figure 4. The values of Langmuir and Freundlich constants and correlation coefficients were determined, and are shown in Table 2.

In general, the Langmuir model fitted the results slightly better than the Freundlich model with all $R^2$ values. This suggests that the adsorption of Ni (II) ions by anode dust is monolayer type.[15] The values of maximal adsorption capacity $q_m$, obtained by Langmuir isotherm show that the adsorption capacity depends on pH and decreases along with an increase pH value of aqueous solution. Maximal capacity of adsorption is achieved at the pH value of 4.5.

## Conclusions

- The adsorption capacity of anode dust for the removal of Ni (II) ions was found to be pH dependent and decreased along with an increase of solution pH.
- The best adsorption of Ni (II) ions was obtained at the pH value of 4.5.
- Equilibrium data can be fitted by Langmuir and Freundlich adsorption isotherms, and the Langmuir

model fitted the results slightly better than the Freundlich model**.**

- The obtained adsorption capacity value is promising in the use of anode dust as an efficient low-cost and nonconventional adsorbent for the removal of Ni (II) ions from solutions.

## Acknowledgement

This work was supported by the Ministry of Science, Education, and Sports of the Republic of Croatia, under the project 124-1241565-1524.

## References

[1] LIN, S. H., LAI, S. L., LEU, H. G. Removal of heavy metals from aqueous solution by chelating resin in a multistage adsorption process. *Journal of Hazardous Materials* ,B76 (2000), 139–153.

[2] PARAB, H., JOSHI, S., SHENOY, N., LALI, A., SARMA, U. S., SUDERSANAN, M., Determination of kinetics and equilibrium parameters of the batch adsorption of Co(II), Cr(III) and Ni(II) onto coir pith. *Process Biochemistry,*41 (2006), 609–615.

[3] ABU AL-RUB, F. A., KANDAH, M., AL-DABAYBEH N., Nickel removal from aqueous solutions using sheep manure wastes. *Engineering in Life Sciences,* 2 (2002), 111–116.

[4] ABU AL-RUB, F.A., KANDAH, M., AL-DABAYBEH, N. (2003): Competitive adsorption of nickel and cadmium on sheep manure wastes; experimental and prediction studies. *Separation and Science Technology,* 38 (2003), 483–497.

[5] HASAR, H., Adsorption of nickel (II) from aqueous solution onto activated carbon prepared from almond husk. *Journal of Hazardous Materials*, B97 (2003), 49–57.

[6] ŠTRKALJ, A., MALINA, J., RAĐENOVIĆ, A.: Waste mould sand-potential low-cost sorbent for nickel and chromium ions from aqueous solution. *RMZ-Materials and geoenvironment*, 56 (2009), 118–125.

[7] RAĐENOVIĆ, A., MALINA, J., ŠTRKALJ, A.: Distribucijski koeficijent uklanjanja $Ni^{2+}$ iona iz vodenih otopina pomoću visokopećnog mulja. Proc. of 13 Int. Conf. MATRIB 08/Grilec, K. (ed.), Vela Luka, (2007),180–184.

[8] ĆURKOVIĆ, L., CERJAN-STEFANOVIĆ, Š., RASTOVČAN - MIOČ, A. (2001): Batch $Pb^{2+}$ and $Cu^{2+}$ removal by electric furnace slag. *Water Research,* 35 (2001), 3436–3440.

[9] ZUBOULIS, A., KYDROS, K. A.: Use of red mud for toxic metals removal: the case of nickel. *Journal of Chemical Technology and Biotechnology,* 58 (1993), 95–101.

[10] THONSTAD, J., FELLNER, P., HAARBERG, G. M., HIVEŠ, J., KVANDE, H., STERTEN, A. (2001): Aluminium Electrolysis, Aluminium-Verlag, Düsseldorf.

[11] GRJOTHEIM, K., KVANDE, H. (1993): Introduction to Aluminium Electrolysis, Aluminium-Verlag, Düsseldorf.

[12] FRIES J., GETROS, H. (1977): Organic Reagents for Trace Analysis. E. Merck Darmstadt.

[13] ŠTRKALJ, A. (2009): *Sorpcija Cr (VI) i Ni (II) iona iz vodenih otopina na ugljičnoj anodnoj prašini,* Ph. D. Thesis. Sisak: University of Zagreb, Faculty of Metallurgy, Sisak; 201 p.

[14] RADOVIĆ, LJ. R. (2001): Chemistry and Physics of Carbon, Marcel Dekker, New York.

[15] PIMENTEL, P. M., MELO, M. A. F., MELO, D. M. A., ASSUNCAO, A. L. C., HENRIQUE, D. M., SILVA JR., C. N., GONZALEZ, G.: Kinetics and thermodynamics of Cu(II) adsorption on oil shale wastes. *Fuel Processing and Technology,* 89 (2008), 62–67.

# Hardenability modeling

# Modeliranje prekaljivosti

Miha Kovačič[1, 2, *]

[1]ŠTORE STEEL, d. o. o., Štore, Slovenia
[2]University of Nova Gorica, Laboratory for Multiphase Processes, Nova Gorica, Slovenia

*Corresponding author. E-mail: miha.kovacic@store-steel.si

**Received:** October 9, 2009 **Accepted:** January 28, 2010

**Abstract:** The paper presents the use of genetic programming and linear regression method for hardenability modeling for 51CrV4 spring steel. The experimental data on chemical composition, distance from the specimen face and Jominy test results of 74 batches were collected. On the basis of the experimental data set, a mathematical model for the Jominy test was developed by genetic programming and linear regression. The models were also tested on the basis of experimental data on 871 batches. The results show that the genetically developed model performs better and the results can be easily used also in practice.

**Izvleček:** V članku je predstavljena uporaba genetskega programiranja in linearne regresije pri modeliranju prekaljivosti vzmetnega jekla 51CrV4. Uporabljeni so podatki 74 šarž: kemična analiza, razdalja od čelne ploskve in rezultati Jominyjevega preizkusa. Na podlagi teh podatkov smo z genetskim programiranjem in linearno regresijo izdelali matematična modela za rezultate Jominyjevega preizkusa. Oba modela smo preverili z eksperimentalnimi podatki 871 šarž. Rezultati kažejo, da se genetsko dobljeni model vede bolje in da se lahko rezultati raziskave zlahka uporabijo v praksi.

**Key words:** hardenability, Jominy test, spring steel, modeling, genetic programming
**Ključne besede:** prekaljivost, Jominyjev preizkus, vzmetno jeklo, modeliranje, genetsko programiranje

*Original scientific paper*

## Introduction

Hardenability is a steel property which describes the depth to which the steel may be hardened during quenching. The Jominy test is a method for determining the hardenability of steel which involves heating a test piece from the steel (25 mm diameter and 100 mm long) to an austenitising temperature and quenching from one end with a controlled and standardised jet of water. After quenching the hardness profile is measured at intervals from the quenched end.

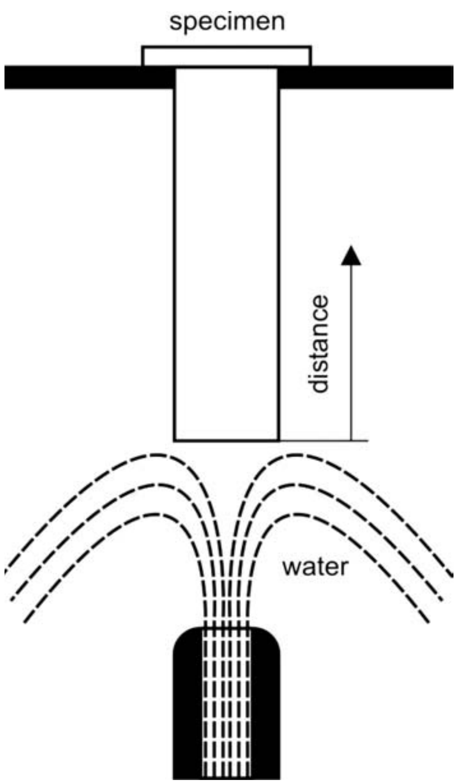


**Figure 1.** Jominy test

Several attempts for Jominy test modeling have been made[1–4] including the artificial intelligence approach. [3]

In this paper genetic modeling and linear regression method for a Jominy test modeling is proposed. Genetic programming has been successfully implemented into several manufacturing processes. [5, 6]

## Experimental setup

The experiment was performed with 51CrV4 spring steel specimens collected in the period of October 2003 to September 2007 in the factory Štore Steel Ltd. [7] Distance from the specimen face (1.5 mm, 9 mm, 15 mm, 30 mm, 50 mm) and chemical composition (mass fractions of C, Si, Mn, P, S, Cr, Mo, Ni, Al, Cu, Ti, V, Sn, Ca, N) were used for mathematical modeling of the Jominy test (Table 1).

Training data set (74 batches) was used Jominy test results prediction, whereas the testing data set (871) was used for verifying the model. The average chemical composition of 51CrV4 spring steel used in the research is shown in table 2.

**Table 1.** Experimental data (mass fraction, *w*/%)

| Batch # | Distance *D*/mm | C | Si | Mn | P | S | Cr | Mo | Ni | Al | Cu | Ti | V | Sn | Ca | N | Jominy [HRC] |
|---|---|---|---|---|---|---|---|---|---|---|---|---|---|---|---|---|---|
| 1 | 2 | 0.52 | 0.3 | 1.04 | 0.01 | 0.001 | 1.13 | 0.02 | 0.11 | 0.017 | 0.17 | 0.004 | 0.16 | 0.012 | 0.001 | 0.007 | 62 |
| 1 | 9 | 0.52 | 0.3 | 1.04 | 0.01 | 0.001 | 1.13 | 0.02 | 0.11 | 0.017 | 0.17 | 0.004 | 0.16 | 0.012 | 0.001 | 0.007 | 62 |
| 1 | 15 | 0.52 | 0.3 | 1.04 | 0.01 | 0.001 | 1.13 | 0.02 | 0.11 | 0.017 | 0.17 | 0.004 | 0.16 | 0.012 | 0.001 | 0.007 | 58 |
| 1 | 30 | 0.52 | 0.3 | 1.04 | 0.01 | 0.001 | 1.13 | 0.02 | 0.11 | 0.017 | 0.17 | 0.004 | 0.16 | 0.012 | 0.001 | 0.007 | 50 |
| 1 | 50 | 0.52 | 0.3 | 1.04 | 0.01 | 0.001 | 1.13 | 0.02 | 0.11 | 0.017 | 0.17 | 0.004 | 0.16 | 0.012 | 0.001 | 0.007 | 43 |
| 2 | 2 | 0.52 | 0.3 | 1.03 | 0.009 | 0.002 | 1.14 | 0.02 | 0.1 | 0.015 | 0.17 | 0.003 | 0.16 | 0.011 | 0.001 | 0.008 | 61 |
| 2 | 9 | 0.52 | 0.3 | 1.03 | 0.009 | 0.002 | 1.14 | 0.02 | 0.1 | 0.015 | 0.17 | 0.003 | 0.16 | 0.011 | 0.001 | 0.008 | 61 |
| 2 | 15 | 0.52 | 0.3 | 1.03 | 0.009 | 0.002 | 1.14 | 0.02 | 0.1 | 0.015 | 0.17 | 0.003 | 0.16 | 0.011 | 0.001 | 0.008 | 58 |
| 2 | 30 | 0.52 | 0.3 | 1.03 | 0.009 | 0.002 | 1.14 | 0.02 | 0.1 | 0.015 | 0.17 | 0.003 | 0.16 | 0.011 | 0.001 | 0.008 | 56 |
| 2 | 50 | 0.52 | 0.3 | 1.03 | 0.009 | 0.002 | 1.14 | 0.02 | 0.1 | 0.015 | 0.17 | 0.003 | 0.16 | 0.011 | 0.001 | 0.008 | 45 |
| 3 | 2 | 0.55 | 0.26 | 1.03 | 0.014 | 0.004 | 1.12 | 0.03 | 0.08 | 0.013 | 0.18 | 0.002 | 0.16 | 0.009 | 0.0011 | 0.008 | 62 |
| 3 | 9 | 0.55 | 0.26 | 1.03 | 0.014 | 0.004 | 1.12 | 0.03 | 0.08 | 0.013 | 0.18 | 0.002 | 0.16 | 0.009 | 0.0011 | 0.008 | 59 |
| 3 | 15 | 0.55 | 0.26 | 1.03 | 0.014 | 0.004 | 1.12 | 0.03 | 0.08 | 0.013 | 0.18 | 0.002 | 0.16 | 0.009 | 0.0011 | 0.008 | 57 |
| 3 | 30 | 0.55 | 0.26 | 1.03 | 0.014 | 0.004 | 1.12 | 0.03 | 0.08 | 0.013 | 0.18 | 0.002 | 0.16 | 0.009 | 0.0011 | 0.008 | 53 |
| 3 | 50 | 0.55 | 0.26 | 1.03 | 0.014 | 0.004 | 1.12 | 0.03 | 0.08 | 0.013 | 0.18 | 0.002 | 0.16 | 0.009 | 0.0011 | 0.008 | 45 |
| ⋮ | ⋮ | ⋮ | ⋮ | ⋮ | ⋮ | ⋮ | ⋮ | ⋮ | ⋮ | ⋮ | ⋮ | ⋮ | ⋮ | ⋮ | ⋮ | ⋮ | ⋮ |
| 945 | 2 | 0.52 | 0.3 | 1.09 | 0.015 | 0.01 | 1.16 | 0.02 | 0.08 | 0.013 | 0.14 | 0.003 | 0.11 | 0.013 | 0.0013 | 0.012 | 63 |
| 945 | 9 | 0.52 | 0.3 | 1.09 | 0.015 | 0.01 | 1.16 | 0.02 | 0.08 | 0.013 | 0.14 | 0.003 | 0.11 | 0.013 | 0.0013 | 0.012 | 59 |
| 945 | 15 | 0.52 | 0.3 | 1.09 | 0.015 | 0.01 | 1.16 | 0.02 | 0.08 | 0.013 | 0.14 | 0.003 | 0.11 | 0.013 | 0.0013 | 0.012 | 55 |
| 945 | 30 | 0.52 | 0.3 | 1.09 | 0.015 | 0.01 | 1.16 | 0.02 | 0.08 | 0.013 | 0.14 | 0.003 | 0.11 | 0.013 | 0.0013 | 0.012 | 51 |
| 945 | 50 | 0.52 | 0.3 | 1.09 | 0.015 | 0.01 | 1.16 | 0.02 | 0.08 | 0.013 | 0.14 | 0.003 | 0.11 | 0.013 | 0.0013 | 0.012 | 46 |

**Table 2.** The average chemical composition of 51CrV4 spring steel used in the research

| | *w*/% | Average | St. dev | | *w*/% | Average | St. dev |
|---|---|---|---|---|---|---|---|
| Training data set | C | 0.524 | 0.012345 | Testing data set | C | 0.520875 | 0.011203 |
| | Si | 0.280667 | 0.03214 | | Si | 0.276695 | 0.033691 |
| | Mn | 1.006267 | 0.060607 | | Mn | 0.997613 | 0.064439 |
| | P | 0.012973 | 0.0022 | | P | 0.012589 | 0.00226 |
| | S | 0.005133 | 0.003087 | | S | 0.004957 | 0.002668 |
| | Cr | 1.104933 | 0.068353 | | Cr | 1.103564 | 0.063644 |
| | Mo | 0.038533 | 0.020139 | | Mo | 0.043035 | 0.023867 |
| | Ni | 0.102667 | 0.019982 | | Ni | 0.10568 | 0.020528 |
| | Al | 0.016587 | 0.005825 | | Al | 0.016961 | 0.005442 |
| | Cu | 0.160133 | 0.029319 | | Cu | 0.161231 | 0.029322 |
| | Ti | 0.003493 | 0.003126 | | Ti | 0.004577 | 0.005245 |
| | V | 0.139067 | 0.022609 | | V | 0.141328 | 0.021955 |
| | Sn | 0.011093 | 0.001595 | | Sn | 0.011248 | 0.001757 |
| | Ca | 0.001283 | 0.000365 | | Ca | 0.001283 | 0.000374 |
| | N | 0.010587 | 0.001908 | | N | 0.010857 | 0.002206 |

## Jominy test and genetic programming

Genetic programming is probably the most general evolutionary optimization method. The organisms that undergo adaptation are in fact mathematical expressions (models) for Jominy test prediction consisting of the available function genes (i.e., square root and basic arithmetical functions) and terminal genes (i.e., independent input parameters, and random floating-point constants). In our case the models consist of: function genes of addition, subtraction, multiplication, division and square root operation, terminal genes of distance from specimen face *D* and chemical composition (mass fractions of C, Si, Mn, P, S, Cr, Mo, Ni, Al, Cu, Ti, V, Sn, Ca, N).

Random computer programs of various forms and lengths are generated by means of selected genes at the beginning of simulated evolution. Afterwards, the varying of computer programs during several iterations, known as generations, by means of genetic operations is performed. After completion of varying of computer programs a new generation is obtained that is also evaluated and compared with the experimental data. The process of changing and evaluating organisms is repeated until the termination criterion of the process is fulfilled. This was the prescribed maximum number of generations.

For the process of simulated evolutions the following evolutionary parameters were selected: size of population of organisms 500, the greatest number of generations 200, reproduction probability 0.4, crossover probability 0.6, the greatest permissible depth in creation of population 6, the greatest permissible depth after the operation of crossover of two organisms 10 and the smallest permissible depth of organisms in generating new organisms 2. Genetic operations of reproduction and crossover were used. For selection of organisms the tournament method with tournament size 7 was used.

We have developed 100 independent civilizations of mathematical models for prediction of the Jominy test.

To make the presentation more clear let us have a look at the development of one of the independent civilizations with previously mentioned genes.

The result of the blind random searching for mathematical models in the initial generation is bad. The best mathematical model for prediction of the Jominy test in generation 1 is:

$$\begin{aligned}&-35.15+118.66\cdot C+13.72\cdot Cr+9.25\cdot Cu+15.13\cdot Mn\\&+20.71\cdot Mo-126.73\cdot N+12.73\cdot Ni+54.83\cdot P+10.55\cdot Si\end{aligned} \quad (1)$$

with average deviation (%) for training data (74 batches) 92.62 %.

A slightly better model has been developed in generation 50:

$$29.27+60.38\cdot C-0.00276\,(33.44\cdot Al+9.25\cdot Cu)\,D^2 \quad (2)$$

with average deviation for training data (74 batches) 13.06 %.

The best model occurred in generation 156:

$$\begin{aligned}&29.27+60.38\cdot C-D\cdot Si\\&+Mo(Mo-Mn^2(60.38+60.38\cdot C+Mn)Mo+Si(120.76\cdot Si^2)\\&+Si^2(60.38\cdot Si+120.76\cdot Si^2+Mn\cdot Si^7)\\&+Si(120.76\cdot Si+362.28\cdot Si^2+Si(120.76\cdot Si+181.14\cdot Si^2)))\end{aligned} \quad (3)$$

with average deviation for training data (74 batches) 4.22 %.

**Table 3.** The linear regression results

| | | Unstandardized Coefficients | | Standardized Coefficients | $t$ | Sig. |
|---|---|---|---|---|---|---|
| Model | | *B* | Std. Error | *Beta* | | |
| 1 | (Constant) | 63.462 | 8.019 | | 7.914 | 0.000 |
| | Distance | –0.284 | 0.009 | –0.846 | –30.985 | 0.000* |
| | C | 3.875 | 16.277 | 0.008 | 0.238 | 0.812 |
| | Si | –0.981 | 5.298 | –0.005 | –0.185 | 0.853 |
| | Mn | 1.845 | 4.886 | 0.019 | 0.378 | 0.706 |
| | P | 37.209 | 39.616 | 0.029 | 0.939 | 0.348 |
| | S | 1.445 | 38.137 | 0.001 | 0.038 | 0.970 |
| | Cr | –2.365 | 4.697 | –0.028 | –0.503 | 0.615 |
| | Mo | 12.553 | 9.045 | 0.044 | 1.388 | 0.166 |
| | Ni | –17.477 | 9.130 | –0.060 | –1.914 | 0.056 |
| | Al | –33.779 | 28.771 | –0.038 | –1.174 | 0.241 |
| | Cu | 0.263 | 6.863 | 0.001 | 0.038 | 0.969 |
| | Ti | 18.319 | 68.077 | 0.012 | 0.269 | 0.788 |
| | V | –10.336 | 8.404 | –0.040 | –1.230 | 0.220 |
| | Sn | –47.154 | 108.512 | –0.013 | –0.435 | 0.664 |
| | N | 93.117 | 102.366 | 0.040 | 0.910 | 0.364 |

*Statistical significance ($p < 0.05$)

The linear regression model is:

$$\begin{gathered}63.462 - 0.284 \cdot D + 3.875 \cdot C - 0.981 \cdot Si + 1.845 \cdot Mn + 37.209 \cdot P + 1.445 \cdot S \\ - 2.365 \cdot Cr + 12.553 \cdot Mo - 17.477 \cdot \mathrm{Ni} - 33.779 \cdot Al + 0.263 \cdot Cu + 18.319 \cdot Ti \\ - 10.336 \cdot V - 47.154 \cdot Sn + 93.117 \cdot N\end{gathered} \tag{4}$$

$W = w(\mathrm{W})$; W = C, Si, Mn, P, S, Cr, Mo, Ni, Al, Cu, Ti, V, Sn, N
with average deviation for training data (74 batches) 4.25 %.

The average mass fraction deviation of the best model for testing data (871 batches) is 14.92 %.

The only statistically influential parameter ($p < 0.05$) in the linear regression model is distance from the edge ($p = 0.000$).

The average deviation of the best model for testing data (871 batches) is 4.37 %.

As the models are developed by simulated evolution based on probability, there is no guarantee that the models will contain all available independent parameters. During previous studies it was established experimentally that genetic programming for building of models, usually uses only parameters leading to successful solutions, whereas parameters not having decisive influence on the output parameter(s) are on the average more frequently eliminated by simulated evolution. [5, 6] Thus in our case, by analyzing the parameters present (i.e., remaining) in the best model, the influence of an individual parameter on the Jominy test can be indirectly estimated.

From sixteen terminal genes - monitored parameters (distance from specimen face, mass fractions of C, Si, Mn, P, S, Cr, Mo, Ni, Al, Cu, Ti, V, Sn, Ca, N) only five were present in the best model for Jominy test prediction.

It is possible to conclude that the distance from specimen face, mass fractions of C, Si, Mn and Mo are the most influential parameters for 51CrV4 spring steel hardenability.

## Jominy test and linear regression

The results of linear regression modeling results are presented in the next table (Table 3).

## Conclusion

In this paper prediction of the Jominy test by genetic programming and linear regression was performed. Prediction models were developed on the basis of experimental data on the chemical composition and distance from the specimen face of the 51CrV4 spring steel.

A training data set (74 batches) was used for Jominy test results prediction, whereas the testing data set (871 batches) was used for verifying the model.

Genetic programming predicts the Jominy test with average deviation for training data (74 batches) 4.22 % and 4.37 % for testing data (871 batches). With the genetic programming method we can also assume that the influence of the mass fractions of P, S, Cr, Ni, Al, Cu, Ti, V, Sn, Ca and N on Jominy test results is relatively small.

Linear regression predicts the Jominy test with average deviation for training data (74 batches) 4.25 % and 14.92 % for testing data (871 batches). The only statistically influential parameter ($p < 0.05$) in the linear regression model is distance from the edge ($p = 0.000$).

The results show that both approaches give pretty the same idea about influencing parameters and also the genetically developed model performs better. The results can be easily practically used for chemical composition optimization.

## REFERENCES

[1] Yazdi, A., Z., Sajjad, S., A., Zebarjad, S. M., Nezhad, M., S., M. (2007): Prediction of Hardness at Different Points of Jominy Specimen Using Quench Factor Analysis Method. *Journal of Materials Processing Technology*, Vol. 199, 1–3, 124–129.

[2] SONG, Y., P., LIU, G., Q., LIU, S., X., LIU, J., T., FENG, C., M. (2007): Improved Nonlinear Equation Method for Numerical Prediction of Jominy End-Quench Curves. *Journal of Iron and Steel Research*, Vol. 14/1, 37–41.

[3] DOBRZANSKI, L., A., SITEK, W. (1999): The modeling of hardenability using neural networks. *Journal of Materials Processing Technology*. Vol. 92–93, 8–14.

[4] HÖMBERG, D. (1993): A numerical simulation of the jominy end-quench test, *Acta Materialia*, Vol. 44/11, 4375–4385.

[5] KOVAČIČ, M., BALIČ, J., BREZOČNIK, M. (2004): Evolutionary approach for cutting forces prediction in milling. *Journal of Materials Processing Technology*, 155–156, 1647–1652.

[6] KOVAČIČ, M., ŠARLER, B. (2009): Application of the genetic programming for increasing the soft annealing productivity in steel industry. *Materials and manufacturing processes*, Vol. 24/3, 369–374.

[7] Dostopno na svetovnem spletu: www.store-steel.si

# Estimation of Groundwater Recharge under various land covers in parts of Western ghat, Karnataka, India.

# Ocena napajanja podzemne vode na območjih z različno pokrovnostjo tal v delih zahodnega Gathsa, Karnataka, Indija

Purandara B. K.[1,*], Venkatesh B.[1] & V. K. Choubey[2]

[1]National Institute of Hydrology, 11, I main, II cross, Hanuman Nagar, Belgaum - 590 001, Karnataka, India
[2]National Institute of Hydrology, Jal Vigyan Bhavan, Roorkee – 247667, India

*Corresponding author. E-mail: purandarabk@yahoo.com

**Received:** July 2, 2009 **Accepted:** February 24, 2010

**Abstract:** Land use practices are assumed to have important impacts on availability of water resources. These impacts can be both positive and negative. Therefore, it is essential to understand the impact of land cover changes on hydrological regime. In this connection, the present study has been carried out to estimate the groundwater recharge under various land covers, viz, natural forest, degraded and afforested regions. Extensive field investigations were carried out to determine the soil hydraulic properties and retention characteristics of soils, which are basic input parameters for modeling. SWIM model was applied to estimate the ground recharge. It is observed that, the groundwater recharge is higher in forested catchments and afforested regions. The minimum recharge was noticed in degraded forests. The present study throws a light on forest management strategies to be adopted for maximizing the water resources.

**Izvleček:** Infiltracija je eden najpomembnejših parametrov pri modeliranju hidroloških procesov in ključni dejavnik pri hidroloških spremembah, ki so posledica človekove dejavnosti. Kljub temu je vpliv tovrstnih sprememb na hidrološki krog slabo razumljen. Ena pomembnejših nalog hidrologov je ocena vplivov sprememb rabe tal na podzemni del hidrološkega kroga. Da bi bolje razumeli vpliv, posebej na napajanje podzemne vode, je bila študija izvedena na območjih pokrajine Uttara Kannada v indijski zvezni državi Karnataka, kjer

*Original scientific paper*

poteka obsežno pogozdovanje z eksotičnimi vrstami dreves (npr. Accacia auriculiformis). Lokalno prebivalstvo na tem območju je zaskrbljeno zaradi vpliva pogozdovanja na zaloge in razpoložljivost podzemne vode. Zato je osnovni cilj študije ocena napajanja podzemne vode v odvisnosti od različnih pokrovnosti tal. Obsežne terenske raziskave so bile izvedene za določitev hidravličnih lastnosti tal, ki so osnovni vhodni parametri za modeliranje. Za oceno napajanja je bil uporabljen model SWIM. Ugotovljeno je bilo, da je napajanje podzemne vode največje na napajalnih zaledjih, pokritih z gozdom, in na pogozdenih območjih, najmanjše pa na degradiranih območjih. Gledano v celoti, študija osvetljuje določene aspekte strategije upravljanja z gozdovi na degradiranih območjih, ki lahko prispevajo k ohranjanju vodnih virov.

**Key words:** Groundwater, Recharge, infiltration, Hydraulic conductivity, Soil Water Infiltration Movement Model (SWIM**),** Western Ghats
**Ključne besede:** podzemna voda, napajanje, infiltracija, prepustnost, SWIM-model, zahodni Ghats

## Introduction

Tropical forests in India have undergone dramatic land use changes in the last few decades. The myriad of changes that have, and still are, taking place are the effect of an equally large number of local causes and factors, highlighting a complexity that tends to defy easy generalizations. One of the important factor which lead to such dramatic change is the population explosion combined with more and more industrialization. The ultimate result of such a growth was deforestation in order to meet the local people needs. Of late, the degraded and the open land in the forests have been brought under the forest cover by extensive plantation. In many developing countries, extensive areas are undergoing land use changes. The largest changes in terms of land area, and arguably also in terms of hydrological impacts, often arise from afforestation and deforestation. Increasing areas are undergoing afforestation with fast growing monocultures of often exotic tree species.

There are world wide concern that increased establishment of plantation of exotic forest species for wood, fiber production, either as result of conversion of native forests and scrublands or afforestation of pasture and native grassland may have a detrimental effect on the environment. One of the most interesting questions put forward is that, what happens to water yield when the headwater catchments are planted with monoculture species. There are only limited studies carried out to evaluate the hydrological impacts of plantation. In India, during the last few years, considerable effort has been made to understand the impact of forest degradation on the soil hydrological regime. However, studies are quite limited as far as the impact of forest degradation on groundwater regime in western ghat region.

The Western Ghat region is the origin and primary catchment of many rivers (west and east flowing) in peninsular India. The lives of the majority of the rural population in the four southern states (Kerala, Tamil Nadu, Andhra Pradesh and Karnataka) plus parts of Maharashtra are thus critically dependent upon the watershed services provided by the Western Ghats forests. The portion of the Western Ghats that lies in Karnataka state, contains the major portion of the forests. It is reported that, there has been an increased anthropogenic activities in the western ghat mountain region, a rapid change in variety of land-use and land cover are taking place, which could have very significant impact on the water regime of the region, which includes the baseflow and groundwater recharge.

In the present study is an attempt to understand the impact of the land-uses on the groundwater recharge under different rainfall regimes with change in land-use conditions. In order to facilitate the analysis, SWIM (Soil Water and Infiltration Movement) model is chosen. It is selected in view of its simplicity and use of input parameters (soil moisture characteristics) that can be directly measured in the field/laboratory.

## Materials and methds

### Study Area

Uttara Kannada is a district with an area of 10,291 km$^2$, with its administrative headquarters at Karwar (Figure 1). The main geographic feature of the district is the Western Ghats (WG), which runs from north to south through the district. Between the WG and the sea is narrow coastal strip, which varies from 8 km to 24 km in width. Behind the coastal plain are flat topped hills from 60 m to 100 m in height, and behind these hills are the ridges and peaks of the WG. East of the WG is the upland, part of the vast Deccan plateau.

In the WG region, majority of the rain falls during June- September., i.e., south-west monsoon. More than 90 % of the annual rainfall occurs during the four monsoon months, with an average number 120–140 rainy days per year. During the monsoon, a major portion of the rainfall is contributed by four to five spells each lasting 8–10 days.

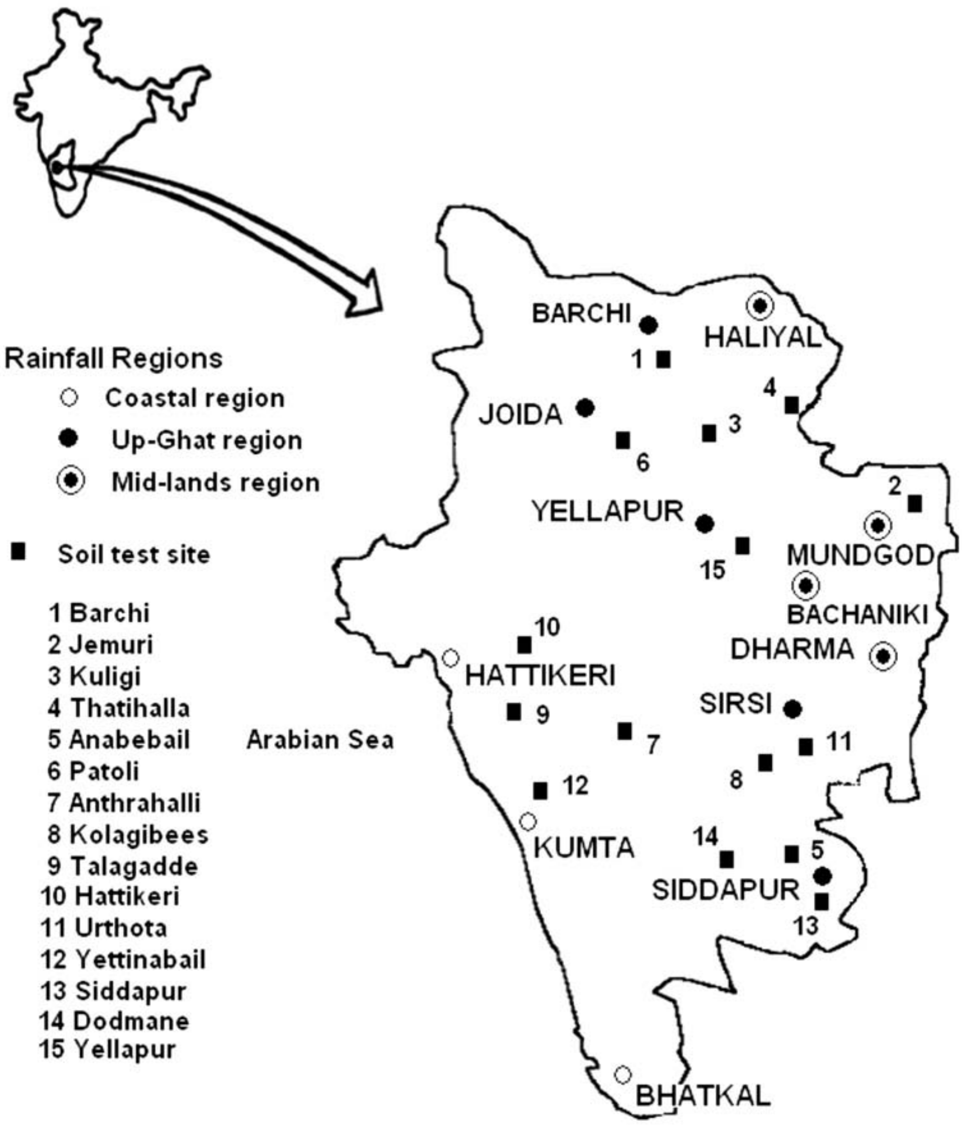


**Figure 1.** Index map of Study area with location of raingauges and experimental sites.

During such spells, daily values are very high. However, intensities are relatively moderate and rainfall occurs during most part of the day (PUTTY, 1994). PUTTY et al. (2000) reported that 15-minute intensities seldom exceed 80 mm/h and contribute about 2 % of the annual rainfall, while hourly intensities of 60 mm/h contribute less than 1 % of the annual rainfall.

### Geology and Soils

Geologically, the study area consists of Pre-Cambrian formations with gneiss and intrusive granites (mostly along the coastal tracts and adjoining areas towards east). In the northern part of the study area basaltic rocks of Upper Cretaceous age are seen. Soil is deep particularly in coastal areas (few feet to few meters). Laterites are commonly found in coastal areas and plateau region is covered by black soils, where as the up-ghat region is characterized by both red and mixed soils. By contrast, large areas along the coastal tracts of North Kanara district, the parts of Western Ghat are severely degraded with laterite (Geologically Recent in age) induced by natural climatic variability. In the plateau areas of the Western Ghats, deep forest soils rich in humus. Black soil is found locally, i.e. in areas having elevation above 500–600 m. Generally, regions with heavy rainfall and dissected topography (slope varying between 12–15 %) are devoid of black soil indicating that, climate, topography and lack of drainage are more important than nature of underlying rocks in the formation of black soil.

The Karnataka Forest Department (KFD) has taken up various reforestation strategies depending upon the state of land degradation. The major species used for the afforestation activities are Teak and acacia ariculiformis.

## Methodology

### Rainfall Analysis

The entire Uttara Kannada district has been divided into three distinct regions based on the elevation. The three regions are Coastal, Up-ghats and Plateau. The automatic raingauge stations covered under coastal region are, Kumta, Aversa and Bhatkal. Sirsi, Yellapur, Joida and Siddapur are included under the Up-ghat region. Raingauge stations available in the plateau region are Mundgod, Dharma, Barchi, Bachaniki and Haliyal. The rainfall intensity and duration data for these rainfall stations were extracted from the hourly rainfall charts (The Water Resources Development Organisation, Govt. of Karnataka, maintains these stations). The records from the raingauge stations in each region were taken together to give regional record totals in station years. This amalgamation of annual maximum values assumes that they are independent of the stations and they are representative of their regions defined from the criteria. These compounded records were then subjected to an analysis using the Gumbel's frequency distribution with the probability weighted moment method.

As the first step of the analysis, the values of maximum intensities for 1 h, 2 h, 3 h and 5 h duration from all 12 stations were considered. The frequencies of all these maximum intensity values were computed using the Weibull plotting position procedure. A multiple regression model is used to develop a relationship of intensity versus duration and frequency of the form of, $I$ = 112,47 $D^{-0.341}$ $T^{0.21}$, The multiple correlation coefficient obtained was 0.80

**Field Investigations**

Field experiments were carried out for the determination of saturated hydraulic conductivity in three typical zones by using Disc permeameter (PERROUX & WHITE, 1988) and Guelph permeameter. In each location a plot of 10 m/10 m was selected and carried out 6–8 experiments in order to get a proper representation. Data has been subjected to statistical analysis to get log mean values. LSD and F tests were also carried out for the analysis.

**Laboratory Investigations**

Laboratory investigations included determination of saturated moisture content, and soil moisture retention characteristics using the pressure plate apparatus.

## MODELING

Daily rainfall and evaporation data of 1986 to 2000 were used for the study. Water balance components like runoff, evapotranspiration and drainage (recharge to groundwater from rainfall) were determined through SWIM.

SWIM is an acronym that stands for Soil Water Infiltration and Movement Model. It is a software package developed within the CSIRO Division of soils for simulating infiltration, evapotranspiration, and redistribution. The model is based on a numerical solution of the Richards' equation and the advection-dispersion equation. It can be used to simulate runoff, infiltration, redistribution, solute transport and redistribution of solutes, plant uptake and transpiration, soil evaporation, deep drainage and leaching. Soil water and solute transport properties, initial conditions, and time dependent boundary conditions (e.g., precipitation, evaporative demand, solute input) need to be supplied by the user in order to run the model. The governing partial differential equation (Richards' equation) applicable for one-dimensional flow in the unsaturated zone can be written as:

$$\frac{\partial \theta}{\partial t} = \frac{\partial}{\partial x} K\left[\frac{\partial \psi}{\partial x} + \frac{dz}{dx}\right] + S$$

where,
$\theta$ = volumetric water content [cm³/cm³]; water/soil
$t$ = time [h]
$x$ = distance into the soil [cm]
$K$ = hydraulic conductivity

[$cm^2$ /(cm/h); water/soil]
$\psi$ = matric potential [cm]; water
$z$ = gravitational potential[cm] and
$S$ = sink strength[$cm^3$/($cm^3$/h)]; water/soil

The model deals with a one-dimensional soil profile. For a vertical soil profile, this means that it may be vertically inhomogeneous, but must be horizontally uniform. This assumption has two consequences of importance in many common simulations. There is only one hydraulic conductivity function for each layer, so that any macropore, or bypass flow can only accounted for in a limited way. Secondly, the calculated solute concentrations apply to the whole soil layer, which means that there is no concentration gradient from the bulk soil to near the root surface. The presence of such a concentration gradient may in reality affect the soil osmotic potential and hence water and solute uptake (Verburg et al, 1996).

**Model Conceptualization**

In order to simulate the water balance components of the study area, a soil profile in each zone, viz., coastal, up ghat and plateau areas were considered with a thicknes of about 150 cm. Vapour conductivity is not taken into consideration nor is the effect of osmotic potential. There are two hydraulic property sets (for upper and lower soil horizons) that applied to 16 nodes of the 150 cm deep profile. Hysterises is not taken into account. Initially, there is no water ponded on the surface. Runoff is governed by a simple power law function and a surface conductance function. No by pass flow was included. A matric potential gradient of 0, i.e., `unit gradient' has been applied as bottom boundary condition through out the simulation. Cumulative rainfall and evaporation records (daily) for the period 1986–2000 were given as the input for determination of water balance components (runoff, evapotranspiration and drainage). The model parameters (soil hydraulic properties and moisture characteristics) were actually measured in the field and laboratory. Therefore, the model does not require any calibration as such.

Input Data for SWIM Model

1. Rainfall: Based upon the available information, two distinct soil layers were identified. The following input data was used for simulation of soil moisture movement through SWIM. Daily rainfall data of Honnavar, Barchi and Siddapur were used.
2. Evaporation: Daily evaporation data of Honnavar (coastal), Barchi (plateau) and Siddapur (Up ghat) were considered for the analysis.
3. Saturated Hydraulic Conductivity:

Saturated hydraulic conductivity was measured at 9 locations in the study area by using disc permeameter (locations are shown in Figure 1).The average saturated hydraulic conductivity values for the surface was measured by using disc permeameter and lower layer by using Guelph permeameter.

4. van Genuchten Parameters: The collected soil samples from the study area were analysed in the laboratory by pressure plate apparatus for soil moisture retention characteristics. The averaged van-Genuchten parameters for the two soil layers were obtained by non-linear regression analysis (Table 1).
5. Vegetation: Forested watershed, minimum xylem potential = –15000 cm, exponential root growth with depth and sigmoid with time were assumed for the study.

**Table 1.** Measured saturated hydraulic conductivity and van Genuchten Parameters for the Two Soil Layers

| Zones | Land use type | Soil Layers Depth (cm) | Sample size | Log-mean Ksat (mm/h) | Van-Genuchten Parameter | |
|---|---|---|---|---|---|---|
| | | | | | $\alpha$ | $n$ |
| Coastal | Natural Forest | Surface | 10 | 93.92 | 0.0192 | 1.6161 |
| | | 120–150 | 10 | 44.74 | 0.0105 | 1.6270 |
| | Degraded Forest | Surface | 12 | 6.73 | 0.0201 | 1.7008 |
| | | 120–150 | 12 | 0.20 | 0.0298 | 1.5353 |
| | Afforested | Surface | 10 | 88.20 | 0.0792 | 1.2586 |
| | | 120–150 | 10 | 88.20 | 0.8118 | 1.2446 |
| Plateau | Natural forest | Surface | 15 | 11.88 | 0.0044 | 1.9400 |
| | | 120 – 150 | 15 | 0.21 | 0.0110 | 1.8151 |
| | Degraded Forest | Surface | 12 | 6.21 | 0.0119 | 1.6320 |
| | | 120–150 | 12 | 0.40 | 0.0123 | 1.6296 |
| | Afforested | Surface | 15 | 6.01 | 0.0050 | 1.8698 |
| | | 120–150 | 15 | 0.60 | 0.0051 | 1.7644 |
| Up-Ghat | Natural Forest | Surface | 20 | 179.64 | 0.0253 | 1.4570 |
| | | 120–150 | 20 | 1.66 | 0.0104 | 1.4514 |
| | Degraded Forest | Surface | 20 | 2.78 | 0.0214 | 1.3563 |
| | | 120–150 | 20 | 2.78 | 0.0201 | 1.5861 |
| | Afforested | Surface | 20 | 90.00 | 0.0125 | 1.6925 |
| | | 120 –150 | 20 | 43.2 | 0.003 | 1.7701 |

## Results and Discussion

### Regional Analysis of Rainfall

Data of all the station that are grouped under three regions were pooled together to fit Gumbel distribution. The results obtained from fitting Gumbel distribution for individual stations and region wise were compared with the observed values. The estimates obtained from fitted distribution matches the observed values with an error of (10–15).

Table 2, reveals that the rainfall intensity is higher in coastal region for the return periods 2 and 5 years. The return period 10, 25 and 50 years show higher intensity in region III, compared to Region I. However, it is interesting to note that in Region II, the intensity is comparatively lower for all the return periods than the other two regions. This is true for only for intensity duration of 1 h. In the case of 2 h, 3 h and 5 h duration, the intensity is higher in up ghat region than in plateau region. The coastal region is distinct with the higher intensity than the other two regions.

### Statistical and Numerical Analyses

Statistical methods provide a satisfactory tool for hydrological analyses. Tukey (1977) indicated that the K data frequency distributions are closely approximated by the log-normal function. These observations are in close agreement with other field investigations (Bonell et al., 1983; Talsma, et. al., 1980) Consequently the use of log-means for interlayer comparison of K is more appropriate measure than the arithmetic means (Talsma, 1965; Nielsen et. al., 1973). The use of further statistical and numerical analysis on the K data is confined to the sur-

**Table 2.** Rainfall intensity –duration estimates for different regions for selected return period

| RP* | Region I | | | | Region II | | | | Region III | | | |
|---|---|---|---|---|---|---|---|---|---|---|---|---|
| | 1 h | 2 h | 3 h | 5 h | 1 h | 2 h | 3 h | 5 h | 1 h | 2 h | 3 h | 5 h |
| 2 | 34.06 | 28.41 | 29.19 | 20.27 | 26.06 | 21.34 | 14.27 | 11.98 | 29.23 | 17.17 | 12.04 | 9.64 |
| 5 | 42.40 | 41.14 | 39.14 | 31.3 | 38.01 | 29.09 | 22.00 | 18.14 | 41.75 | 25.73 | 18.25 | 14.82 |
| 10 | 47.57 | 49.57 | 45.73 | 38.60 | 45.57 | 34.23 | 27.11 | 22.22 | 50.04 | 31.4 | 22.37 | 18.26 |
| 25 | 54.10 | 60.22 | 54.05 | 47.82 | 55.12 | 40.72 | 33.57 | 27.38 | 60.51 | 38.56 | 27.56 | 22.60 |
| 50 | 58.94 | 68.12 | 60.23 | 54.66 | 62.2 | 45.53 | 38.37 | 31.21 | 68.28 | 43.87 | 31.41 | 25.82 |

Return Period, Region I – Coastal, Region II – Up Ghat, Region III – Plateau
Values are in mm/hr

face and layer between 120–150 cm, as these controls the runoff process. A significance level of 0.01 was used to test differences between specific pairs of sites. However, results indicated that, both F-test ($F < 0.001$) and Least Significant Difference was significant at this level.

The measured saturated hydraulic conductivities are plotted as box plots to view the variation within the measured values. The length of the box reflects the inter-quartile range, and the fence or tails of the box plots are marked by the extremes if there are no outliers, or else by the largest and smallest observation that does not qualify for an outlier. The outliers are defined as data points more than 1.5 times the inter-quartile range away from the upper or lower quartile. The middle horizontal bar on the box plot represents the median of the data.

The saturated hydraulic conductivity observed for soils in the undisturbed forests and also in afforested regions is comparatively higher in the lateritic soils, followed by red soil and least is observed in black cotton soils (Figure 2). Another set of data observed across an array of land use types, showed that the saturated hydraulic conductivity is maximum in forest and plantations (afforested land). Minimum saturated hydraulic conductivity was observed in degraded forests. However, saturated hydraulic conductivity in afforested region depends upon both soil type and also the type of plantation, such as teak, causarina or Acacia. A diagrammatic representation of the variation in saturated hydraulic conductivity with land use type is shown in Figure 3. Similar observation was made by VENKATESH et al. (2004) for Barchi watershed in a plateau region. It is reported that in regions afforested with teak plantation has the lowest $K_s$ value as compared to the forest and degraded lands.

The computed rainfall intensities for different frequencies are superimposed on these box plots to identify the possible runoff generation mechanism. From the Figure 2 it is evident that, the red and lateritic soils are more permeable than the black soils. However, in black soils, the mean Ks are exceeded by the rainfall intensities even at 1 in 1 year and above, indicating the domination of infiltration excess overland flow (Hortonian overland flow) occurrences.

The box-plot.3, depicts that, the natural forest and acacia plantation are comparatively has higher permeability than the other land-uses considered for the analysis. From the box-plot, it is observed that, the $K_s$ values in natural forest are much higher than the rainfall intensities at 1 in 50 years, indicating that in such regions the probability of having Hortonian overland flow is rare. However, PUTTY et al. (2000) reported the pipe flow phenomenon in such conditions.

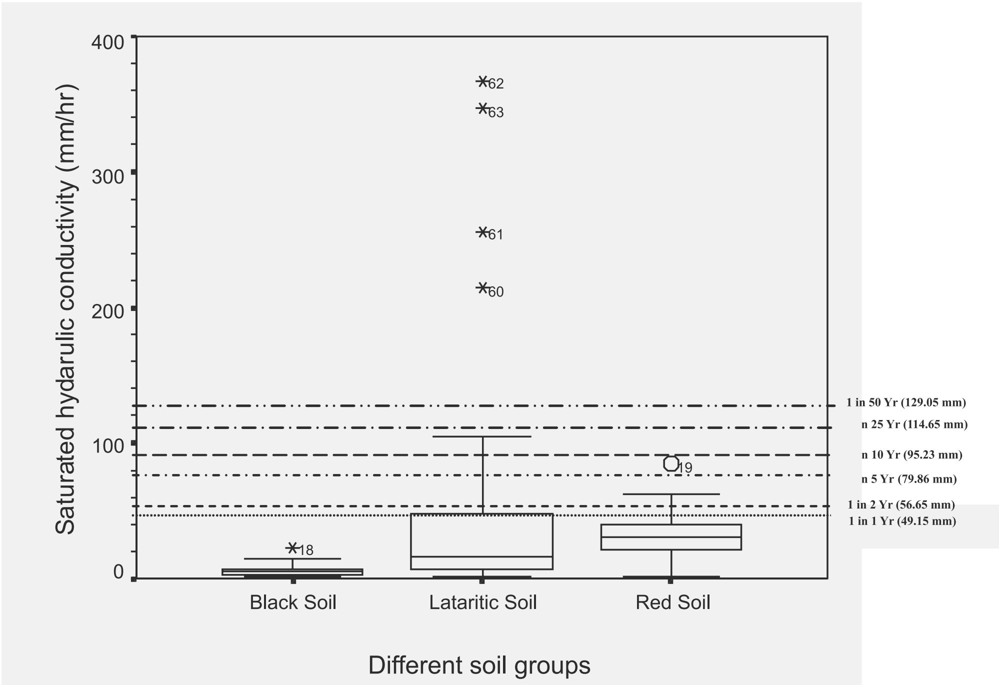


**Figure 2.** Saturated hydraulic conductivity, $K_s$ as a function of soil

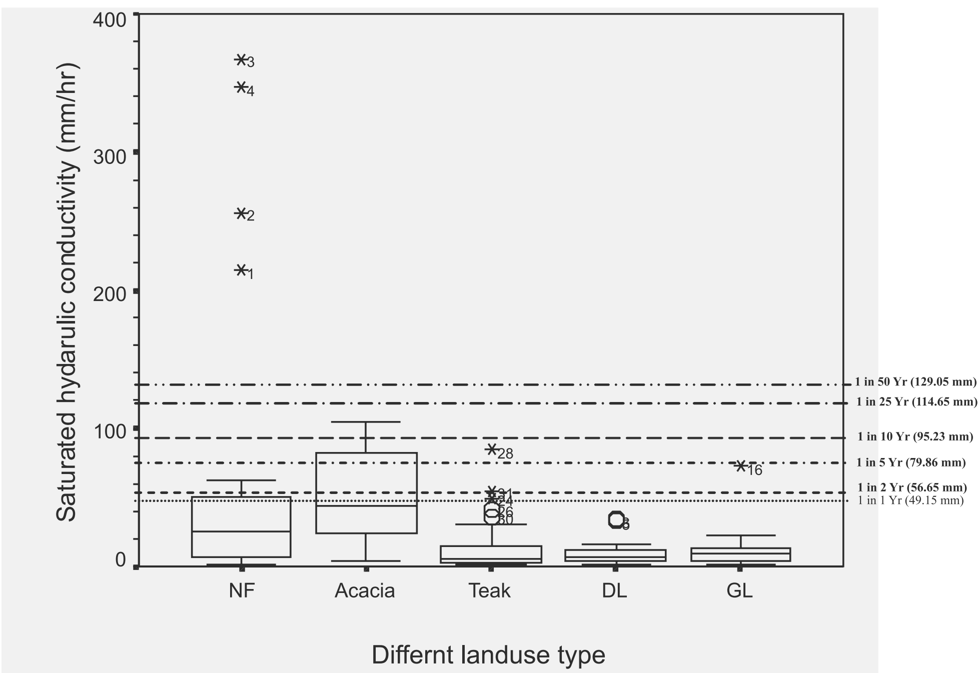


**Figure 3.** Saturated hydraulic conductivity, $K_s$ as a function of land-use

**Table 3.** Estimates of Groundwater Recharge using SWIM Model

| Sl No | Zones | Rainfall records Considered | Land use type | Average rainfall (mm) | Recharge percentage |
|---|---|---|---|---|---|
| 1 | Coastal | 1986–2000 | Forest | 3090–4192 | 52–55 |
| 2 | | | Degraded land | | 28–30 |
| 3 | | | Afforested land | | 60–65 |
| 4 | Plateau | 1986–1999 | Forest | 941–1521 | 30–35 |
| 5 | | | Degraded land | | 18–22 |
| 6 | | | Afforested land | | 22–25 |
| 7 | Up Ghat | 1989–2000 | Forest | 2489–2734 | 50–55 |
| 8 | | | Degraded land | | 28–32 |
| 9 | | | Affores ted land | | 48–52 |

**Simulations using SWIM Model**

The water balance estimated for the coastal region (using SWIM model) in three plots, namely, natural forest, degraded forest, afforested land, it is found that with an average rainfall of 3663 mm rainfall, the rainfall got apportioned into 1648 mm as runoff, 1200 mm as evapotranspiration, and 811 mm as deep drainage. The estimation of evapo–transpiration by the SWIM model is based on the potential evaporation. The PE values were available for only one station in each region. Therefore, no variation was observed in the estimated ET amount under different land use. The variation observed in the recharge percentage during the study period (for the data of 1986 to 2000) was 51–55 % in natural forest, 28–30 % in degraded forest and 60–65 % in areas where the afforestation was done about 10 years back. The runoff coefficient observed for the catchments in coastal area varied between 0.17 and 0.85. The minimum was noted in the forested plots and maximum is on degraded forests. This shows that there is a wide variation in runoff characteristics due to continuous change in land use and climatic conditions. Other important observation made was that high recharge and deep drainages are the characteristic features in coastal region due to high permeable lateritic rocks. Similar observations reported for the basins originating from WG of Karnataka (SHETTY, 1999).

In the plateau area, especially, in black cotton soils (vertisol), the estimated recharge in natural forest was 30–35 %, degraded forests, 18–22 % and 22–25 % in afforested lands. SWIM model analysis carried out for the Barchi nala catchment showed that with an average rainfall of 1303 mm, 524 mm is evapo–transpiration and 350 mm was estimated runoff. The deep drainage component was only 410 mm.

Hydrologically, the up lands of the WG are characterized by steep slopes and high rainfall. The major part of the WG is covered by lateritic soil underlain by crystalline rocks. The runoff percentage estimated is 43 %. The average rainfall in the area is 2361 mm. SWIM model results showed that 878 mm as evapotranspiration and 1015 mm runoff. The drainage component estimated was 461 mm. This is quite lower than that estimated for the coastal region but higher than that of plateau region.

Baseflow indices were estimated for two regions (Venkatesh et al., 2002), one dominated by red soils and the other is black cotton soils. In the black cotton soil area it is found that, the baseflow index showed high value (0.51) as compared to the red soil region (0.36). This variation is attributed to the fact that, in red soil region major part of the rainfall infiltrated into deeper zones and increased the ground water recharge, where as in the black cotton soil area, the deep drainage component is quite lower due to low infiltration rates as observed in this part of the study area.

## Conclusions

The application of SWIM has been demonstrated for different land use in parts of WG of North Kanara district of Karnataka, India. The advantage of the model is that it can be used both for laboratory and field studies to simulate the soil water and solute transport and can also be used for understanding the impact of different land use management hydrologic regime of the area. In this study, simulations using the SWIM has been substantiated by the field experiments to understand the runoff generation dynamics under different land–use conditions.

Following are some of the important conclusions drawn from the study

1. The impact of afforestation showed a considerable increase in infiltration and hydraulic conductivity and also generates infiltration excess overland flow at higher rainfall intensities.
2. The results obtained through SWIM model indicated that there is marked differences in recharge percentages as the land cover changes (i.e., converting the land from degraded has been brought under Acacia plantation in the present case). This higher groundwater recharge may contribute to the

dry season flows in the streams.

3. The current study clearly indicated that selective reforestation/afforestation with specific species may lead to improve the surface hydraulic properties and encourage greater percolation and conversely, inhibits the occurrence infiltration excess overland flow.

## REFERENCES

BONELL. M., GILMOUR, D. A. & CASSELLS, D. S. (1983): A preliminary survey of the hydraulic properties of rainforest soils in tropical north–east Queens land and their implication fpr the runoff process. *In J.* de Ploey (ed.) Rainfall simulation, runoff and soil Erosion, Catena Supplement 4, Braunschweig, pp 57–78.

NIELSEN, D. R., BIGGAR, J. W. & ERH, K. T. (1973): Spatial variability of field measured soil water properties. *Hilgardia*, Vol. 42, pp 215–259.

PERROUX, K. M. & WHITE, I. (1988): Designs for disc Permeameters. *Soil Sci. Soc. Am. J.*, Vol. 52, pp. 1205–1215.

PUTTY,Y. R. (1994): The Mechanisms of Streamfflow Generation in the Sahyadri Ranges (Western Ghats) of South India. Ph. D Thesis, Indian Institute of Science, Bangalore, India.

PUTTTY, Y. R., PRASAD, V. S. R. K. & RAMASWAMY, R. (2000): A study on rainfall intensity pattern in the Western Ghats, Karnataka, Proceedings of Regional Workshop. *Watershed Development Management and Evaluation in theWestern Ghats Region of India*, pp. 44–51

SHETTY, A. V. (1999): Rainfall–Runoff modelling of Western Ghat Region of Karnataka. *Technical Report*, National Institute of Hydrology, Roorkee.

SNEDECOR, G. W. & COCHRAN, W. G. (1967): Statistical methods, 6$^{th}$ Edition, Iowa State University Press, Iowa, USA, pp 593.

TALSMA & HALLAM (1980): Hydraulic conductivity measurement of Forest Catchments. *Aust. J. Soil Res.*, Vol. 30, pp 139–148.

TALSMA, T. (1965): Sample size estimates in permeability studies. Proceedings of American Society of Eivil Engineers, 91, pp 76–77.

TUKEY, J. W. (1977): Exploratory Data Analysis, Addison–Wesley, Reading, Massachusetts, USA, pp. 688.

VENKATESH B, PURANDARA, B. K. & CHANDRAMOHAN T. (2004): Analysis of Spatial Variability of Hydraulic Conductivity of Forest Soils. *Integrated Water Resources Planning and Management*; ed. By K. S. Raju, A. K. Sarkar & M. L. Dash. Published by Jain Brothers new Delhi. pp.125–133.

VENKATESH B. & CHANDRAKUMAR S. (2002): Development of Base Flow Indices For Rivers In Hard Rock Region. *Technical Report*, National Institute of Hydrology, Roorkee.

# Jurassic and Cretaceous neptunian dikes in drowning successions of the Julian High (Julian Alps, NW Slovenia)

# Neptunski dajki v potopitvenih zaporedjih Julijskega platoja (Julijske Alpe, SZ Slovenija)

Andrej Šmuc[1,*]

[1]University of Ljubljana, Faculty of natural science, Department of Geology, Privoz 11, SI-1000 Ljubljana, Slovenia

*Corresponding author. E-mail: andrej.smuc@ntf.uni-lj.si

**Received:** January 12, 2010 **Accepted:** January 31, 2010

**Abstract**: In the Julian Alps the Jurassic neptunian dikes are common features of the drowning successions of the Julian High. In the research area, comprising Ravni Laz, Lužnica Lake and Triglav Lakes Valley areas, neptunian dikes are present in the Pliensbachian shallow – water limestone and in the Bajocian to the Tithonian Prehodavci formations. The dikes were formed by two mechanisms: A) the initiation of the voids by mechanical fracturing and later reshaping by dissolution, B) formation solely by mechanical fracturing of the host rock. The time span of dike infillings ranges from the Bajocian to late Cretaceous in age. According to the age of the host rock and neptunian dike infillings, the following phases of neptunian dike formation in the investigated area are recognized: Pliensbachian and/or Bajocian phase, Late Kimmeridgian-Early Tithonian phase and Late Cretaceous (pre-Senonian) phase.

**Izvleček:** V Julijskih Alpah se v jurskih potopitvenih sekvencah Julijskega praga pogosto pojavljajo neptunski dajki. Na raziskanem območju Ravnega Laza, Jezera v Lužnici ter Doline Triglavskih jezer se dajki pojavljajo v pliensbachijskih plitvovodnih apnencih in znotraj bajocijske do tithonijske Prehodavške formacije. Zapolnitve dajkov so od bajocijske do zgornjekredne starosti. Dajki so nastali na dva načina: A) z mehanskim razpokanjem

*Original scientific paper*

matične kamnine, razpoke pa so bile kasneje preoblikovane z raztapljanjem; B) nastanek izključno z mehanskim razpokanjem matične kamnine. Na podlagi raziskav matične kamnine in zapolnitev smo določili naslednje faze nastajanja dajkov: pliensbachijska in/ali bajocijska faza, kimmeridgijska faza in zgornjekredna faza.

**Key words:** neptunian dikes, Julian High, Jurassic, Cretaceous, Julian Alps

**Ključne besede:** neptunski dajki, Julijski prag, jura, kreda, Julijske Alpe

## Introduction

Neptunian dikes are defined as bodies of younger sediment filling fissures in rocks exposed on the seafloor. They are of great importance in the paleogeographic interpretation of an area because 1) fracture fillings often preserve unique bits of stratigraphic and paleontological information, which can be missing in normal bed-on-bed successions, 2) understanding the mechanism of opening and infilling is of great help in highlighting the relative importance of extensional tectonics, slope instability and sub-aerial or submarine dissolution.

In Slovenia the most frequent occurrences of neptunian dikes are in the western part of the Julian Alps. The dikes outcrop at Kanin, near Učeja, in the surroundings of Bovec at the Mangart Saddle and in the Krn ridge. The host rocks of the dikes are Triassic, Jurassic and Cretaceous carbonate rocks. The dikes themselves are of Jurassic and Cretaceous ages. The present study investigated in detail the neptunian dikes of Julian Carbonate Platform-Julian High drowning successions in three key areas; the Ravni Laz area under the Kanin massive, the Lužnica Lake area in the eastern part of the Krn ridge and the neptunian dikes of the Triglav Lakes Valley.

The aims of this study were to define the stratigraphical distribution of neptunian dikes in the aforementioned areas, to define their frequency, to decipher all varieties of neptunian dike forms and their infillings and to interpret geological processes that were responsible for their formation.

## Geological setting

The Julian Alps are located in the NW part of Slovenia and NE part of Italy. Structurally, they belong to the Julian

Nappe and, together with the underlying Tolmin Nappe, they represent the easternmost continuation of the Southern Alps (Figure 1). In the Julian Alps the Paleogene Dinarides intersect with the Neogene Southern Alps. The area was first deformed by SW-vergent thrusts related to the most external Dinarides during the Oligocene – early Miocene and then by S to SSE-vergent ''Alpine'' thrusting since the late Miocene (Doglioni & Siorpaes, 1990; Bresnan et al., 1998; Placer, 1999; Placer, 2008; Placer & Čar, 1998; Mellere et al., 2000; Vrabec & Fodor, 2006). At the Miocene-Pliocene transition the major strike-slip deformation started in the Julian Alps (Vrabec & Fodor, 2006). From the Neogene to the present NW-SE trending dextral faults cut the area and displaced both the Dinaric and South Alpine fold-and-thrust structures.

Paleogeographically, the area in the Jurassic belonged to the Adriatic-Apulian microcontinent, bordered by the Alpine Tethys and the Vardar Ocean (Stampfli et al., 2001). From the Late Triassic to the earliest Jurassic, the area of the Julian Alps belonged to the Julian Carbonate Platform. During Early Jurassic rifting, the platform was dissected into blocks, forming a horst-and-graben structure. Some of these blocks became part of an isolated pelagic carbonate platform named the Julian High (Figure 2), while other blocks formed deeper basins, for example, the Bovec Trough (Šmuc, 2005; Šmuc & Goričan, 2005).

Neptunian dikes are present only in the drowning successions of the Julian High and they are completely absent in the Bovec Trough.

In general, the drowning succession of the Julian High is represented by Pliensbachian platform limestones of the Julian Carbonate Platform that are unconformably overlain by Bajocian to lower Tithonian highly-condensed limestones of the Prehodavci Formation or by middle Cretaceous Scaglia variegata or Senonian Scaglia rossa. Distinct features of all Julian High successions are numerous polyphase neptunian dikes that occur in Pliensbachian shallow water limestones and in the Prehodavci Formation. In the most extreme cases the dikes represent the only preserved Jurassic sediments that are otherwise missing from bed-on-bed successions.

## Previous research

The Jurassic neptunian dikes are well documented in the Carpathians (Aubrecht, 1997; Luczynski, 2001), Sicily (Mallarino, 2002; Martire & Pavia, 2004) and the in Southern Alps (Lehner, 1991; Winterer et al., 1991; Martire, 1992) while in Slovenia detailed studies

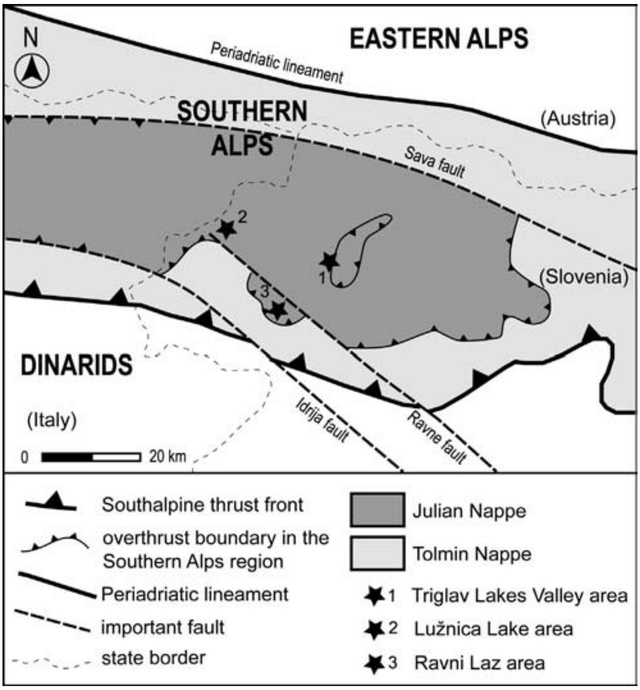


**Figure 1.** Location of the studied area with marked larger geotectonic units and regional faults

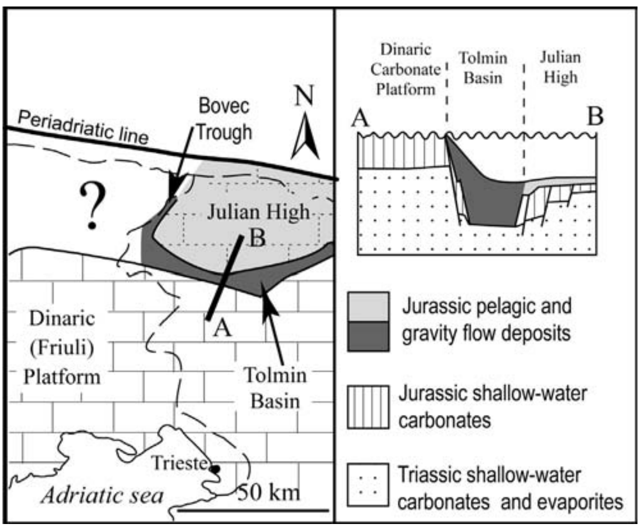


**Figure 2.** Present-day position of paleogeographic units (compiled from Buser (1989) and Placer (1999, 2008) and schematic cross-section (A-B) at the end of the Jurassic

of the neptunian dikes are scarce (Babić, 1981; Črne et al., 2007, Šmuc, 2005).

The neptunian dikes in the Julian Alps were first reported by Babić (1981). He observed and described fractures in the Upper Triassic Dachstein Limestone that were filled with the angular Upper Triassic and Lower Jurassic limestone clasts embedded in a red Middle-Upper Jurassic matrix. He interpreted them as neptunian dikes that were formed by extensional fracturing and later filled with pelagic sediments in the marine environment. Buser (1986, 1987, 1996) observed heavily karstified Jurassic fractures in the Dachstein limestone that were filled with assumed Bajocian-Bathonian grey-red crinoidal and micritic limestone. He suggested that these fractures were intensively karstified during the Early Jurassic emersion of the platform and later, when the platform drowned, filled with marine sediments.

Šmuc (2005) described in detail the Jurassic and Cretaceous successions of the Julian Alps. Within investigated sections he reported neptunian dikes from the Mangart area, Ravni Laz, Lužnica Lake and Triglav Lakes Valley. Neptunian dikes from the Mangart area were investigated in detail by Črne et al. (2007), whereas a detailed analysis of the neptunian dikes in the Lužnica Lake, Ravni Laz and Triglav Lakes Valley areas is presented in this article.

Research of the Mt. Mangart dikes system by Črne et al. (2007) represents an exemplar study of the complex neptunian dike system. The dikes at Mt. Mangart exhibit several different geometries: dissolution cavities, thin penetrative fractures, larger fractures and laterally confined breccia bodies. They were filled by two main generations of infillings. The first generation is Pliensbachian in age and represented by bioclastic limestone subdivided into five microfacies. The second generation is composed of breccias with a marly matrix. The timing of the second generation is only broadly assigned from the Pliensbachian to the Late Cretaceous.

## Description of neptunian dikes and interpretation of their formation

The research areas of Lužnica Lake, Ravni Laz and Triglav Lakes Valley paleogeographically belong to the Upper Triassic – Lower Jurassic Julian Carbonate Platform and Middle to Upper Jurassic Julian High. In all of the investigated sections the drowning succession starts with the Pliensbachian platform limestone that is unconformably overlain by condensed limestone of the Bajocian to lower Tithonian Prehodavci Formation (Šmuc, 2005) (Figure 3).

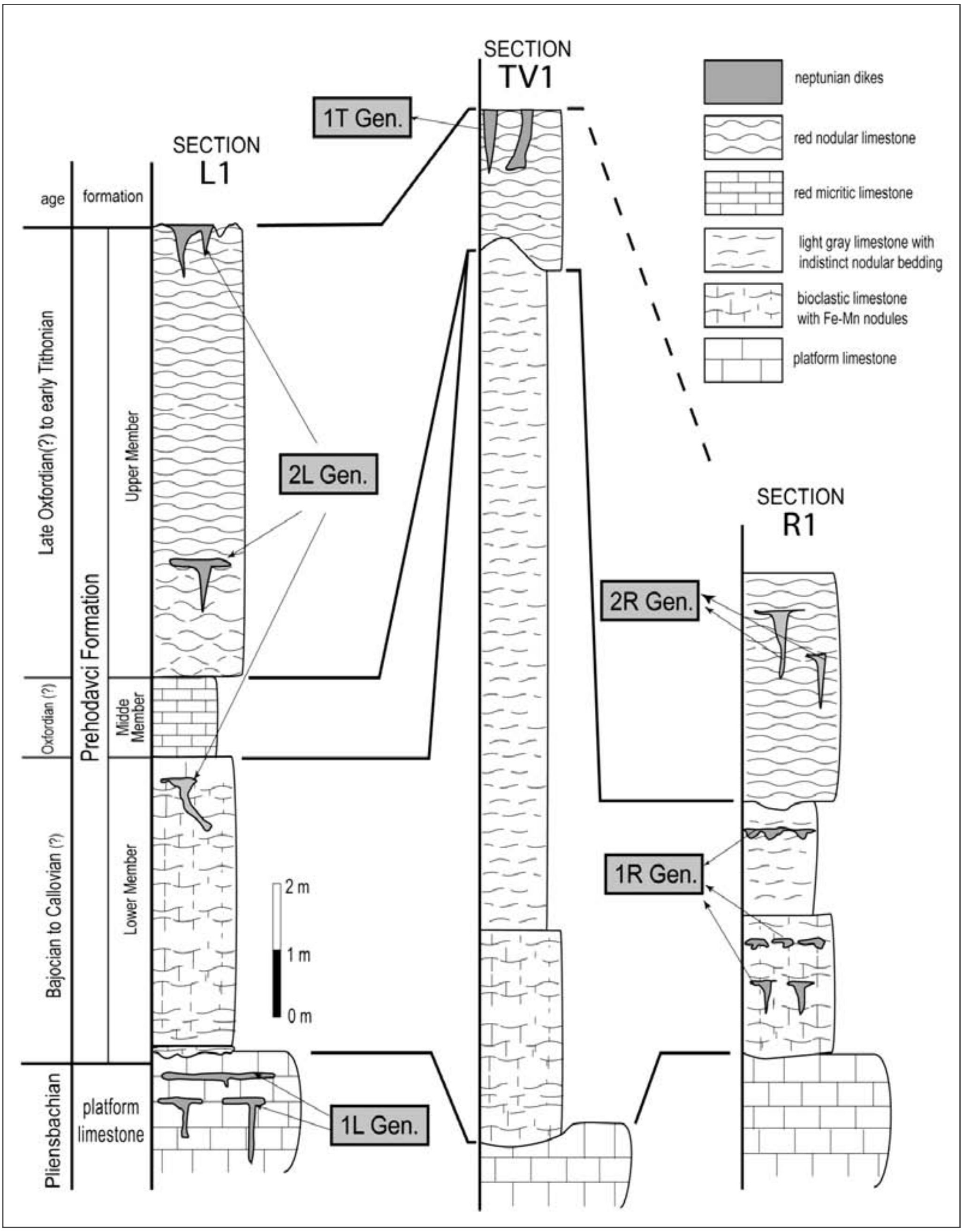


**Figure 3.** Lithostratigraphic sections of the investigated areas with marked occurrence of the neptunian dikes

The Lower Jurassic platform limestone is primarily a massive and bedded oolitic limestone that in places alternates with beds of micritic limestone, laminated dolomite and dolomitic limestone (Buser, 1986; Jurkovšek, 1986; Jurkovšek et al., 1990; Šmuc, 2005; Šmuc & Goričan, 2005). The limestone was deposited in a variety of different peritidal environments ranging from intertidal to a high-energy subtidal environment.

The Prehodavci Formation unconformably overlies the Lower Jurassic platform limestone (Figure 3). The contact is represented by a highly irregular unconformity surface that marks a stratigraphical gap comprising at least Toarcian to Aalenian. The Prehodavci Formation consists of condensed limestone of Ammonitico Rosso type and is subdivided into three members (Šmuc, 2005). The Lower Member (Bajocian to? Callovian) is composed of condensed, red, bedded bioclastic limestone with Fe-Mn nodules that gradually passes into light grey, indistinctly nodular limestone. The Middle Member (early Oxfordian?) consists of thin-bedded micritic limestone. The Upper Member (late Oxfordian? to early Tithonian) unconformably overlies the Lower or Middle Members. It is represented by red nodular limestone and red marly limestone with abundant *Saccocoma* sp. (Šmuc, 2005).

Neptunian dikes are present in all of the investigated sections (Figure 3). In the Triglav Lakes Valley and in Ravni Laz area the neptunian dikes only occur in the Prehodavci Formation while in the Lužnica Lake area neptunian dikes are also present in the Lower Jurassic shallow-water limestone.

**Neptunian dikes at Lužnica Lake section**

At Lužnica Lake (section L1 in Figure 3, $y = 399234$ $x = 124072$ $z = 1865$) the neptunian dikes occur in Pliensbachian platform limestone and in the Prehodavci Formation. Two generations of neptunian dikes were recognized.

***I. Generation***

The dikes located in the Pliensbachian platform limestone represent I generation (1L Gen. in Fig. 3). They are elongated, mostly sub-vertical, bed-crossing and occasionally bed-parallel oval cavities with smooth walls filled with younger limestone. The neptunian dikes are up to 10 cm wide and can cut up to 70 cm deep into the host rock. The neptunian dikes show polyphase laminated infillings. The oldest sediment is microsparitic limestone with rare ostracods, followed by a wackestone-packstone with echinoderm fragments, small sparite grains and Fe-Mn encrusted clasts that grade into wackestone with planktonic foraminifera (Protoglobigerinids), be-

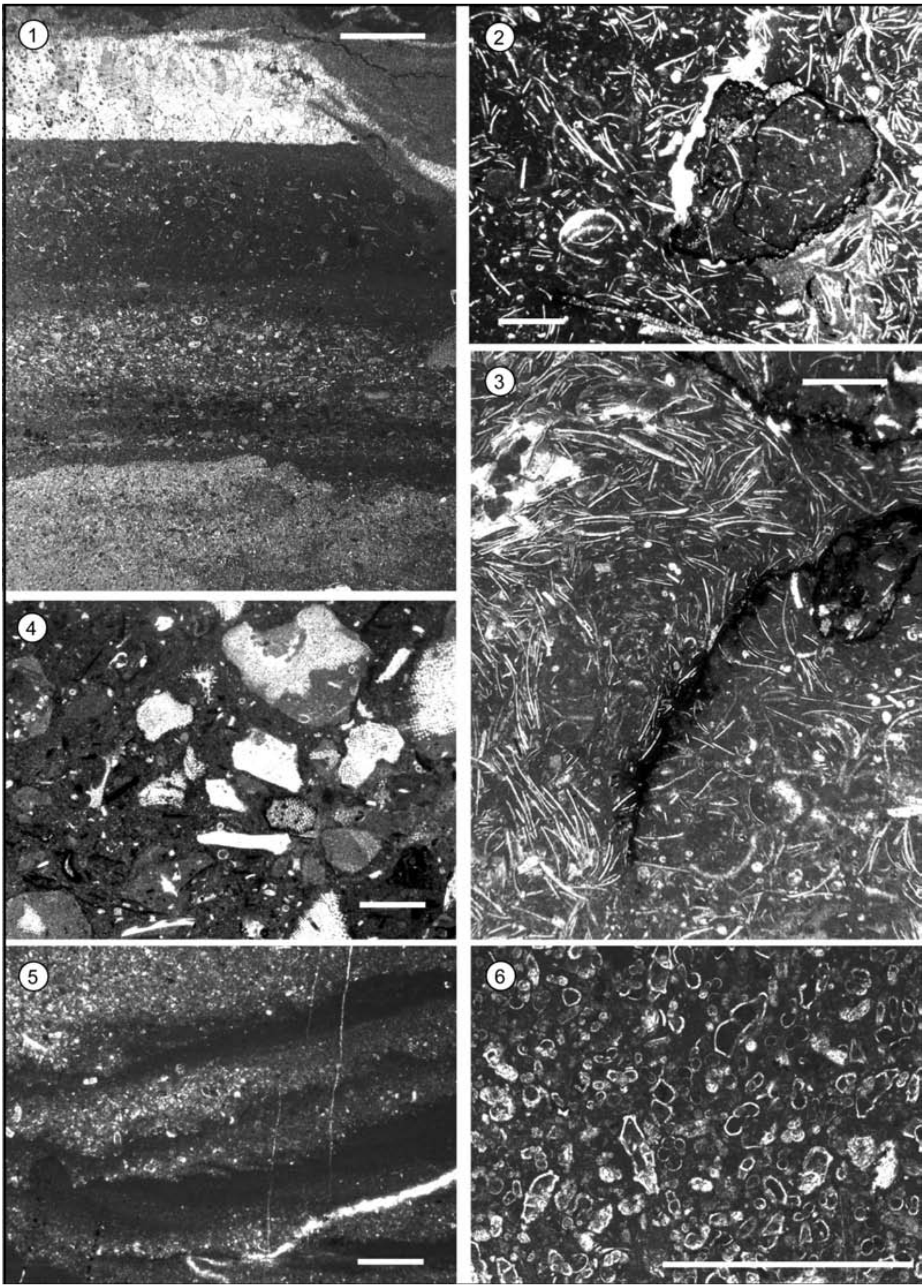
1
2
3
4
5
6

**Plate 1**

Pl. 1, Fig. 1: 1L Generation of neptunian dikes filled with wackestone with small sparite grains (lower part of the photograph) overlain by wackestone-packstone with planktonic foraminifera (Protoglobigerinids), belemnites, echinoderm fragments, filaments and occasional benthic foraminifera (middle part of the photograph). In the uppermost part the infill is calcite cement. The scale bar is 1 mm long.

Pl. 1, Fig. 2: 2L Generation of neptunian dikes filled with packstone mainly composed of filaments and encrusted intraclasts of bioclastic limestone. The scale bar is 1 mm long.

Pl. 1, Fig. 3: 2L Generation of neptunian dikes filled with packstone mainly composed of filaments and encrusted intraclasts of host rocks. The scale bar is 1 mm long.

Pl. 1, Fig. 4: 1R Generation of neptunian dikes filled with lower Berriasian fine-grained breccias. The breccia is clast-supported and composed of lithoclasts of wackestone to mudstone with echinoderm fragments, benthic foraminifera and calpionelids Calpionella elliptica (Cadisch). The scale bar is 1 mm long.

Pl. 1, Fig. 5: 2R Generation of neptunian dikes. The laminated infill in the upper part of the neptunian dikes is composed of alternatiing packstone laminae up to 5 mm thick and thinner mudstone. The scale bar is 1 mm long.

Pl. 1, Fig. 6: 2R Generation of neptunian dikes filled with Upper Cretaceous wackestone-packstone with planktonic globular foraminifera, globotruncanids and rare echinoderm fragments. The scale bar is 1 mm long.

lemnites, echinoderm fragments, filaments and rare benthic foraminifera (Pl. 1, Fig. 1). The clasts of the host rock are occasionally observed. The matrix is micrite to microsparite. On the basis of the presence of planktonic foraminifera, (Protoglobigerinids) this neptunian dike infill is Bajocian. The Bajocian infillings are in places additionally cut by younger dikes that are partly filled by a radiaxial fibrous calcite cement and micrite. The uppermost Bajocian sediments are occasionally encrusted with Fe-Mn oxides and the remaining pore space is filled by upper Tithonian mudstones with *Calpionella alpina* (Lorenz).

***II. Generation***

The II generation of neptunian dikes occurs in the Prehodavci Formation (2L Gen. in Fig. 3). The dikes are represented by sub-vertical and bed-parallel cavities up to few dm in diameter showing smooth and straight walls. In the Lower Member the neptunian dikes are filled with packstone mainly composed of filaments and encrusted intraclasts of bioclastic limestone (Pl. 1, Fig. 2). Other grains include echinoderm fragments and gastropod protoconchs. In the Upper Member of the Prehodavci Formation the infill is characterized by an Upper Kimmeridgian to Lower Tithonian packstone composed of numerous filaments, *Saccocoma* sp. fragments and intraclasts of host rock (Pl. 1, Fig. 3). In places the dikes are also filled with mudstone with calpionellids (*Calpionella alpina* (Lorenz)) of Tithonian age.

The overall geometry, smooth walls and clasts of the host rock of the I. generation of neptunian dikes indicate formation of the cavities by mechanical fracturing. However, subsequent reshaping of the existing voids by dissolution is also indicated (small scale undulation of the walls). Neptunian dikes of the II generation were formed due to mechanical fracturing of the host rock and were later episodically filled with younger sea-bottom sediments. The infilling of the dikes is represented by autochthonous and allochthonous sediments. Autochthonous sediments are clasts of the Prehodavci Formation, derived from the walls of the fracture, while all other sediments are allochthonous and derived from an active sea bottom surface.

***Neptunian dikes at Ravni Laz***

At Ravni Laz (section R1 in Fig. 3*, y* = 388997 *x* = 134741 *z* = 720), neptunian dikes occur only in the Prehodavci Formation. The neptunian dikes are subparallel to the bedding and occur in a distinct horizon within the Prehodavci Formation. On the basis of the stratigraphic position and age of infillings, two different generations of neptunian dikes were recognized.

***I. Generation***

I generation (1R.Gen. in Fig. 3) occurs in the Lower Member of the Prehodavci Formation and is filled with Kimmeridgian to lower Berriasian limestone. The geometry of the dikes is bed-crossing fractures down to 0.5 m deep, however, smaller oval cavities with undulating walls that occur in a distinct horizon are also observed. The base of these neptunian dikes is characterized by laminated and graded packstone to mudstone with abundant fragments of *Saccocoma* sp. The remaining space in the dikes is filled with graded microsparitic limestone composed of echinoderm fragments, calpionellids (*Calpionella alpina* (Lorenz)) and intraclasts of packstones with *Saccocoma* sp. In places, the neptunian dikes of the I. generation are filled only by fine-grained clast-supported carbonate breccias (Pl. 1, Fig. 4). The clasts consist of lithoclasts of mudstone to wackestone with echinoderm fragments, benthic foraminifera (*Lenticulina* sp., Textularidae) and *Calpionella elliptica* (Cadisch). Other grains include individual echinoderm fragments and Fe-Mn encrusted bioclasts.

***II. Generation***

The II generation of neptunian dikes (2R Gen. in Fig. 3) occurs in the Upper Member of the Prehodavci Formation and is filled by late Cretaceous deposits. These dikes are up to 10 cm wide bed-crossing and bed- parallel cavi-

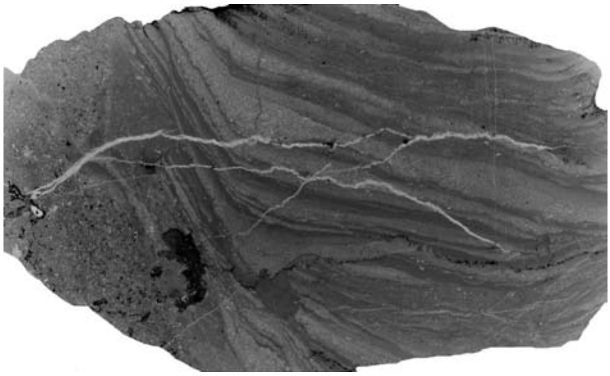

**Figure 4.** 2R Generation of neptunian dikes. On the left side of the photograph is wackestone with planktic globular foraminifera and globotruncanids. On the right side of the photograph is horizontal and oblique laminated infill represented by thicker packstone and thinner mudstone layers. The photograph is 5.5 cm wide.

ties, with undulating wall geometries in places. The dikes are filled with red-brown wackestone with planktonic globular foraminifera, globotruncanids and rare echinoderm fragments (Pl. 1, Fig. 5). In the upper part of the dike, the infilling is grey in colour, laminated and graded. Laminations are bed-parallel and oblique (Fig. 4). The laminations are represented by alternations of up to a few mm thick packstone and thinner layers of mudstone (Pl. 1, Fig. 6). In places, packstone grades into mudstone. The packstone is exclusively composed of fragmented globotruncanids and extremely rare echinoderm fragments.

The geometry of the neptunian dikes of the Ravni Laz section is characterized by bed-crossing and bed-parallel fractures, smooth walls of the host rock and also by undulating oval cavities. Thus the formation of the cavities was most probably caused by initial mechanical fracturing of the host rock and also subsequent dissolution in places, the latter causing reshaping of the existing voids. All of the different infillings of the neptunian dikes represent allochthonous sediments as is evidenced by the marked age difference of the host rock and infilling. The sedimentary structures, such as grading and lamination, are result of minor turbidity currents which episodically transported the sediment into the open voids (Sarti et al., 2000). The oblique laminations usually occur in the vicinity of the cavity walls (Figure 4) and most are probably formed as a result of the impact of minor turbidity currents with the cavity walls.

***Neptunian dikes in Triglav Lakes Valley***

Neptunian dikes in the Triglav Lakes Valley (section TV1, Figure 3, $y$ = 40755 $x$ = 134509 $z$ = 2000) are developed only in the uppermost part of the Prehodavci Formation (1T Gen. in Fig. 3) as bed-crossing fractures up to 50 cm deep and a few tens of cm wide (Figure 5), with a preferential SE – NW orientation (Pl. 2, Figs. 1 and 2). In places the neptunian dikes exhibit a jigsaw structure (Pl. 2, Figs. 1 and 2). The walls of the fractures are usually encrusted with Fe-Mn oxides. The fractures are filled with two different breccias. The first breccia consists of fragments of ammonite moulds and centimetre-sized lithoclasts of red wackestone to packstone with disarticulated valves of thin-shelled bivalves and calcified radiolarians of the red nodular facies (Pl. 2, Fig. 3). The matrix of this breccia is packstone with filaments, rare echinoderm fragments, belemnites and foraminifera (*Lenticulina* sp.) The second breccia is composed of euhedral grains of terrigenous quartz, lithoclasts of red nodular limestone, packstone with calcified radiolarian moulds and wackestone with aptychi (Pl. 2, Fig. 4). The matrix of the breccia is wackestone with echinoderm fragments, opaque minerals and Fe-Mn incrusted bioclasts.

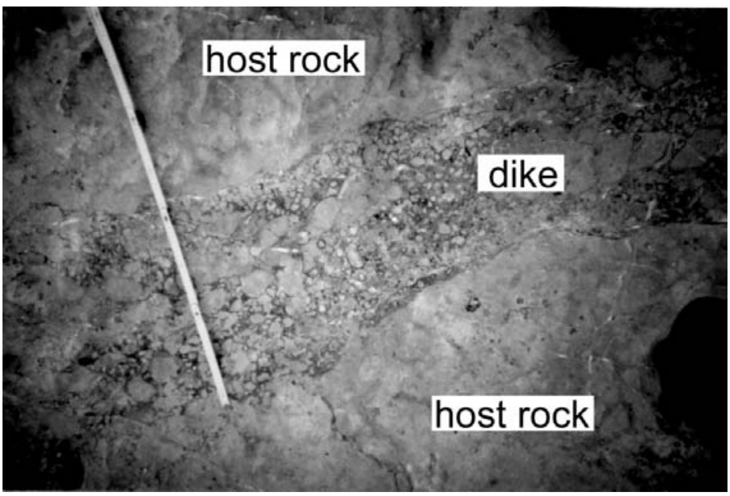


**Figure 5.** Photograph of the neptunian dike outcropping in the bed surface of the Upper Member of the Prehodavci Formation from the Triglav Lakes Valley. The photograph is approximately 1m wide

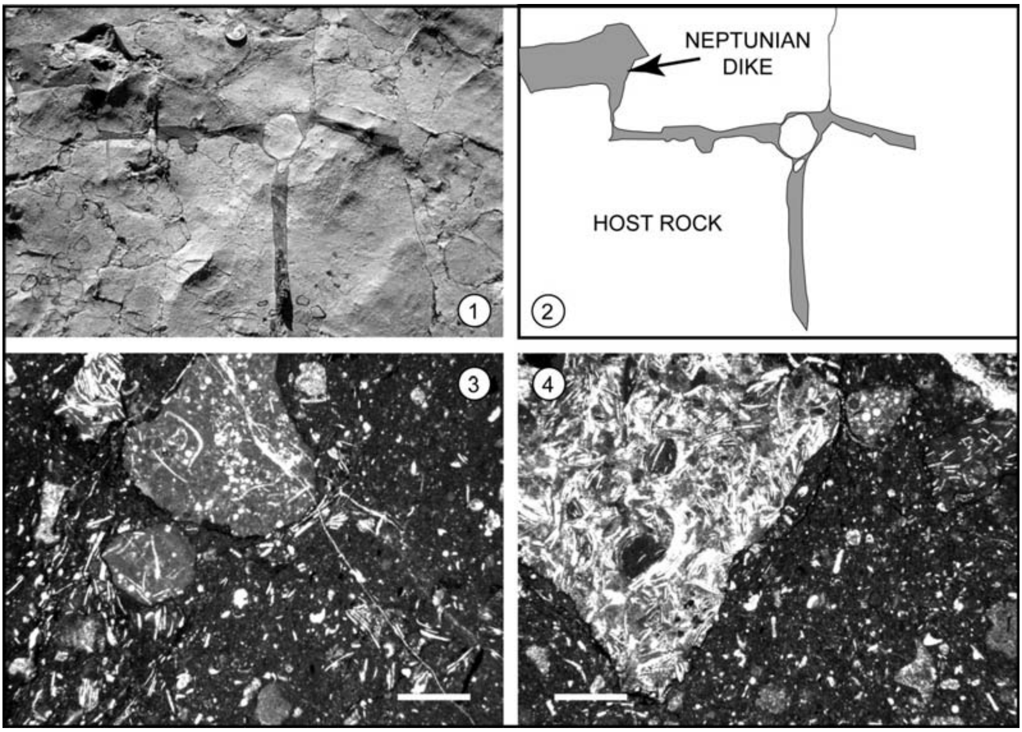


**Plate 2**
Pl. 2, Fig1: 1T Generation of neptunian dikes. Neptunian dikes with jigsaw structure. Host rock is limestone of the Prehodavci Formation.
Pl. 2, Fig. 2: Sketch of the neptunian dike in Pl. 2, Fig. 1.
Pl. 2, Fig. 3: 1T Generation of neptunian dikes. First breccia with lithoclasts of red wackestone to packstone with calcified radiolarians and filaments. The matrix of breccia is wackestone-packstone with filaments and rare echinoderm fragments.
Pl. 2, Fig. 4: 1T Generation of neptunian dikes. Second breccia composed of lithoclasts packstone with filaments and calcified radiolarian moulds and intraclasts of red nodular limestone. The matrix of the breccia is wackestone with echinoderm fragments.

The dikes are clearly open fractures formed due to a brittle fracturing of a well-lithified host rock. The jigsaw structure additionally indicates a mechanical deformation by penetrative fracturing of the host rock (Cozzi, 2000). Fe-Mn impregnated walls of the fractures indicates phases of non-deposition following fracture formation.

## Discussion

### Neptunian dike formation

The formation of the neptunian dikes in the investigated areas was the result of two different mechanisms. Neptunian dikes of I. generation of Lužnica Lake and I and II generation in Ravni Laz are bed-crossing or bed-parallel oval cavities with smooth and undulating walls and represent a group of neptunian dikes in which at least reshaping of the voids by dissolution is indicated. This reshaping by dissolution can occur by meteoric waters, indicating an episode of sub-aerial exposure and karstic dissolution or it can occur on the sea-floor. The episode of sub-aerial exposure is a valid hypothesis for the I generation of neptunian dikes in Lužnica Lake. Namely they are located in the Lower Jurassic shallow-water limestone stratigraphically under the unconformity surface separating shallow-water limestone and the Prehodavci Formation. Similar, but more intensively karstified Jurassic fractures in the Dachstein Limestones were reported by Buser (1986, 1987, 1996) and attributed to emersion during the Early Jurassic. The emersion scenario, however, is difficult to apply for the I and II generation of neptunian dikes in Ravni Laz. The dikes are located within the Prehodavci Formation that represents typical deposits of a pelagic plateau with depth of the deposition at least a few ten to hundreds of metres (Martire, 1996). The dissolution and reshaping of the voids most probably occurred on the seafloor in a phreatic marine environment. However, in both cases the initiation of the voids was probably related to mechanical fracturing.

The second group of neptunian dikes includes dikes that were formed only by a mechanical fracturing of the host rock. This group includes the II generation of neptunian dikes in the Lužnica Lake and dikes from the Triglav Lakes Valley. The dikes are bed-crossing straight fractures filled with autochthonous sediments derived from the walls of fracture. The jigsaw structure of the fractures that is present in places indicates a mechanical deformation by penetrative fracturing of the host rock (Cozzi, 2000) which is commonly the result of a seismic shock (Montenat et al., 1991, Cozzi, 2000).

### Timing of the neptunian dike formations

The detailed study of the neptunian dikes from Ravni Laz, Lužnica Lake and Triglav Lakes Valley areas revealed the following main phases of neptunian dike formation.

#### *1. Pliensbachian or Bajocian phase*

The I generation of neptunian dikes from Lužnica Lake represents the oldest investigated neptunian dikes.

They were formed in the Pliensbachian shallow-water host rock and filled with Bajocian and Tithonian deposits. These neptunian dikes are correlative with I. generation of neptunian dikes from Mt. Mangart (same host rock and mechanism of void formation) (Črne et al., 2007). Črne et al. (2007) determined that void initiation as well as infilling with sediments occurred in the Pliensbachian. The dikes from Lužnica Lake however are filled by younger strata ranging from Bajocian to Tithonian. Thus, two possible explanations exist:

A). I generation of the neptunian dikes from Lužnica Lake formed in the Pliensbachian and started to communicate with the seafloor no earlier than the Bajocian. In this case, dike formation is related to the Julian Carbonate dissection that occurred during that time (Šmuc, 2005; Šmuc & Goričan, 2005). The fragmentation of the platform caused fracturing of the host rock and differential subsidence of blocks. Some blocks were most probably emerged and this caused reshaping of the initial voids by meteoric waters. The Early Jurassic tectonic event is widely recognized across the entire south Tethyan passive margin and a great number of dikes was formed at that age (Winterer & Bosellini, 1981; Winterer et al., 1991; Bertotti, 1993; Sarti et al., 1992, Clari & Masetti, 2002).

B). another possibility is that I generation of neptunian dikes at Lužnica Lake were formed in the Bajocian. If the dikes were formed in the Bajocian, their formation was related to the Bajocian tectonic phase that caused deepening of the Julian High and the beginning of the sedimentation of the Prehodavci Formation (Šmuc, 2005). The accelerated subsidence pulse is well documented in the Southern Alps (Winterer & Bosellini, 1981; Martire, 1992, 1996; Winterer, 1998) and also in the successions of the Slovenian Basin (Rožič & Popit, 2006; Rožič, 2009)

***2) Late Kimmeridgian-Early Tithonian phase***

Neptunian dikes of this phase (II generation of dikes from Lužnica Lake and I generation of dikes from Ravni Laz and neptunian dikes from Triglav Lakes Valley) are mainly located in the Upper Member of the Prehodavci Formation. The same age – mainly Late Kimmeridian to Early Tithonian – was determined for the host rock and for the oldest dike infillings. This suggests that opening of the voids occurred soon after the deposition of the Upper Member. The dikes are filled with Kimmeridgian to Berriasian deposits. Different infillings of the dikes in different areas represent rather local lateral variations in the sedimentary environments, and most possibly also tectonic styles of deformation. Additionally, some of the voids (Lužnica Lake and Ravni Laz) exhibit relatively continuous infilling ranging from Kimmeridgian to Late Tithonian, while the dikes at Triglav Lakes Valley exhibit phases of deposition and non-deposition as proved by Fe-Mn incrustations of the walls of neptunian dikes and also of clasts of the infillings.

The Late Kimmeridgian – Early Tithonian phase of the neptunian dike formation is tentatively related to the onset of convergent plate movements in the Dinaric Tethys that caused normal faulting and differential subsidence in the external domains (DOZET, 1994; DOZET et al., 1996; VLAHOVIĆ et al., 2005).

***3) Late Cretaceous phase (pre-Senonian)***

Neptunian dikes in the Prehodavci Formation that are filled with Late Cretaceous limestone with globotruncanids are present only in the Ravni Laz section. The late Cretaceous phase is most probably related to the tectonic pulse in the Late Cretaceous, more precisely, before the Senonian.

## CONCLUSIONS

Neptunian dikes in the investigated area of the Julian High are present in the Pliensbachian shallow-water limestone and in the Prehodavci Formation. The following generations of dikes were defined.

Lužnica Lake

I. generation dikes are located in the Pliensbachian shallow-water limestone host rock and filled with Bajocian to Tithonian limestone. II generation is represented by dikes in the Prehodavci Formation that are filled by Upper Kimmeridgian to Lower Tithonian sediments.

Ravni Laz:

I. generation is represented by dikes in the Lower Member of the Prehodavci Formation filled with Kimmeridgian to Berriasian sediments. II generation of dikes is placed in the Upper Member of the Prehodavci Formation and filled with late Cretaceous deposits.

Triglav Lakes Valley

The dikes occur in the Upper Member of the Prehodavci Formation and are filled by Late Kimmeridgian and Early Tithonian breccias.

The dikes were formed by two different mechanisms; A) the initiation of the voids by mechanical fracturing and later reshaping of the voids by dissolution. The reshaping by dissolution occurred by meteoric waters indicating an episode of sub-aerial exposure and karstic dissolution (I generation of Lužnica Lake dikes) or it could have occurred on the seafloor in a phreatic marine environment (I and II generation of dikes from Ravni Laz). B) The dikes were formed only by mechanical fracturing of the host rock and in places by penetrative fracturing of the host rock as a result of seismic shock. This group includes the II generation of neptunian dikes in the Lužnica Lake and dikes from the Triglav Lakes Valley.

According to the age of the host rock and neptunian dike infillings, three main phases of neptunian dike formation in the investigated area are recognized: Pliensbachian and/or Bajocian phase, Late Kimmeridgian-Early Tithonian phase, and Late Cretaceous (pre-Senonian) phase.

## References


Aubrecht, R. (1997): Indications of the middle Jurassic emergence in the Czorsztyn unit (Pieniny Klippen belt, western Carpathians). *Geol. Carpath.*; Vol. 48, pp. 71–84.

Babić, L. (1981): The origin of ''Krn breccia'' and the role of the Krn area in the Upper Triassic and Jurassic history of the Julian Alps. *Vestnik zavoda geol.geofiz. istraživanja NR Srbije*; Vol. 38/39, pp. 59–87.

Bertotti, G., Picotti, V., Bernoulli, D. & Castellarin, A. (1993): From rifting to drifting: tectonic evolution of the South-Alpine upper crust from the Triassic to the Early Cretaceous. *Sedimentary Geology*; Vol. 86, pp. 53–76.

Bresnan, G., Snidarcig, A. & Venturini, C. (1998): Present stata of tectonic stress of the Friulli area (eastern Southern Alps). *Tectonophysics*; Vol. 292, pp. 211–227.

Buser, S. (1986): Basic Geological map of SFRJ 1:100.000, sheet Tolmin in Videm. Zvezni geološki Zavod, Beograd.

Buser, S. (1987): Explanatory note to Basic Geological Map of SFRJ 1:100.000, list Tolmin in Videm. Zvezni geološki Zavod, 103 pp., Beograd.

Buser, S. (1996): Geology of Western Slovenia and its paleogeographical evolution. In: Drobne, K., Goričan, Š. & Kotnik, B. (Eds.) International workshop Postojna 1996: The Role of Impact Processes in the Geological and Biological Evolution of Planet Earth, pp. 111–123.

Clari, P. & Masetti, D. (2002): The Trento Ridge and the Belluno Basin. In: Santantonio, M. (Ed.) General Field Trip Guidebook. VI International Symposium on the Jurassic System, 12-22 September 2002, pp. 271–315.

Cozzi, A. (2000): Synsedimentary tensional features in Upper Triassic shallow-water platform carbonates of the Carnian Prealps (northern Italy) and their importance as paleostress indicators. *Basin Res.*; Vol. 12, pp. 133–146.

Črne, A., Šmuc, A. & Skaberne, D. (2007): Jurassic neptunian dikes at Mt Mangart (Julian Alps, NW Slovenia). *Facies*; Vol. 53, pp. 249–265.

Doglioni, C. & Siorpaes C. (1990): Polyphase deformation in the Col Bechei area (Dolomites-Northeastern Italy). *Eclogae Geologicae Helvetiae*; Vol. 83, pp. 701–710.

Dozet, S. (1994): Malmian bauxites at Kočevska reka and Kočevje. *RMZ-materials and geoenvironment*; Vol. 41, pp. 215–219.

DOZET, S., MIŠIČ, M. & ZUZA, T. (1996): Malm bauxite occurences in Logatec, Nanos and Kočevje area. *RMZ - materials and geoenvironment*; Vol 43, No.1-2, pp. 23–35.

JURKOVŠEK, B. (1986): Basic Geological map of SFRJ 1:100.000, sheet Beljak in Ponteba. Zvezni geološki Zavod, Beograd.

JURKOVŠEK, B., ŠRIBAR, L., OGORELEC, B. & KOLAR-JURKOVŠEK, T. (1990): Pelagic Jurassic and Cretaceous beds in the western part of the Julian Alps. *Geologija*; Vol. 31/32, pp. 285–328.

LEHNER, B. L. (1991): Neptunian dikes along a drowned carbonate platform margin; an indication for recurrent extensional tectonic activity. *Terra Nova*; Vol. 3, pp. 593–602.

LUCZYNSKI, P. (2001): Development history of Middle Jurassic neptunian dykes in the High-Tatric series, Tatra Mountains, Poland. *Acta. Geol. Pol.*; Vol. 51, pp. 237–252.

MALLARINO, G. (2002): Neptunian dikes along submarine escarpments: examples from the Jurasic of Monte Kumeta (Sicily). *Boll. Soc. Geol. Ital.;* Vol. 121, pp. 377–390.

MARTIRE, L. (1992): Sequence stratigraphy and condensed pelagic sediments. An example from the Rosso Ammonitico Veronese, northeasters Italy. *Palaeogeography, Palaeoclimatology, Palaeoecology*; Vol. 94, pp. 169–191.

MARTIRE, L. (1996): Stratigraphy, Facies and Synsedimentary Tectonics in the Jurassic Rosso Ammonitico Veronese (Altopiano di Asiago, NE Italy). *Facies*. Vol. 35, pp. 209–236.

MARTIRE, L. & PAVIA, G. (2004): Jurassic sedimentary and tectonic processes at Montagna Grande (Trapanese domain, Western Sicily, Italy). *Rivista Italiana di Palentologia e Stratigrafia*; Vol. 110, No. 1, pp. 23–33.

MARTIRE L., PAVIA G., POCHETTINO M., & CECCA, F. (2000): The Middle-Upper Jurassic of Montagna Grande (Trapani): age, facies and depositional geometries. *Mem. Soc. Geol Ital.*; Vol. 55, pp. 219–255.

MELLERE, D., STEFANI, C. & ANGEVINE, C. (2000): Polyphase tectonics trough subsidence analysis: the Oligo-Miocene Venetian and Friulli basin, north-east Italy. *Basin research;* Vol. 12, pp. 159–182.

Montenat C., Barrier P., & Ott d'Estevou, P. (1991): Some aspects of the recent tectonics in the strati of Messina, Italy. *Tectonophysics*; Vol. 194, pp. 203–215.

PLACER, L. (1999): Contribution to the macrotectonic subdivision of the border region between Southern Alps and External Dinarides. *Ge-*

*ologija*; Vol. 41, pp. 223–255.

Placer, L. (2008): Principles of the tectonic subdivision of Slovenia. *Geologija;* Vol. 51, No. 2, pp.205–217.

Placer, L. & Čar, J. (1998): Structure of Mt. Blegoš between the Inner and Outer Dinarides. *Geologija*; Vol. 40, pp. 305–323.

Rožič, B. & Popit T. (2006): Resedimented Limestones in Middle and Upper Jurassoc Succession of the Slovenian Basin. *Geologija*, Vol. 49, N. 2, pp. 219-234.

Rožič, B. (2009): Perbla and Tolmin formations: revsied Toarcian to Tithonian stratigraphy of the Tolmin Basin (NW Slovenia) and regional correlations. *Bull. Soc. géol. Fr.*; Vol. 180, N. 5, pp. 411–430.

Sarti, M., Bosellini, A. & Winterer, E. L. (1992): Basin Geometry and Architecture of a Tethyan Passive Margin, Southern Alps. *AAPG Memoir*; Vol. 53, pp. 241–258.

Sarti, M., Winterer EL., & Luciani, V. (2000); Repeated gravity-controled fracturing and dilation of Jurassic limestone over 130 m.y. and filling by episodic microturbidity currents in Cretaceous and Paleogene sediments (Taormina, Sicily). *Mem. Soc. Geol Ital.*Vol. 55, pp. 251–260.

Stampfli, G. M., Mosar, J., Favre, P., Pillevuit, A. & Vannay, J. C. (2001): Permo_mesozoic evolution of the western Tethys realm: the Neo-Tethys East Mediterranean Basin Conenction. In: Ziegler, P. A., Cavazza, E., Robertson, A. H. F. & Crasquin-Soleau, S. (Eds) Peri Tethys Memoir 6: Pery-Tethyan Rift/Wrench Basins and passive Margins. *Memoires du Museum national d'historie naturelle* ; Vol.186, pp. 51–108.

Šmuc, A. 2005: Jurassic and Cretaceous stratigraphy and sedimentary evolution of the Julian Alps, Slovenia. Založba ZRC; 98 p.

Šmuc, A. & Goričan, Š. (2005): Jurassic sedimentary evolution from carbonate platform to deep-water basin: a succession at Mt Mangart (Slovenian-Italian border). *Rivista Italiana di Paleontologia e Stratigrafia*; Vol. 111, No. 2, pp. 45–70.

Vlahović, I., Tišljar, J. Velić, I. & Matičec, D. (2005): Evolution of the Adriatic Carbonate Platform: Palaeogeography, main events and depositional dynamics. *Palaeogeography, Palaeoclimatology, Palaeoecology;* Vol. 220, pp. 333–360.

Vrabec, M. & Fodor, L. (2006): Late Cenozoic Tectonics of Slovenia: Structural styles at the Northeastern Corner of the Adriatic Microplate. In: Pinter, N., Grenerczy, G., Weber, J., Stein, S., Medak, D. (Eds), *The Adria Microplate: GPS Geodesy, Tectonics and Hazards*, pp. 151–168.

Winterer, E. L. & Bosellini, A. (1981): Subsidence and sedimentation on Jurassic Passive Continetal Margin, Southern Alps, Italy. *AAPG Bulletin*; Vol. 65, pp. 394–421.

Winterer, E. L., Metzler, C. V. & Sarti, M. (1991): Neptunian dikes and associated breccias (Southern Alps, Italy and Switzerland): role of gravity sliding in open and closed systems. *Sedimentology*; Vol. 38, pp. 381–404.

Winterer, E. L. (1998): Paleobathymetry of Mediteranean Tethyan Jurassic pelagic sediments. *Memorie della Societa Geologica Italiana*; Vol. 53, pp. 97–131.

# Revision of coal reserves and placement of exploitation fields in exploitation of the lignite deposit in Premogovnik Velenje

# Revizija rezerv premoga in umeščanje odkopnih polj pri eksploataciji ležišča lignita v Premogovniku Velenje

Milan Medved[1,] *, Bojan Lajlar[1], Vladimir Malenković[2], Evgen Dervarič[3]

[1]Premogovnik Velenje, d. d., Partizanska 78, SI-3320 Velenje, Slovenia
[2]HTZ, I. P., d. o. o., Partizanska 78, 3320 Velenje, Slovenia
[3]University of Ljubljana, Faculty of Natural Sciences and Engineering, Aškerčeva 12, SI-1000 Ljubljana, Slovenia

*Corresponding author. E-mail: milan.medved@rlv.si

**Received:** March 30, 2010 **Accepted:** May 25, 2010

**Abstract:** Coal (brown coal and lignite) is the only fossil fuel available in Slovenia, representing approximately 21 % of primary energy consumption. Due to environmental reasons, the use of coal is directed only to thermal energy generating facilities with appropriate flue gas cleaning technologies.

Premogovnik Velenje (PV) is a modern equipped and highly productive coal mine providing lignite exclusively to Termoelektrarna Šoštanj for its production of electricity and thermal energy. PV exploits a deposit of exceptional dimensions in which they developed their own, highly productive exploitation method with underground production and can compete, in productivity and coal prices, with the world's best underground coal mines. The quantities of domestic production of coal cover 78.0 % of all planned demands for solid fuels.

In the Šaleška dolina valley, the balance sheet reserves of coal in coal deposit in PV amount to 171 million tonne on 31st December 2008 and 131,67 million tonne of exploitation reserves with average calorific value of 10.47 GJ/t. Projections for further production of coal are related to long-term operation of the Šoštanj Thermal Power Plant (TEŠ) which will invest in the 600 MW generator unit 6. PV is the only supplier of coal for TEŠ. Until the year 2021, the level

*Original scientific paper*

of production of coal will amount to 4 million tonne per year. In the period until the year 2040, it will gradually decrease to the level of 2 million tonne per year and will remain at this level until the end of exploitation of the Velenje exploitation field in the year 2054.

**Izvleček:** Premog (rjavi premog in lignit) je edino fosilno gorivo, ki je na razpolago v Sloveniji in pomeni približno 21 % rabe primarne energije. Zaradi okoljskih razlogov je uporaba premoga usmerjena le na termoenergetske objekte, ki imajo ustrezne tehnologije čiščenja dimnih plinov.

Premogovnik Velenje (PV) je moderno opremljen in visoko produktiven premogovnik, ki lignit dobavlja izključno Termoelektrarni Šoštanj za proizvodnjo električne energije in toplote. PV izkorišča nahajališče izjemnih dimenzij, v katerem je razvil lastno, visoko produktivno odkopno metodo s podzemno proizvodnjo, ki se po produktivnosti in ceni premoga kosa z najboljšimi podzemnimi premogovniki v svetu. Količina domače proizvodnje premoga zadostuje za 78,0 % vseh načrtovanih potreb po trdnih gorivih.

V Šaleški dolini ležišče premoga v PV je na dan 31. 12. 2008 razpolagalo s 171 milijoni ton bilančnih zalog, od tega je 131,67 milijona ton eksploatacijskih zalog s povprečno kurilno vrednostjo 10,47 GJ/t. Projekcije za nadaljnjo proizvodnjo premoga so vezane na dolgoročno obratovanje Termoelektrarne Šoštanj (TEŠ), ki bo izvedla investicijo v blok 6 moči 600 MW. PV je edini dobavitelj premoga za TEŠ. Velikost proizvodnje premoga bo do leta 2021 4 milijone ton na leto, do leta 2040 bo postopno upadala do 2 milijona ton na leto in se na tem nivoju obdržala do konca eksploatacije velenjskega odkopnega polja v letu 2054.

**Key words:** coal, exploitation reserves, exploitation filed, exploitation losses

**Ključne besede:** premog, eksploatacijske rezerve, odkopno polje, odkopne izgube

## INTRODUCTION

Long-term plans of Premogovnik Velenje are closely connected to electricity generation in the thermal power plant Termoelektrarna Šoštanj. Exploitation of coal in PV is carried out in three mines or areas divided to the mine Pesje, and the mine Preloge which is divided to south and north wing. In the mines Pesje and Preloge, the exploitation is carried out at long-wall exploitation sites measuring 130 m to 160 m with exploitation height of 10 m or more, and in the north part of the mine Preloge, the dimension of exploitation floors exceed long-wall lengths of 200 m or more, but the exploitation height is, in accordance with the criteria for safe exploitation, limited to 6 m. With the export report: »Revision of coal reserves in Premogovnik Velenje based on conceptual solutions until the finalisation of exploitation in the Velenje exploitation field«, the reserves of coal in individual exploitation fields and their development until the finalisation of exploitation in the Velenje exploitation field were verified at the Faculty of Natural Sciences and Engineering in Ljubljana. The purpose of this article is to present basic reference points for exploitation of coal until the year 2054, i.e. until the time when all reserves in this field will have been exploited.

## Geological and hydrogeological conditions in the deposit

Geological and hydrogeological conditions in the deposit were well researched in the past. All findings of the geological and hydrogeological research were taken into consideration in the elaboration of conceptual solutions for the excavation presented in the continuation of the text.

### *Geology*

Geologic data was acquired by research work (drilling) performed both on the surface and in the mine and by monitoring of the constructed lines. 705 bores were drilled from the surface, in the total length of 205 km. 2265 bores were drilled from the mine facilities, with the total length of approximately 90 km.

The acquired data give an excellent image of the entire coal deposit (coal layer, footline layers, hanging wall layers) Based on these data, conceptual solutions have been elaborated to enable precise calculations of the amounts of coal exploited in the future according to the processed conceptual solutions.

### *Hydrogeology*

Hydrogeological research of the layer, footline and hanging wall layers, carried out in the previous period, gave all hydrologic factors that have to be considered for safe exploitation. Based on analyses of this data, the drainage measures were adopted (drainage of sands in the hanging wall, drainage of the Triassic base, drainage of lithothamnium limestone) to establish conditions for exploitation on the entire coal layer in the mine Velenje.

### *Drainage of first sands above the coal layer*

In the last three decades, there was intensive draining of Pliocene sands in the hanging wall by drainage facilities both from the surface and from the mine. In the wider area of the north wing and the central part, water pressures were lowered by more than 20 bar, so for further exploitation it was only necessary to maintain the existing status by constructing impress filters from the mine facilities.

***Drainage of the Triassic base***

Triassic stones representing the base in the area of the north wing and in the mine Škale, have been in the last few decades intensively drained by drainage facilities constructed from the mine (the upper height points of the Triassic base are shown in Annex No. 3).

The underground water levels have been lowered by more than 300 m. The current situation of groundwater levels is shown in Annex No. 4 and provides safe exploitation of the entire coal layer in the area of the mine Velenje. It is understandable that such situation will have to be maintained and monitored until the finalisation of the exploitation.

**Excavation technology and permitted excavation heights**

The excavation of the layer covered in the conceptual solutions will be performed with the Velenje long-wall exploitation method described in the mining project »Velenje exploitation method«, project No.: RP-36/95 ML, Rudnik lignita Velenje. The method is still being developed and improved in the technological and organisational point of view, particularly in the sense of increasing production from one excavation, increasing the efficiency rate of a layer, employee safety, humanisation of work and better economy.

**Conceptual solutions to excavation**

In Premogovnik Velenje, coal production is currently running in two mines, i.e.:

- in the mine Pesje and
- in the mine Preloge (south and north wing).

Permits for execution of works in these areas were acquired on the basis of the following mining projects:

- »Supplementing of the concept of exploitation of the north-western section of the mine Preloge«, RP-183/2000 ML,
- »Preparation and exploitation of the panel G1/A«, RP-205/2001ML,
- »Continuation of excavation in the mine Pesje from k. +40 to k. –40«, RP-13/91,
- »Continuation of exploitation in the south wing of the mine Preloge until the finalisation of exploitation«, RP-54/91.

The above listed conceptual solutions covered the production of PV until the year 2025.

With the purpose of prolonging the production of coal at PV, they initiated a search for conceptual solutions for the continuation of exploitation in the existing mines (the hanging wall section and the footwall section of the mine Pesje, the north wing of the mine Preloge) and for opening a new part of the mine Preloge called CD pillar. In March 2007, the mining project »Exploitation of the mine Pesje from k. –40 to the depression bottom and CD pillar«, project No.: RP-325/007TK, was prepared, followed by the expert report »Exploitation of the north wing of the mine Preloge«, expert report No.: TK002/07, in June 2007.

Coal for further production of PV is still available in the remaining pillars and in the areas where excavation was abandoned in the past.

**Delimitation of mines of Premogovnik Velenje**

With the decision on exploitation of the pillar between the north and the south wing of the mine Preloge, the needs emerged for denomination of the pillar and reasonable separation of the mine Preloge. It should be noted that the delimitation has been elaborated at the level of the first floor of CD pillar. The area is wider in the depth and it extends to the exploited part of the south wing of the mine Preloge in the south and to the exploited part of the north wing of the mine Preloge in the north.

The mine Pesje is spreading westward where significantly different conditions for coal exploitation appear compared to the existing area, so it was divided in the footwall section and the hanging wall section. It should be noted that the delimitation has been elaborated at the level of the floor k. –50 in the mine Pesje.

**Basic reference points and considered principles in the search of conceptual solutions for the preparation and exploitation in the mines of Premogovnik Velenje**

***The mine Pesje* – Footwall section**

In searching for technical solutions for the preparation and exploitation of this area, the following limitations and requirements were taken into consideration:

- limitations of the exploitation field: on the eastern side the exploitation field is limited by the border of quality coal, on the southern side the exploitation field is limited by the pillar protecting the facilities on the surface, on the northern side the area is limited by the exploited floors of the former north wing of the mine Preloge, and on the western side the area enters the hanging wall section of the mine Pesje,
- the area is exploited in the direction from north-east to south-west, with the excavations following from

footline to hanging wall (from east to west),
- the floor height in the footline section of the mine Pesje amounts to 15 m,
- the footline section of the mine Pesje is ventilated with fresh air from entrance ventilation network of the NOP shaft over the conveyance line to the excavation site and over the delivery line into the exit ventilation network of the ventilation shaft Pesje,
- in the footline section of the mine Pesje, there is no simultaneous operation of several excavations,
- a pillar between two excavation panels on a floor amounts to 15 m and is acquired at the next floor,
- the width of excavation panels is up to 140 m,
- the length of remaining conveyance line after excavation is at least 80 m (currently necessary length for the dismantling of conveyance machinery),
- the conveyance line is at the hanging wall side,
- the existing mine facilities are used to the greatest extent.

***The mine Pesje - Hanging wall section***

From the geological and hydrogeological point of view, the hanging wall section of the mine Pesje is very similar to the area of north wing of the mine Preloge. The following requirements arise from the mining project »Velenje exploitation method«, project No. RP-36/95 ML and from the mining project »Supplementing of the concept of exploitation of the north-western and central section of the mine Preloge«, project No. RP-183/2000 ML:

- the placement of exploitation panels in the coal layer must ensure that the crumbling process in the areas with smaller thickness of isolation layers is entirely carried out in coal,
- the coal remaining above the first exploitation panel (where the crumbling process took place) must not remain uncrumbled in must not be exploited on the following floors,
- intermediate pillars between the exploitation panels are not permitted and are collected with the blind section of the excavation,
- all passages in excavation must be gradual.

Considering the above mentioned aspects, the following limitations and requirements were taken into consideration while searching for technical solutions for the preparation and exploitation of this area:

- limitations of the exploitation field: in the east the area is limited by the hanging wall section of the mine Pesje, on the south-eastern side the exploitation field is limited by the

pillar protecting main connections for the area in question and the mine Preloge, on the western side the area enters the north wing of the mine Preloge, on the north-eastern side the area is limited by excavated floors of the former north-eastern wing of the mine Preloge,
- the area is exploited in the direction from north-east to south-west, with the excavations following from west to east,
- the hanging wall section of the mine Pesje will be exploited as follows: in the area where the isolation layer is thinner than 15 m, coal will only be exploited from the footline section, and in the area where the isolation layer is thicker than 15 m, coal will be exploited from the hanging wall section as well; in such events, a gradual transition from footline exploitation to hanging wall exploitation will be necessary,
- planned excavation height of the exploitation panels in the hanging wall section of the mine Pesje is 8–10 m. Planned excavation height of the substratum will be 6 m,
- the hanging wall section of the mine Pesje is ventilated with fresh air from entrance ventilation network of the NOP shaft over the conveyance line to the excavation site and over the delivery line of the excavation site into the exit ventilation network of the ventilation shaft Šoštanj,
- in the footline section of the mine Pesje, there is no simultaneous operation of several excavations,
- a pillar between two excavation panels in the area in question amounts to 20 m and is acquired from the blind area at the conveyance side of the excavation,
- the width of excavation panels is up to 150 m,
- the length of remaining conveyance line after excavation is at least 80 m (currently necessary length for the dismantling of conveyance machinery),
- the conveyance line is on the eastern side,
- the existing mine facilities are used to the greatest extent.

In the mine Pesje, simultaneous operation of two exploitation panels is planned (one in the hanging wall section and one in the footline section), according to the system A-F, B-E and C-D. The exploitation sites C and D start excavation works in a 3-month interval.

***The Mine Preloge - CD pillar***

From the geological and hydrogeological point of view, the area of CD pillar is very similar to the area of north wing of the mine Preloge. Similar requirements to those in the hanging wall section of the mine Pesje were taken in consideration here. Other limitations and requirements are the following:

- limitations of the exploitation field: on the eastern side the area is limited by the protective pillar for exploitation panels of the hanging wall section of the mine Pesje, on the southern side the exploitation field extends to the south wing of the mine of Preloge, on the western side the area is limited by the facilities protecting the main mine pumping site at k. –130, and on the northern side the area enters the G panels of the north wing of the mine Preloge,
- the area is exploited in the direction from east to west, with the excavations following from north to south,
- in the area where the isolation layer is thinner than 15 m, coal will only be exploited from the footline section, and in the area where the isolation layer is thicker than 15 m, coal will be exploited from the hanging wall section as well. In such events, a gradual transition from footline exploitation to hanging wall exploitation will be necessary,
- planned excavation height of the exploitation panels in the hanging wall section of CD pillar is 8–10 m (in the section where the superstratum is exploited). Planned excavation height of the substratum will be 6 m.
- excavations in CD pillar are ventilated with fresh air from entrance ventilation network of the entrance ventilation shaft Šoštanj II over the delivery line to the excavation site and over the conveyance line into the exit ventilation network of the ventilation shaft Šoštanj,
- there is no simultaneous operation of several excavations in CD pillar,
- a pillar between two excavation panels on a floor amounts to 20 m and is acquired from the blind area at the conveyance side of the excavation,
- the width of excavation panels is up to 215 m,
- the length of remaining conveyance line after excavation is at least 80 m,
- the conveyance line is on the southern side,
- the existing mine facilities are used to the greatest extent.

***North wing***

The following requirements arise from the mining project »Velenje exploitation method«, project No. RP-36/95 ML and from the mining project »Supplementing of the concept of exploitation of the north-western and central section of the mine Preloge«, project No. RP-183/2000 ML and must be taken into consideration while planning the excavation in this area:

- the placement of exploitation panels in the coal layer must ensure

that the crumbling process in the areas with smaller thickness of isolation layers is entirely carried out in coal,
- the coal remaining above the first exploitation panel (where the crumbling process took place) must not remain uncrumbled in must not be exploited on the following panels,
- intermediate pillars between the exploitation panels are not permitted and are collected with the blind section of the excavation,
- all passages in excavation must be gradual.

Considering the above mentioned aspects, the following limitations and requirements were taken into consideration while searching for technical solutions for the preparation and exploitation of this area:
- limitations of the exploitation field: on the eastern side the exploitation field is limited by the hanging wall section of the mine Pesje, on the southern side the exploitation field is limited by the pillar protecting the main communications for the north wing of the mine Preloge, on the northern side the area is limited by the border of quality coal and by an area with thin isolation layer in the hanging wall, and on the western side the area is limited by the border of quality coal,
- the area is exploited in the direction from north to south, with the excavations following from footline to hanging wall (from west to east),
- the floor height in the north wing of the mine Preloge amounts to 9 m,
- the north wing of the mine Preloge is ventilated with fresh air from entrance ventilation network of the entrance ventilation shaft Šoštanj II over the delivery line to the excavation site and into the exit ventilation network of the ventilation shaft Šoštanjin the north wing of the mine Preloge, there is no simultaneous operation of several excavations,
- a pillar between two excavation panels on a floor amounts to 20 m and is acquired from the blind area at the conveyance side of the excavation,
- the length of remaining conveyance line after excavation is at least 80 m,
- the existing mine facilities are used to the greatest extent.

Exploitation of G area will be performed according to the Velenje exploitation method (mining project »Velenje exploitation method«, project No.: RP-36/95 ML). On all panels of G area, the exploitation will be carried out by excavation of coal from the substratum of the exploitation site.

Permitted exploitation heights in the north wing of the mine Preloge have been determined on the basis of the expert report »Hydrogeological basis for exploitation of the mine Preloge and CD pillar« (expert report No.: 01/07-HGS) and amount to 6 m, while floor heights amount to 9 m.

***South wing***

From the geological and hydrogeological point of view, the south wing of the mine Preloge is not a demanding area for exploitation. In searching for technical solutions for the preparation and exploitation of this area, the following limitations and requirements were taken into consideration:

- limitations of the exploitation field: on the eastern side the exploitation field is limited by the pillars protecting the main communications for the north wing of the mine Preloge, on the southern side the exploitation field is limited by the pillar protecting the facilities on the surface and by the border of quality coal, on the northern side the area is limited by the pillar protecting the main ventilation facilities of the ventilation network of the ventilation shaft Šoštanj, and on the western side the area is limited by the pillar protecting the facilities of the ventilation network of the ventilation shaft Šoštanj.
- the area is exploited in the direction from west to east, with the excavations following from footline to hanging wall (from south to north),
- the floor height in the south wing of the mine Preloge amounts to 10 m,
- the south wing of the mine Preloge is ventilated with fresh air from entrance ventilation network of the shaft NOP over the conveyance line to the excavation site and into the exit ventilation network of the ventilation shaft Šoštanj,
- in the south wing of the mine Preloge, there is no simultaneous operation of several excavations,
- a pillar between two excavation panels on a floor amounts to 20 m and is acquired at the next floor,
- the length of remaining conveyance line after excavation is at least 80 m,
- the existing mine facilities are used to the greatest extent.

**Temporal integration of excavation in the relevant area**

The exploitation fields in Premogovnik Velenje are mutually approaching, which causes an increase of their mutual influence dictating reasonable integration of individual exploitation fields and individual exploitation panels to achieve the necessary production dynamics.

Exploitation of coal in the south wing of the mine Preloge will continue in the current manner to the depression bottom - presumably to the floor k. –140.

Roadways of the exploitation panel on the floor k. –140 will be used as connections for CD pillar and the north wing of the mine Preloge from the floor G3 on. It will be exploited after finalised exploitation of the mentioned areas.

The exploitation field CD pillar will be included in the production after finalised exploitation in the south wing of the mine Preloge and after finalised exploitation of the third level of G panels in the north wing of the mine Preloge. Three more levels of CD pillar will be exploited, followed by the exploitation of the G area where three further levels will be exploited. The exploitation will continue in the same sense to the bottom of the coal layer in both areas.

The integration of exploitation panels in the mine Pesje will be carried out depending on the advancement of exploitation of G area. The contact between the G area and the mine Pesje is situated in the area with thinner isolation layers. In order to preserve them intact, the deepening of the mine Pesje in this area must follow the deepening of the G area in a timely manner.

## Spatial integration of exploitation of the treated areas

### *Spatial integration of the south wing of the mine Preloge*

Exploitation of the south wing of the mine Preloge will continue to the depression bottom (presumably to the fl. –140). Roadways to the excavation sites will be connected to the existing main lines.

Roadways of the exploitation panel k. –140 will be used as connections for the exploitation of CD pillar and the north wing of the mine Preloge. According to valid concepts, it will be exploited after finalised exploitation of the mentioned areas.

### *Spatial integration of the north wing of the mine Preloge*

Exploitation of the north wing of the mine Preloge will be continued to the exploitation site G3/C. Due to demanding dynamics of excavation, this exploitation must be included in the production process after the exploitation site F k. –65 which will represent the first exploitation of the hanging wall section of the mine Pesje and will demolish the existing connections for the G area. They will be replaced by the above mentioned roadways of the exploitation site k. –140 and new connections of the hanging wall section of the mine Pesje.

After the third level of G panels, three level of CD pillar will be exploited, followed by the preparations for the fourth level of CD pillar which will serve as a connection for the remaining levels of the G area.

***Spatial integration of the mine Pesje from k. –40 on***

With the existing main lines in the mine Pesje, it will be possible to connect to the exploitation panels of the floor k. –50 and exploitation panels A and B on the floor k. –65. For the connection of other exploitation sites in the mine Pesje, a construction of new main lines will be necessary.

***Spatial integration of CD pillar***

The beginning of exploitation of CD pillar is planned for the year 2012. Until then, the exploitation in the mine Pesje will take place on the floor k. –65, spreading to the hanging wall section of the mine Pesje. The exploitation panel F k. –65 will demolish the main connections for the G area. For these reasons, new main communications for the G area and CD pillar will be constructed and will, after finalised excavations in the mentioned area, serve as roadways for the exploitation site k. –140.

The spatial integration of Velenje coal mine exploitation area is shown on Figure 1.

**Excavation parameters**

The parameters for preparation and exploitation for the panels exploited with the currently known technology are shown below. The technology may change in the future, which will influence the preparation and exploitation of the panels, also in the sense of a better efficiency rate of the layer.

***The mine Pesje***

Parameters for excavation of exploitation panels at floors k. –50, k. –65 and k. –80 in the mine Pesje are shown in Tables 1 to 3.

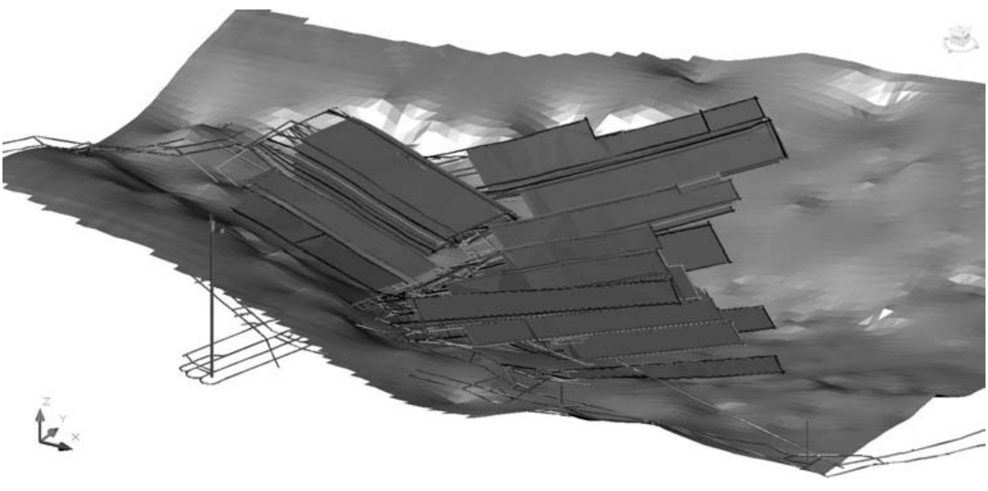

**Figure 1.** Velenje coal mine exploitation fields

**Table 1.** Parameters at excavation of floor level k. –50

| ET. k. –50 | | A k. –50 | B k. –50 | C k. –50 | Total |
|---|---|---|---|---|---|
| Excavation panel length | m | 434 | 670 | 680 | **1 784** |
| Excavation panel width | m | 140 | 140 | 140 | **420** |
| Total roadways | m | 2 298 | 1 130 | 1 664 | **5 092** |
| Advacement of development works | m/d | 5.0 | 5.0 | 5.0 | |
| Production of development works | t | 59 748 | 29 380 | 43 264 | **132 392** |
| Advancement of excavation panel | m/d | 4.2 | 3.3 | 4.6 | |
| Production of excavation panel | t | 1 088 589 | 1 696 324 | 1 565 678 | **4 350 591** |
| Length of transport routes | m | 1 670 | 1 550 | 1 430 | |
| Length of demolished roadways | m | 310 | 525 | 321 | |
| Calorific value | MJ/kg | 9.36 | 10.85 | 11.76 | |
| Energy from excavation panels | GJ | 10 189 193 | 18 405 115 | 18 412 373 | **47 006 682** |
| **Total energy** | | | | | **48 447 566** |

**Table 2.** Parameters at excavation of floor k. –65

| ET. k. –65 | | A k. –65 | B k. –65 | C k. –65 | D k. –65 | E k. –65 | F k. –65 | Total |
|---|---|---|---|---|---|---|---|---|
| Excavation panel length | m | 433 | 678 | 670 | 614 | 427 | 440 | 3 262 |
| Excavation panel width | m | 131 | 131 | 131 | 134 | 118 | 147 | 792 |
| Total roadways | m | 2 250 | 1 133 | 1 770 | 1 775 | 1 360 | 2 580 | 10 868 |
| Advacement of development works | m/d | 5.0 | 5.0 | 5.0 | 5.0 | 5.0 | 5.0 | |
| Production of development works | T | 58 500 | 29 458 | 46 020 | 46 150 | 35 360 | 67 080 | 282 568 |
| Advancement of excavation panel | m/d | 4.6 | 4.6 | 3.3 | 3.3 | 6.0 | 4.8 | |
| Production of excavation panel | t | 977 200 | 1 606 021 | 1 565 957 | 1 272 004 | 437 474 | 548 787 | 6 407 443 |
| Length of transport routes | m | 1 635 | 1 530 | 1 400 | 1 570 | 1 640 | 1 840 | |
| Length of demolished roadways | m | 440 | 450 | 257 | 386 | 380 | 150 | 72 210 077 |
| Calorific value | MJ/kg | 9.50 | 10.85 | 11.71 | 12.02 | 12.09 | 12.00 | |
| Energy from excavation panels | GJ | 9 283 400 | 17 425 328 | 18 337 356 | 15 289 488 | 5 289 061 | 6 585 444 | |
| Total energy | | | | | | | | 75 413 909 |

**Table 3.** Parameters at excavation of floor k. –80

| ET. k. –80 | | A k. –80 | B k. –80 | C k. –80 | D k. –80 | E k. –80 | F k. –80 | Total |
|---|---|---|---|---|---|---|---|---|
| Excavation panel length | m | 358 | 681 | 742 | 590 | 410 | 397 | 3 178 |
| Excavation panel width | m | 130 | 130 | 130 | 135 | 140 | 134 | 799 |
| Total roadways | m | 2 240 | 983 | 1 935 | 1 730 | 1 340 | 1 160 | 9 388 |
| Advacement of development works | m/d | 6.0 | 6.0 | 6.0 | 6.0 | 6.0 | 6.0 | |
| Production of development works | T | 58 240 | 25 558 | 50 310 | 44 980 | 34 840 | 30 160 | 244 088 |
| Advancement of excavation panel | m/d | 3.5 | 3.7 | 3.1 | 3.4 | 5.2 | 5.0 | |
| Production of excavation panel | t | 935 622 | 1 834 813 | 1 968 334 | 1 178 527 | 476 890 | 551 022 | 6 945 208 |
| Length of transport routes | m | 1 645 | 1 570 | 1 440 | 1 600 | 1 680 | 1 850 | |
| Length of demolished roadways | m | 330 | 420 | 260 | 380 | 380 | 190 | 76 794 319 |
| Calorific value | MJ/kg | 9.06 | 10.57 | 11.46 | 11.94 | 12.02 | 11.91 | |
| Energy from excavation panels | GJ | 8 476 735 | 19 393 973 | 22 557 108 | 14 071 612 | 5 732 218 | 6 562 672 | |
| Total energy | | | | | | | | 79 513 100 |

Parameters at exploitation of the entire area of the mine Pesje from k. –40 to the depression bottom:

- planned production 48 037 315 tonne
- average calorific value of coal 9.8 GJ per tonne
- planned production of energy 470 765 687 GJ
- required length of constructed lines 60 800 m
- planned production of appliances 1 580 800 tonne
- norm for construction of lines 1.22 m per 1000 tonne

***CD pillar in the mine Preloge***

Parameters for excavation of exploitation panels at the first three levels of CD pillar in the mine Preloge are shown in Table 4:

**Table 4.** Parameters for excavation of the first three levels of CD pillar

<table>
<tr><th colspan="2">CD1-3</th><th>CD1</th><th>CD2</th><th>CD3/a</th><th>CD3/b</th><th>Total</th></tr>
<tr><td>Excavation panel length</td><td>m</td><td>677</td><td>658</td><td>635</td><td>635</td><td>2 605</td></tr>
<tr><td>Excavation panel width</td><td>m</td><td>190</td><td>222</td><td>112</td><td>120</td><td>644</td></tr>
<tr><td>Total roadways</td><td>m</td><td>4 780</td><td>2 005</td><td>1 880</td><td>1 620</td><td>10 285</td></tr>
<tr><td>Advacement of development works</td><td>m/d</td><td>5.0</td><td>5.0</td><td>5.0</td><td>5.0</td><td></td></tr>
<tr><td>Production of development works</td><td>T</td><td>124 280</td><td>52 130</td><td>48 880</td><td>42 120</td><td>267 410</td></tr>
<tr><td>Advancement of excavation panel</td><td>m/d</td><td>3.0</td><td>3.9</td><td>4.0</td><td>5.0</td><td></td></tr>
<tr><td>Production of excavation panel</td><td>t</td><td>1 458 664</td><td>1 252 237</td><td>743 133</td><td>796 214</td><td>4 250 248</td></tr>
<tr><td>Length of transport routes</td><td>m</td><td>3 150</td><td>3 150</td><td>3 100</td><td>3 020</td><td rowspan="4">50 368 923</td></tr>
<tr><td>Length of demolished roadways</td><td>m</td><td>185</td><td>210</td><td>250</td><td>250</td></tr>
<tr><td>Calorific value</td><td>MJ/kg</td><td>12.00</td><td>11.89</td><td>11.60</td><td>11.75</td></tr>
<tr><td>Energy from excavation panels</td><td>GJ</td><td>17 503 968</td><td>14 889 098</td><td>8 620 343</td><td>9 355 515</td></tr>
<tr><td colspan="6">Total energy</td><td>53 538 425</td></tr>
</table>

Parameters at exploitation of the entire area of CD pillar:

- planned production 13 808 321 tonne
- average calorific value of coal 10.35 GJ per tonne
- planned production of energy 142 916 122 GJ
- required length of constructed lines 25 640 m
- planned production of appliances 666 640 tonne
- norm for construction of lines 1.77 m/ per1000 tonne

***South wing of the mine Preloge***

Parameters for excavation of exploitation panels of the south wing of the mine Preloge are shown in Table 5:

**Table 5.** Parameters for excavation of the south wing of the mine Preloge

| Preloge | | A k. –120 | B k. –120 | A k. –130 | B k. –130 | Total |
|---|---|---|---|---|---|---|
| Excavation panel length | m | 686 | 732 | 690 | 700 | 2 808 |
| Excavation panel width | m | 103 | 136 | 104 | 92 | 435 |
| Total roadways | m | 1 774 | 2 090 | 1 900 | 1 780 | 7 544 |
| Advacement of development works | m/d | 5.0 | 5.0 | 5.0 | 5.0 | |
| Production of development works | T | 46 124 | 54 340 | 49 400 | 46 280 | 196 144 |
| Advancement of excavation panel | m/d | 5.0 | 3.9 | 4.0 | 5.0 | |
| Production of excavation panel | t | 986 840 | 1 373 985 | 1 115 774 | 953 989 | 4 430 588 |
| Length of transport routes | m | 1 250 | 1 125 | 1 050 | 980 | 41 654 947 |
| Length of demolished roadways | m | 250 | 450 | 290 | 390 | |
| Calorific value | MJ/kg | 8.74 | 10.41 | 8.55 | 9.63 | |
| Energy from excavation panels | GJ | 8 624 982 | 14 303 184 | 9 539 868 | 9 186 914 | |
| Total energy | | | | | | 43 511 687 |

Parameters at exploitation of the entire area of the south wing of the mine Preloge:

- planned production 4 446 362 tonne
- average calorific value of coal 10.63 GJ per tonne
- planned production of energy 47 264 828 GJ
- required length of constructed lines 7 544 m
- planned production of appliances 196 144 ton
- norm for construction of lines 1.70 m per 1000 tonne

***North wing of the mine Preloge***

Parameters for excavation of exploitation panels at floors G3, G4 and G5 in the north wing of the mine Preloge are shown in Tables 6 to 8:

**Table 6.** Parameters for excavation of exploitation panels at floor G3 in the north wing of the mine Preloge

<table>
<tr><td colspan="2">ET. G3</td><td>G3/A</td><td>G3/B</td><td>G3/C</td><td>Total</td></tr>
<tr><td>Excavation panel length</td><td>m</td><td>294</td><td>792</td><td>713</td><td>1 799</td></tr>
<tr><td>Excavation panel width</td><td>m</td><td>157</td><td>149</td><td>195</td><td>501</td></tr>
<tr><td>Total roadways</td><td>m</td><td>1 208</td><td>1 890</td><td>1 950</td><td>5 048</td></tr>
<tr><td>Advacement of development works</td><td>m/d</td><td>5.0</td><td>5.0</td><td>5.0</td><td></td></tr>
<tr><td>Production of development works</td><td>T</td><td>31 408</td><td>49 140</td><td>50 700</td><td>131 248</td></tr>
<tr><td>Advancement of excavation panel</td><td>m/d</td><td>3.0</td><td>3.9</td><td>2.8</td><td></td></tr>
<tr><td>Production of excavation panel</td><td>t</td><td>378 034</td><td>942 646</td><td>1 138 697</td><td>2 459 377</td></tr>
<tr><td>Length of transport routes</td><td>m</td><td>2 010</td><td>1 940</td><td>3 180</td><td rowspan="4">27 980 204</td></tr>
<tr><td>Length of demolished roadways</td><td>m</td><td>390</td><td>406</td><td>535</td></tr>
<tr><td>Calorific value</td><td>MJ/kg</td><td>11.57</td><td>11.32</td><td>11.36</td></tr>
<tr><td>Energy from excavation panels</td><td>GJ</td><td>4 373 853</td><td>10 670 753</td><td>12 935 598</td></tr>
<tr><td colspan="5">Total energy</td><td>29 473 488</td></tr>
</table>

**Table 7.** Parameters for excavation of exploitation panels at floor G4 in the north wing of the mine Preloge

<table>
<tr><td colspan="2">ET. G4</td><td>G4/A</td><td>G4/B</td><td>G4/C</td><td>Total</td></tr>
<tr><td>Excavation panel length</td><td>m</td><td>274</td><td>771</td><td>706</td><td>1 751</td></tr>
<tr><td>Excavation panel width</td><td>m</td><td>158</td><td>150</td><td>176</td><td>484</td></tr>
<tr><td>Total roadways</td><td>m</td><td>890</td><td>1 920</td><td>1 770</td><td>4 580</td></tr>
<tr><td>Advacement of development works</td><td>m/d</td><td>5.0</td><td>5.0</td><td>5.0</td><td></td></tr>
<tr><td>Production of development works</td><td>T</td><td>23 140</td><td>49 920</td><td>46 020</td><td>119 080</td></tr>
<tr><td>Advancement of excavation panel</td><td>m/d</td><td>3.0</td><td>3.5</td><td>3.0</td><td></td></tr>
<tr><td>Production of excavation panel</td><td>t</td><td>346 379</td><td>927 428</td><td>994 172</td><td>2 267 979</td></tr>
<tr><td>Length of transport routes</td><td>m</td><td>2 490</td><td>2 600</td><td>2 800</td><td rowspan="4">25 258 942</td></tr>
<tr><td>Length of demolished roadways</td><td>m</td><td>280</td><td>280</td><td>250</td></tr>
<tr><td>Calorific value</td><td>MJ/kg</td><td>11.38</td><td>11.14</td><td>11.05</td></tr>
<tr><td>Energy from excavation panels</td><td>GJ</td><td>3 941 793</td><td>10 331 548</td><td>10 985 601</td></tr>
<tr><td colspan="5">Total energy</td><td>226 585 292</td></tr>
</table>

**Table 8.** Parameters for excavation of exploitation panels at floor G5 in the north wing of the mine Preloge

<table>
<tr><th colspan="2">ET. G5</th><th>G5/B</th><th>G5/C</th><th>Total</th></tr>
<tr><td>Excavation panel length</td><td>m</td><td>751</td><td>691</td><td>1 442</td></tr>
<tr><td>Excavation panel width</td><td>m</td><td>125</td><td>177</td><td>302</td></tr>
<tr><td>Total roadways</td><td>m</td><td>1 990</td><td>1 870</td><td>3 860</td></tr>
<tr><td>Advacement of development works</td><td>m/d</td><td>5.0</td><td>5.0</td><td></td></tr>
<tr><td>Production of development works</td><td>T</td><td>51 740</td><td>48 620</td><td>100 360</td></tr>
<tr><td>Advancement of excavation panel</td><td>m/d</td><td>3.5</td><td>3.0</td><td></td></tr>
<tr><td>Production of excavation panel</td><td>t</td><td>750 310</td><td>978 578</td><td>1 728 888</td></tr>
<tr><td>Length of transport routes</td><td>m</td><td>2 500</td><td>2 600</td><td rowspan="4">18 513 790</td></tr>
<tr><td>Length of demolished roadways</td><td>m</td><td>290</td><td>290</td></tr>
<tr><td>Calorific value</td><td>MJ/kg</td><td>10.85</td><td>10.60</td></tr>
<tr><td>Energy from excavation panels</td><td>GJ</td><td>8 140 864</td><td>10 372 927</td></tr>
<tr><td colspan="4">Total energy</td><td>19 588 639</td></tr>
</table>

Parameters at exploitation of the entire area of the south wing of the mine Preloge:

- planned production 9 065 088 tonne
- average calorific value of coal 10.58 GJ per tonne
- planned production of energy 95 908 631 GJ
- required length of constructed lines 22 050 m
- planned production of appliances 573 300 tonne
- norm for construction of lines 2.43 m per 1000 tonne

**Quantities of coal in pillars and abandoned areas**

They contain a total of approximately 55 million tonne of coal. It is evident from their location that it will be possible to connect S pillar and the remaining part of G and L panels from the existing main communications for the north wing of the mine Preloge and the hanging wall section of the mine Pesje. The unexploited part of the mine Škale will be connected from the footline section of the mine Pesje. The location of NOP pillar does not require the construction of new connections - the existing connections can be used for its exploitation.

After finalised exploitation of conceptually treated G area, the remaining part of G and L panels will be exploited. At the same time, it will be possible to exploit the unexploited part of the mine Škale and S pillar. After finalised exploitation of G and L panels and S pillar, the excavation of NOP pillar will begin and, at the same time, the exploitation in the mine Škale will continue.

In exploitation of the above listed areas, average losses of 10 % to 15 % are expected. Therefore, approximately 49 million tonne of coal can be produced.

## Physical and chemical properties of coal

Physical and chemical properties of coal (shown in Table No. 11) are dealt with in the expert report »Prediction of physical and mechanical parameters and calorific value of lignite until the year 2028«, expert report No. 02/07-HGS. The properties were researched for exploitation panels according to conceptual solutions listed in the mining project »Exploitation of the mine Pesje from k.-40 to the depression bottom and CD pillar«, project No.: RP-325/007TK and in the expert report »Exploitation of the north wing of the mine Preloge«, expert report No.: TK002/07.

## Total quantities of coal at premogovnik Velenje - situation Dec. 31, 2008

**Table 9.** Balance sheet reserves of coal in the Velenje field of PV

| The Velenje field | Reserves (t) |
|---|---:|
| BALANCE SHEET RESERVES (over 8.4 MJ/kg) | 171 000 000 |
| BALANCE SHEET RESERVES – A | 7 729 050 |
| BALANCE SHEET RESERVES – B | 163 270 950 |

**Table 10.** Excavation reserves of coal in the Velenje field of PV

| The Velenje field | Reserves (t) |
|---|---:|
| EXCAVATION RESERVES | 131 670 000 |
| EXCAVATION RESERVES – A | 6 529 000 |
| EXCAVATION RESERVES – B | 125 141 000 |

**Table 11.** Physical and chemical properties of coal at PV

| Physical and chemical properties of coal | |
|---|---:|
| Calorific value | 10.47 MJ/kg |
| Moisture content | 35.23 % |
| Ash content | 15.87 % |
| Sulphur content | 1.39 % |

## Conclusion

Using the confirmed concepts, by using the existing excavation method, a total of approximately 131.67 million tonne of coal can be produced from the Premogovnik Velenje mines situated in Velenje. In calculations of coal reserves of Premogovnik Velenje until the end of exploitation of the Velenje exploitation field, the situation of reserves on 31st December 2008 was taken as a reference point.

It should also be noted that all exploitation concepts have been elaborated on the basis of existing methods for excavation of coal in the mines of PV. Should, in the future, the extraction method change in the sense of reduction of excavation losses, we can predict that it will be possible to produce even more coal at G panels and in CD pillar as planned in the currently valid concepts.

## References

Expert report »Expert report on categorisation, classification and calculation of coal reserves in the area of Velenje coal mine« (situation 31st Dec 1998), Premogovnik Velenje, Technical sector, Velenje, June 1999.

CERTIFICATE of coal reserves within the exploitation area of Velenje coal mine, situation 31st Dec 1998, Republic of Slovenia, MINISTRY OF ECONOMIC AFFAIRS, Ljubljana, 10th Dec 1999.

Concession Contract No. 354-13-737/01, Ljubljana, 21st Jan 2002, Concession-granting authority; Authorised person of the Government of the Republic of Slovenia, mag. Janez Kopač, MINISTER OF THE ENVIRONMENT AND SPATIAL PLANNING, Ljubljana, 21st Jan 2002.

Report »Report on coal reserves on 31st Dec 2004 and comparison with exploitation reserves from long-term exploitation concepts«, Premogovnik Velenje, Technical sector, Velenje, February 2005.

Expert's report »Report on classification and categorisation of coal reserves and sources on 31st Dec 2008«, Premogovnik Velenje, Expert report No E – 09 – IV, Technical sector, Velenje, december 2009.

Expert report »Prediction of physical and mechanical parameters and calorific value of lignite until the year 2028«, expert report No. 02/07-HGS, Premogovnik Velenje, Technical sector, Velenje, February 2007.

Mining project: »Continuation of exploitation in the mine Pesje from k. +40 to k. –40«, RP-13/91, Rudnik lignita Velenje, March 1991, responsible project manager: Marjan Moškon, BSc (Min Eng), revision clause No. 6/25-B/91, Mining Institute Ljubljana, 22nd May 1991.

Mining project: »Continuation of exploitation in the south wing of the mine Preloge until the finalisation of exploitation«, RP-54/91, Rudnik lignita Velenje, August 1993, responsible project manager: mag. Boris Salobir, BSc (Min Eng), revision clause No. 06/28-93, Mining Institute Ljubljana, Ljubljana, 8th Nov 1993.

Mining project: »Concept of exploitation of the north-western section of the mine Preloge«, Project No. m RP28/91, Rudnik lignita Velenje, February 1995, responsible project manager: mag. Boris Salobir, BSc (Min Eng), revision clause No. 261/95, University of Ljubljana, Faculty of Natural Sciences and Engineering, Department of geo-technology and mining , Ljubljana, 2nd Nov 1995.

Mining project »Velenje mining method«, Project No: RP-36/95 ML, Rudnik lignita Velenje, Velenje, June 1996, responsible project manager Marijan Lenart, BSC (Min Eng), revision clause No. 297/97, University of Ljubljana, Faculty of Natural Sciences and Engineering, Department of geotechnology and mining, Ljubljana, 16th July 1997.

Mining project: »Supplementing of the concept of exploitation of the north-western and central section of the mine Preloge «, RP-183/2000 ML, Premogovnik Velenje, July 2000, responsible project manager: Marijan Lenart, BSc (Min Eng), revision clause No. 366/01, University of Ljubljana, Faculty of Natural Sciences and Engineering, Department of geo-technology and mining, Ljubljana, 9th Mar 2001.

Mining project: »Preparation and exploitation of the panel G1/A«, RP-205/2001ML, Premogovnik Velenje, September 2001, responsible project manager: Marijan Lenart, BSc (Min Eng), revision clause No. KC-12/2001, Ciril Kemperle, s. p., projektiranje, revidiranje in svetovanje, Velenje, 2nd Oct 2001.

Expert report: »Concept of mine exploitation in the south wing of the mine Preloge and in A pillar in the mine Pesje«, expert report No.: 1/2004BŠ, Premogovnik Velenje, Velenje, March 2004, responsible project manager: Božo Špegel, BCs (Min Eng).

Mining project: »Exploitation of the mine Pesje from k.-40 to the depression bottom and CD pillar«, project No.: RP-325/007TK, Premogovnik Velenje, March 2007, responsible project manager: Tomaž Kodrič, BSc (Min Eng), revision clause No. 48/2006, Proteus inženiring biro, d. o. o., Velenje, 6th Apr 2007.

Expert report: »Exploitation of the north wing of the mine Preloge«, expert report No.: TK002/07, Premogovnik Velenje, June 2007, responsible project manager: Tomaž Kodrič, BSc (Min Eng).

# 3D analysis of the influence of primary support stiffness on the surface movements during tunnel construction

# 3D-analize vpliva togosti primarnega podporja na razvoj pomikov površine med gradnjo predora

**Jakob Likar**[1, *]

[1]University of Ljubljana, Faculty of Natural Sciences and Engineering, Aškerčeva cesta 12, SI-1000 Ljubljana, Slovenia

*Corresponding author. E-mail: jakob.likar@ntf.uni-lj.si

**Received:** March 18, 2010 **Accepted:** May 18, 2010

**Abstract:** The usage of underground structures is increasing which is the reason that in many cases construction takes place in heavy and difficult geological geotechnical conditions. The main goal to reduce surface settlement on the minimum is connected with stiffness of the primary lining and effective protection excavation face against deformation process realized in rock pillar ahead the excavation. The construction process was modelled with *PLAXIS 3D tunnel program*. Input parameters were determined by 3D back analyses with Soft-Soil-Creep (SSC) constitutive material model, which takes into account rheological phenomena. 3D development of stress-strain fields during the tunnel excavation was performed to show major stress-strain changes in the surrounding rocks and support elements. The calculations showed that during excavation of the top heading substantial deformations are developed ahead of the top heading. Influence of the support stiffness has strong connection with amount of surface movements above the tunnel.

**Izvleček:** Uporaba podzemnih prostorov se v svetu povečuje, kar je pogosto razlog, da v mnogih primerih gradnja poteka v zahtevnih geoloških in geotehničnih razmerah. Glavni cilj podpornih ukrepov v takih primerih je, da se doseže zmanjšanje deformacij površine, ki je naseljena, na najnižjo možno raven. To je v direktni povezavi s togostjo primarne obloge in z učinkovito zaščito izkopnega čela pred procesom razvoja deformacij v hribinskem stebru pred njim.

*Original scientific paper*

Simulacija gradnje predora v obravnavanem primeru je bila izdelana s programskim paketom PLAXIS 3D-predor, ki je ustrezen za tovrstne izračune. Vhodni parametri za izračune so bili določeni s povratnimi 3D-analizami z uporabo materialnega modela Soft-Soil-Creep (SSC), ki omogoča upoštevanje časovno odvisnih procesov v hribinah. 3D-analiza razvoja napetostnih polj in obremenitev podpornega sistema med izkopom predora je bila opravljena tako, da so bile upoštevane različne togosti podpornih elementov. Izračuni so pokazali, da so med izkopom posebej pomembne velikosti deformacij pred izkopnim čelom, ki v skupnem seštevku deformacij, ki se razvijejo v predoru med izkopom in vgradnjo podpornih elementov, lahko močno presegajo dopustne vrednosti. Z izračuni deformacij v 3D-prostoru je bil dokazan realen vpliv togosti primarnega podpornega sistema na razvoj pomikov površine nad predorom.

**Key words:** 3D Finite Element Analysis, SCC constitutive model, tunnelling, stiffness of primary lining, surface movenets

**Ključne besede:** 3D-analize z metodo končnih elementov, konstitutivni model SCC, izkop in primarno podpiranje predora, togost primarne obloge, pomiki površine terena

## Intruduction

The influences of tunnelling on surface in areas of low overburden are sometimes still difficult to predict, despite contemporary computer techniques. The cause for that could be in quite changeable physical and mechanical properties of the surrounding rocks mass and soils and also in selected construction method related with stiffness of primary support, which is installed after the excavation. In technical and scientific literature at this area we could find some numerical models, which deals with relations between stresses and strains in the support system and surrounding rock mass for different distances between closed primary support and the face of excavation also for the particular stiffness of the support system.

In fact this is the effect of the support stiffness in function with surrounding rock mass in which the stiff support system has the biggest contribution. Stiff support system is usually combination of steel support together with shotcrete, rock bolts or anchors and also with additional support systems like steel pipe roof, micro piles, temporary invert with elephant foot, etc. In rocks with low bearing capacity, the arrangement of stresses and the amount of deformations which occurred, could be a serious problem regarding to the acceptable surface subsidence. In reality deformations in tunnel shell usually make no problems with stability and excavation process. The technological procedures are schematic shown in the Figure 1.

Regarding to that, this demands detailed analysis of stiff support effect taking in to account development of deformation fields with excavation progress and installation of primary support.

#### SOME NUMERICAL MODELS WHICH DEALS WITH STIFFNESS OF PRIMARY SUPPORT SYSTEM

The question, which is related with the share of primary state in rock mass, which the support system has to take over, is in professional literature treated in different ways by many authors (WHITTAKER & FRITH, 1990; KIM & EISENSTEIN, 1998; etc.). But in latest past, the usage of complicated models were less desired, because it took a lot of knowledge and time for engineers to obtain some results in practice and on the other hand the input parameters were complicated and difficult to define with standard laboratories tests (Vižintin, 2009a). This causes some problems at planning and execution of detailed laboratories tests, which also could had limited practicability at wider area of the surrounding rock. This fact is quite related with inhomogeneous and anisotropic behaviour and anomalies, which often occur in surrounding mass (Vižintin, 2009b). Reduction factors, which were used by some authors, show us, that they were fully aware of the complexity of rock mass structures.

Experiences that we have with usage of that numerical models indicated, that they are useful for tunnels or others underground objects with low overburden, which are construct in compact rock mass with high cohesion. In cases,

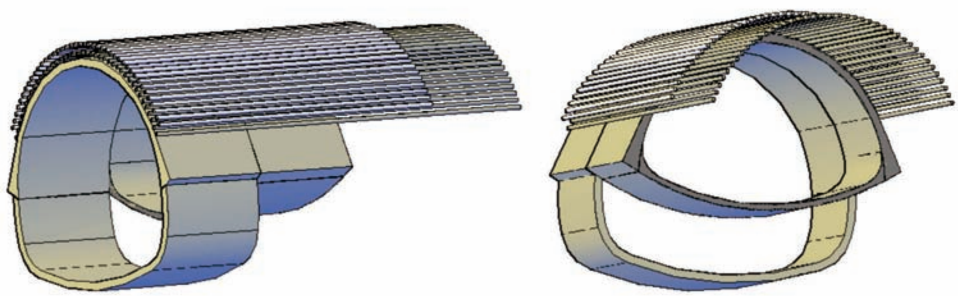

**Figure 1.** Technological sequences during the tunnel tube excavation.

where the rock mass has low cohesion, the results are questionable and not so reliable. Kim in Eisenstein 2006 suggested, that calculation method developed by Schwartz in Einstein 1980, could be used, when the quotient came to $L_d/R < 1$. In this equation the $L_d = 0.7$ m is the distance between the excavation face and the centre of gravity of the latest closed segment of primary lining and $R = 5.5$ m, which is the equivalent radius of excavation.

In present case is $\lambda_d = 0.7 – 0.57$ $(L_d/R) = 0.63$, which corresponds their recommendation.

### Technical particularity of construction of the Trojane tunnel at the section of shallow cover class

The construction of the tunnel at the section of shallow cover class was adjusted to unfavourable conditions. The following working phases were performed:

a) An excavation of top heading was carried out in 5 phases with simultaneous protection of working face by wire mesh Q189, 15 cm thick shotcrete. 35 pieces of 15 m long IBO rock bolts with bearing capacity 250 kN and over covering at 5 m to 7 m were also installed. The amount of excavation step was 0.8 m.

b) After excavation of the 3rd phase, the steel support was installed, which included 2 steel segments IPE 180 and 2 steel micro piles at every side of top heading, with length 6 m and 64 mm in diameter.

c) After excavation of the 4$^{th}$ and 5$^{th}$ phase, temporary invert was installed with the thickness of 25 cm and one layer of wire mesh Q283. Also the second layer of wire mesh Q283 and shot concrete was installed, so that final thickness of primary support came to 35 cm.

d) An installation of pipe roof contained 42 pieces of pipes with 114 mm in diameter and over covering of 5 m to 8 m.

e) An excavation at top heading was followed by excavation and installation of primary support at bench and invert. Distance after working face of top heading was 10 m to 20 m with excavation step 0,8 m.

Figure 2 presents the cross section of the tunnel tube with the supported measures.

### Changes of stress strain relations in rock-support system around the tunnel`s working face

Excavation in low bearing and tectonic damaged rocks like tectonic clays, clay grain and gravel stone, which are present at the section of Trojane was connected with large amount of stress strain changes in front of the working

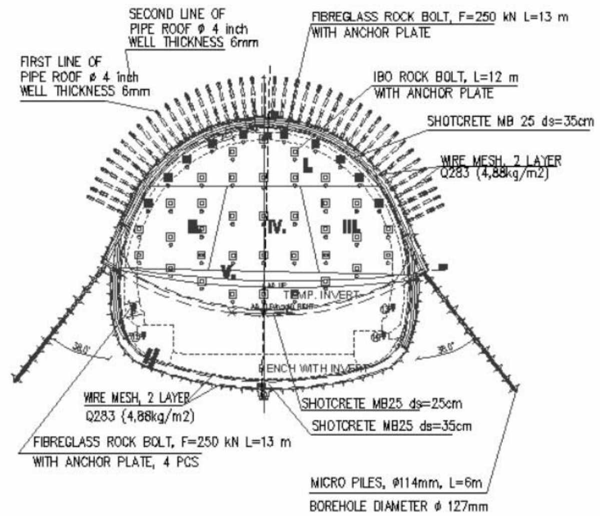


**Figure 2.** Cross section of tunnel tube with supported measures

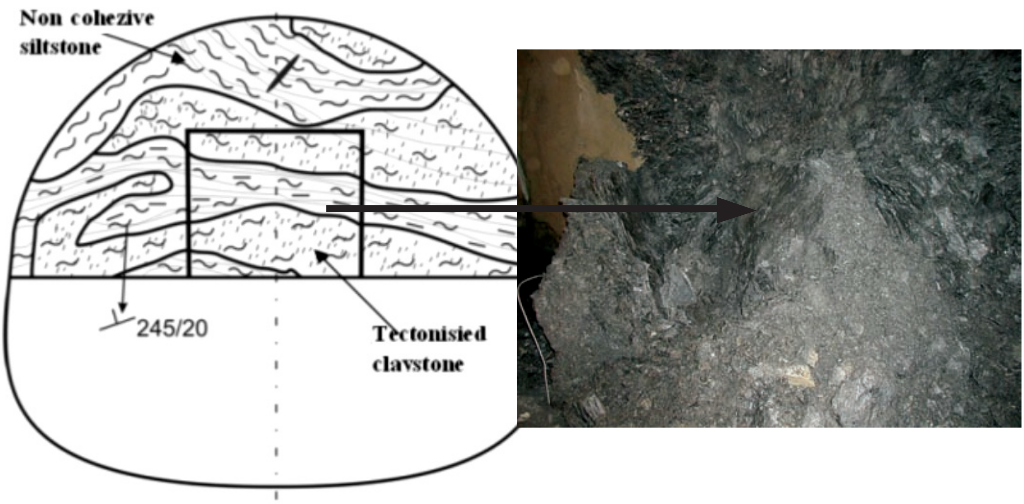


**Figure 3.** Typical geological cross section of the Trojane tunnel (East left tube).

face and wider area around the tunnel. In mostly clayey and relatively soft rocks, the influence was 3D or even 4D in front of the working face, where D stands for the diameter of the tunnel tube. This phenomenon was extremely unfavourable because of influence to the time dependent subsidence at the wider area. From the so far completed analysis and engineering interpretations, it could be estimated that large amounts of clayey components essentially influence the time dependent deformations. That was significant for the right judgment of possible deformations in a long time period.

Very heterogeneous geological structure and primary damaged rocks were often indicated in the differential subsidence of tunnel sidewalls. That also unfavourably affected the governing of the amount of deformations in the tunnel roof and on the influential section at surface.

## Back geostatic analysis of stress strain fields

Modern computer techniques based on numerical methods make quick and qualitative assessment of the changes, which are the result of excavation and installation of the support system. Anyhow, input parameters, which we obtain from standard laboratory and in situ tests, are not always quite realistic, comparing results from analysis obtained with those parameters to actual influences that developed between excavation and support measures. These statements were confirmed during construction of the Trojane tunnel, especially on the sections with clayey material.

Absolute values of the deformations calculated with analysis for estimation were quite smaller than those that actually occurred during the construction and later on. It is interesting that values of the differential deformations were more in accordance with the measured values.

The reasons for increased deformations are:
a) The fact that in two-dimensional analysis the three-dimensional effect is not considered which is essential for this kind of rocks.
b) The fact that input parameters, especially deformational, which we obtain from standard
laboratory and in situ tests are not always quite realistic.

The application of the two-dimensional geostatic analysis for realistic assessment of deformational fields demands much lover values of the input parameters. This contradicts the correct scientific and engineering work. Figure 4 presents in schematic form the influence of excavation on the surface above the tunnel.

### Influence of support system stiffness and rock pillar in front of the excavation face

Influence of the supporting system stiffness on amount and time depended behaviour of deformations is essential for an adequate planning of construction. Increased stiffness of supporting system could be achieved in several ways:

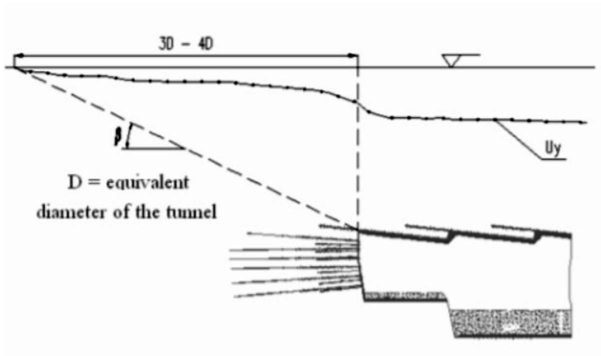


**Figure 4.** Angle of influence and deformations on the surface due to tunnel excavation

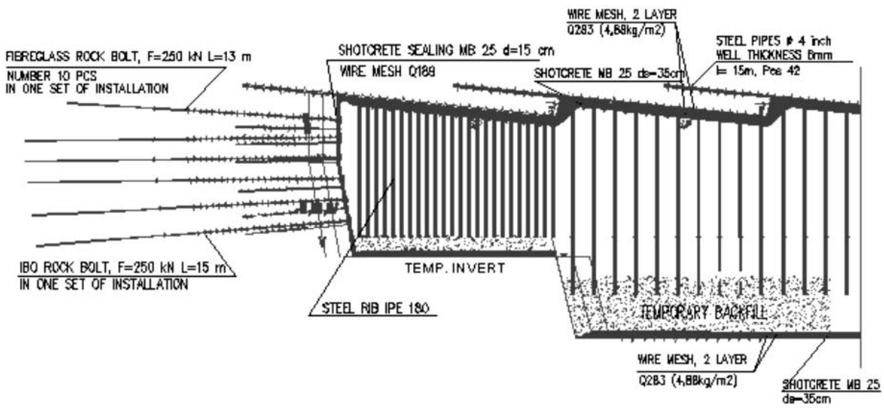


**Figure 5.** Installation of support system, which ensures quick undertaking of additional loads due to excavation tunnel.

a) by installing the supporting system, which ensures a quick undertaking of additional loads, which are the consequence of the excavation;
b) by excavating and supporting its sections, e.g. excavation with side gallery, where balance is reached in smaller cross sections;
c) by installing the auxiliary support elements with low deformability for increasing stiffness of rock pillar in front of the excavation face;
d) by combining it all.

The question of the intensity of increasing the stiffness of rock pillar in front of the working face by installing the auxiliary supporting elements, which allow normal evolution of the technological process of excavation and support, remains. This understanding is essential for normal operation with fewer interruptions and more continuous construction work.

**Results of back geotechnical analysis**

3D analysis of stress strain relations were made with software PLAXIS Tunnel 3D, Version 2.0. Geotechnical input parameters for calculation of stresses and strains in supporting system and surrounding rock were partially determent in previous investigations. The values are presented in Table 1.

The simulation of excavation and primary supporting were carried out in such manner that first, the excavation and supporting in top heading in the length of 10 m were performed.

This was followed by the excavation and installation of supporting elements at bench, invert and top heading for 10 m more. Excavation and supporting step was 0.8 m. Deformations were in amount of 200–250 mm in the tunnel and 150–200 mm on the surface. These values are similar to those measured at many points. A part of these measurements is presented in Figure 6, where we could see irregular subsidence, which is a consequence of the extremely unfavourable geologic and geotechnical conditions on this section.

The way of excavating and supporting was the same at this section, but over covering of the pipe roof in the sections of bigger deformations was greater, even in the range of 8 m. This caused the stiffness to increase in the roof section of top heading together with primary support, which contained 2 steel segments IPE 180, 2 micro piles, wire mesh and shotcrete of final thickness of 35 cm.

The results of calculation are presented in figure 8a and figure 8b in form of deformation field. In calculation was also included passive resistance of rock bolts and shot concrete lining in working face in amount of 250 kN/m$^2$. Comparison between deformation fields obtained with consideration of single pipe roof and over covered pipe roof shows us that influence of increasing stiffness in soft ground is important. Deformations on surface are 20–30% smaller when double pipe roof is used. This was also established during the construction, where in sections with over covered pipe roof deformations were smaller.

Figure 8a and Figure 8b shows differences in deformation fields for normal over covered and fully over covered pipe roof.

**Time dependent processes**

Development of deformations at the time of excavation and primary supporting of the tunnel is distinct in carbonic rock, since evolution of deformations is completed only in time period of 180 days or more.

**Table 1.** Input parameters for calculation with SSC model.

| MODEL PARAMETERS | | Clay schist and mudstone |
|---|---|---|
| Unit weight | $\gamma$ /(kN/m$^3$) | 24 |
| Cohesion | $c$/(kN/m$^2$) | 28 |
| Angle of the internal friction | $\varphi$/$^o$ | 26 |
| Modified swelling index | $\kappa^\bullet$ | 0.035 |
| Modified compression index | $\lambda^\bullet$ | 0.04 |
| Modified creep index | $\mu^\bullet$ | 0.0003 |

**Table 2.** Strength of support elements with different stiffness
Across section; I Moment of Inertia; E Young Modulus

| | A [m^2] | I [m^4] | E [Kn/m^2] | EA [Kn/m] | EI [Knm^2/m] |
|---|---|---|---|---|---|
| **PIPE ROOF 2X** | 1,080 | 0,071411 | 876.000.000,00 | **10.480.000,00** | **406.134,55** |
| **PIPE ROOF 1X** | 0,180 | 0,004574 | 439.000.000,00 | **4.520.000,00** | **31.704,91** |
| SHELL (Es.c. = 3000MPa) | 0,35000 | 0,003572917 | 3.000.000 | 1.050.000,00 | 10.718,75 |
| IPE 180 | 0,00390 | 0,000013200 | 210.000.000 | 2.047.500,00 | 6.930,00 |
| **SHELL+IPE180 (EB.B. = 3000MPa)** | | | | **3.097.500,00** | **17.648,75** |
| SHELL (Es.c. = 7000MPa) | 0,35000 | 0,003572917 | 7.000.000 | 2.450.000,00 | 25.010,42 |
| IPE 180 | 0,00390 | 0,000013200 | 210.000.000 | 2.047.500,00 | 6.930,00 |
| **SHELL+IPE180 (EB.B. = 7000MPa)** | | | | **4.497.500,00** | **31.940,42** |
| SHELL (Es.c. = 7000MPa) | 0,35000 | 0,003572917 | 15.000.000 | 5.250.000,00 | 53.593,75 |
| IPE 180 | 0,00390 | 0,000013200 | 210.000.000 | 2.047.500,00 | 6.930,00 |
| **SHELL+IPE180 (EB.B. = 15000MPa)** | | | | **7.297.500,00** | **60.523,75** |
| SHELL (Es.c = 3000MPa) | 0,35000 | 0,003572917 | 3.000.000 | 1.050.000,00 | 10.718,75 |
| TH 21 | 0,00234 | 0,000003390 | 210.000.000 | 491.400,00 | 711,90 |
| **SHELL+ TH 21 (EB.B. = 3000MPa)** | | | | **1.541.400,00** | **11.430,65** |
| SHELL (Es.c. = 7000MPa) | 0,35000 | 0,003572917 | 7.000.000 | 2.450.000,00 | 25.010,42 |
| TH 21 | 0,00234 | 0,000003390 | 210.000.000 | 491.400,00 | 711,90 |
| **SHELL+ TH 21 (EB.B. = 7000MPa)** | | | | **2.941.400,00** | **25.722,32** |
| SHELL (Es.c = 15000MPa) | 0,35000 | 0,003572917 | 15.000.000 | 5.250.000,00 | 53.593,75 |
| TH 21 | 0,00234 | 0,000003390 | 210.000.000 | 491.400,00 | 711,90 |
| **SHELL+ TH 21 (EB.B. = 15000MPa)** | | | | **5.741.400,00** | **54.305,65** |

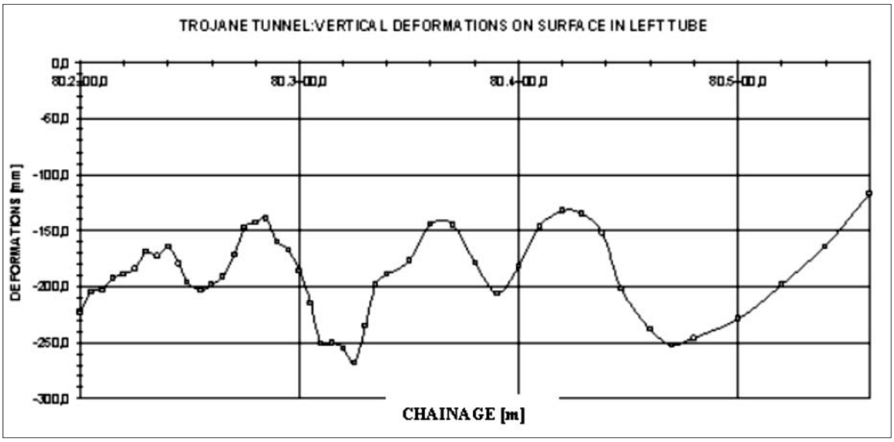


**Figure 6.** Measured subsidence on the surface along the longitudinal axe of the tunnel tube.

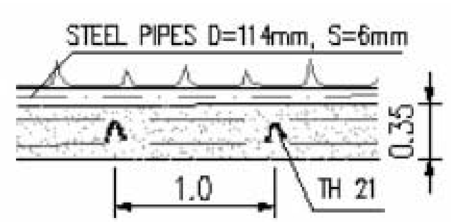


**Figure 7a.** Standard support elements with steel pipes, TH21, wire mesh and shotcrete

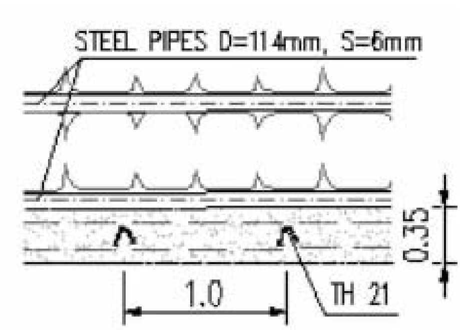


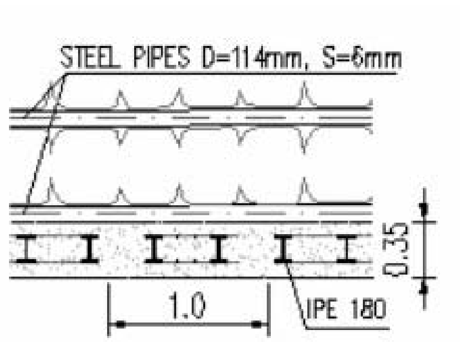


**Figure 7b.** Support elements with double steel pipes, TH21, wire meshes and shotcrete

**Figure 7c.** Support elements with double steel pipes, double IPE180 steel rib, wire meshes and shotcrete

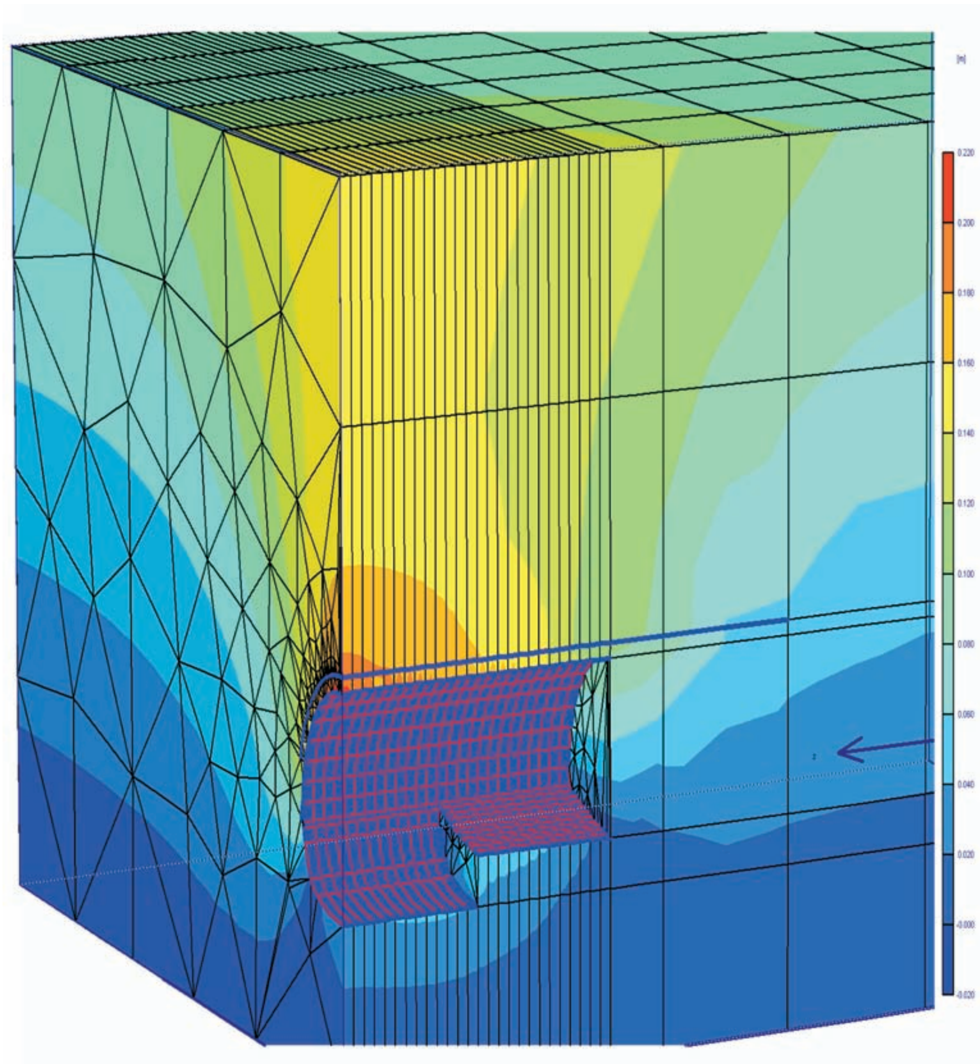

**Figure 8a.** Deformation fields for normally over covered pipe roof

This was also established in analysis with finite element method, where soft soil creep model was used.

In calculation the hardening of shotcrete was simulated, which gives us increased stiffness of support. During the construction, the support stiffness was also increased with installation of stiff steel segments (2 IPE 180 on section of excavation 0.8 m). The weakness of this combined steel and shotcrete system is that quality of filling in the empty spaces around the steel segments is not easily achieved.

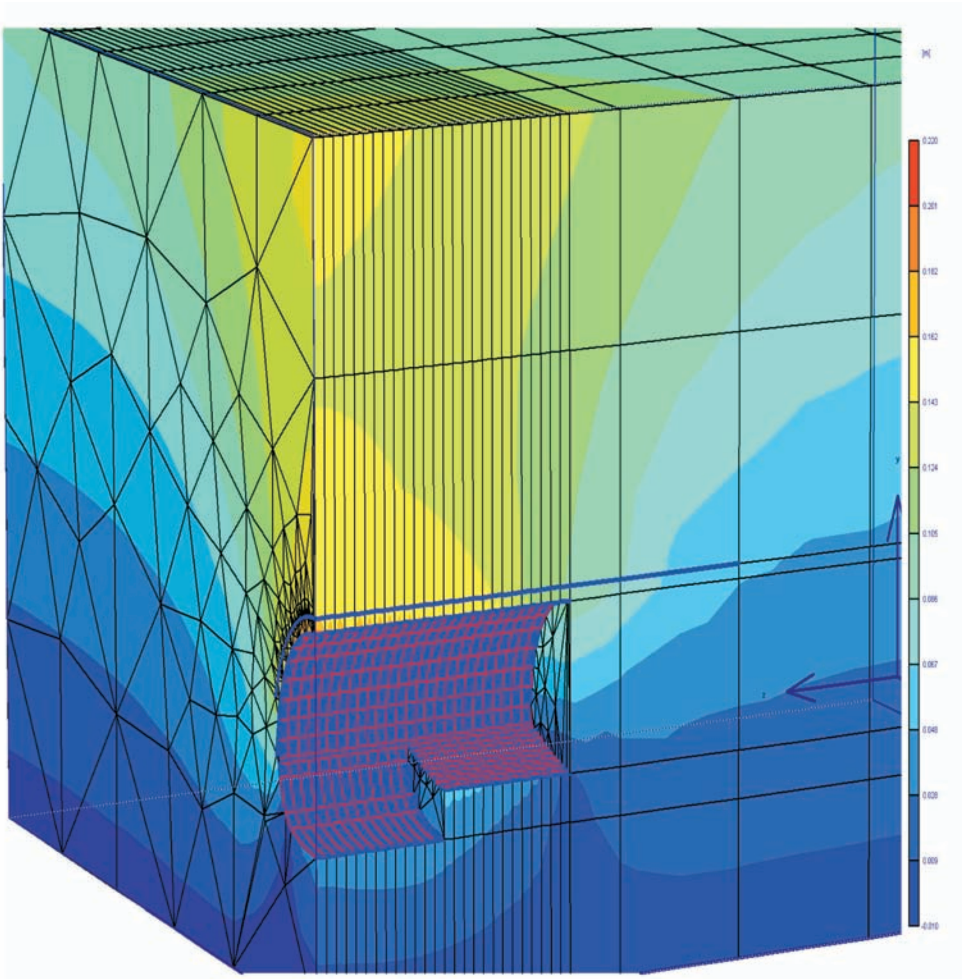

**Figure 8b.** Deformation fields for fully over covered pipe roof

## CONCLUSION

- Tunnel construction in specific conditions such as in low bearing time dependant rocks under habited area depends of the technological procedure and primary support lining, which were used.
- The area of the surface displacements caused by tunnel excavation is closed to geological and geotechnical conditions and type of surface relief with dipping of the natural slopes and local stabilities.
- The results of presented numerical analyses of the surface displacement caused by tunnel construction were usable. Time dependant dis-

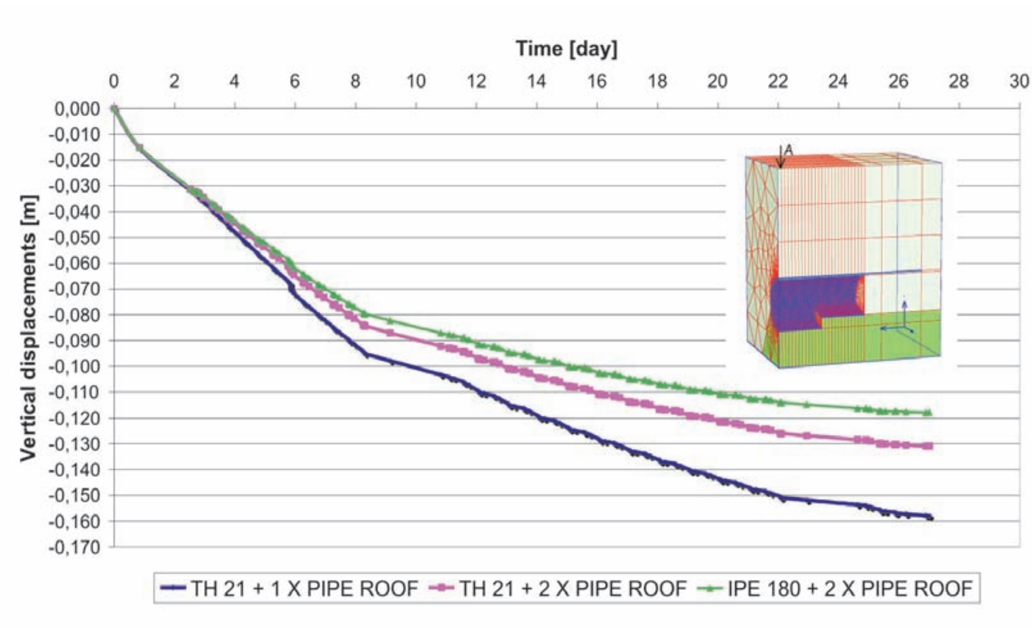


**Figure 9.** Time dependent surface displacements calculated for different stiffness of the primary lining

placements which were presented help us to make danger volume assessment of objects on the surface.

- Comparison between calculated and measured displacement show us, that this method can be used in similar geological and geotechnical circumstances.

## References

Brinkgreve, R. & Vermeer, P. (2004): Plaxis 3D Tunnel-Version 2.; Set of manuals. Plaxis bv Delft, Netherlands.

Karakus, M. (2006): Appraising the methods accounting for 3D tunnelling effects in 2D plain strain FE analysis, Tunnelling and Underground Space Technology, Elsevier, pp.10.

Kim, H. J., Eisenstein, Z. (1998): Prediction of lining loads from case histories. World Tunnel Congress'98, Sao Paolo, Brazil, pp. 299–304.

Venta, M. (2005): Vplivi izkopa podzemnih prostorov na površino v časovno odvisnih kamninah, diplomsko delo, Ljubljana. X, 82 f., grafični prikazi. [COBISS.SI-ID 583007].

Vižintin, G., Veselič, M., Bombač, A., Dervarič, ., Likar, J., Vukelič, Ž. (2009a): The development of a »drive-in« filters dewatering system in the Velenje coal mine using finite-element modelling. Acta geotech. Slov., Vol. 6, 1, str. 50–63.

Vižintin, G., Souvent, P., Veselič, M., Čenčur Curk, B. (2009b): Determination of urban groundwater pollution in alluvial aquifer using linked process models considering urban water cycle. J. Hydrol. (Amst.). [Print ed.], Issues 3–4, Vol. 377, pp. 261–273.

Whittaker, B.N., Frith, R. C. (1990): Tunnelling-Design, Stability and Construction. The Institution of Mining and Metallurgy, London.

Wittke, W. (2000): Stability Analysis for Tunnels. Fundamentals.Verlag Glückauf GmbH. Essen.

Wittke, W. (2002): Statik und Konstruktion der Spritzbetonbauweise. Verlag Glückauf GmbH. Essen.

# Multi-objective methods for welding flux performance optimization

# Več namenske metode za optimizacijo uspešnosti varilnega praška

Ademola David Adeyeye[1,*], Festus Adekunle Oyawale[1]

[1]University of Ibadan, Faculty of Technology, Department of Industrial and production Engineering, Ibadan, Nigeria

*Corresponding author. E-mail: ademola.adeyeye@mail.ui.edu.ng

**Received:** January 11, 2010 **Accepted:** March 30, 2010

**Abstract:** The traditional welding flux development is by lengthy and costly trial and error experiments and the optimum welding flux formulation is not guaranteed. This paper presents discussions on promising multi-objective decision making (MODM) methods that can mitigate the limitations of the traditional approach to welding flux design. The methods are weighted-sum scalarization (WSS), desirability indices, goal programming and compromise programming. The steps a welding flux designer (WFD) may follow to determine the best compromise welding flux, welding flux design situations where each may be useful and trade-off explorations were mentioned. No attempt was made to determine the relative merits of the approaches because the usefulness of each depends on the welding flux design situation. The descriptions only serve as a guide for the WFD to decide which method best suits his needs.

**Izvleček:** Klasični razvoj varilnih praškov poteka z dolgotrajnimi in dragimi preizkušanji in odpravami napak. Pri takšnem načinu ni zagotovljena optimalna sestava varilnega praška. V članku so predstavljene več namenske metode odločanja (MODM), ki odpravijo nekatere omejitve tradicionalnega pristopa raziskav varilnega praška. Uporabljene metode so skalarizacija uteženih vsot (WSS), indeksi zaželjenosti, ciljno programiranje in kompromisno programiranje. Navedeni so koraki za zagotovitev naboljšega varilnega praška, ki naj bi jih sledil načrtovalec varilnega praška (WFD). Prav tako so omenjeni različni preiskani kompromisi za nekatere razmere pri načrtovanju varilnih praškov. Članek ni poskušal odgovoriti na vprašanje relativne vrednoti pristo-

*Professional Paper*

pov, ker je uporabnost vsakega odvisna od razmer za katere razvijamo varilni prašek. Opisane metode naj bi služile samo kot vodilo WFD, za izbiro najustreznejše metode za trenutne potrebe.

**Key words**: welding flux, weighted-sum scalarization, desirability indices, goal programming, compromise programming

**Ključne besede:** varilni prašek, skalarizacija uteženih vsot, indeksi zaželjenosti, ciljno programiranje, kompromisno programiranje

## Introduction

Welding flux design like many real world problems involves multiple objectives which are more often than not conflicting. In the welding flux formulation problem, the welding flux designer (WFD) aims at developing a flux that will deposit weld-metal with the required quality characteristics and at the same time fulfil the operational and environmental requirements. Some of the frequently encountered objectives of WFDs depending on the type of metal, are to get a flux that will deposit weld-metal with maximum acicular ferrite content, maximum charpy impact toughness, maximum tensile strength, minimum diffusible hydrogen content, as well as minimum spatter, minimum fume, minimum toxic content of fume during welding, etc … The conflict of these objectives arises because improvement in one objective can only be made to the detriment of one or more of the other objectives. Because of the conflicting nature of the objectives, it is not feasible to get a flux formulation which optimizes all of them simultaneously. Therefore compromises and balances are often provided and designed into the flux.

The traditional method of achieving the compromises and balances is through tedious trial and error experiments. According to ADEYEYE & OYAWALE[1] the limitations of the traditional trial and error method are mainly due to the paucity of computational models that can be used for the prediction and optimization of flux properties. The traditional approach is time consuming and costly. Consequently, the lead-time for a new welding flux is usually long. The optimality of the flux so designed is difficult to ascertain because of the ever present trial and error and absence of quantitative means of testing optimality. The inability to identify and quantify the direct and interaction effects of the input variables such as levels of flux ingredients is another drawback of the traditional trial and error approach. With the obvious need to overcome these drawbacks, Kanjilal et al,[2-6] introduced a new approach which has great potential to revolutionize welding flux design technology. They used a design of experiment (DoE) method known as mixture design to layout the experiment. Data from the experiment were used to develop regression models that relate the input/predictor variables to the output/response variables. With their approach welding flux design can now be based on quantitative footing, direct and interaction effects of variables that determine the properties of welding flux can be identified and quantified and more insight gained. Some of the phenomena that hitherto could not be explained can now be explained in terms of synergetic or antagonistic interaction effects of input variables.

In a recent paper, Adeyeye & Oyawale[7] proposed a methodology in which the mixture design method used by Kanjilal et al.[2–6] was integrated with mathematical programming optimization technique. This new methodology extended the work of Kanjilal and co-investigators. The methodology was able to identify the optimum welding flux formulation and also assist the WFD to know either it was feasible to achieve desired flux performance level within the input space or not with minimal experimental efforts. However, their study was limited to a situation where the WFD is interested in a single objective. The multiple objectives welding flux design situation is encountered more frequently than the single objective case. The WFD therefore needs well tested and validated optimization tools that can handle multiple objectives and also assist him to explore various trade-off options. There are many optimization methods in multi-objective decision-making (MODM) area which could be used for this purpose. MODM is not new in other areas of arc welding technology but it appears relatively unknown to WFDs and as a result MODM applications in welding flux formulation is yet to be explored.[8–10] In this article, some of the MODM optimization methods are discussed and various welding flux design situations where they could be useful are presented.

## Welding flux design problem

The design of welding flux that meets operational requirements, weld-metal quality requirements, environmental, manufacturability and storage requirements is far from trivial. Operational characteristics such as arc stability, deposition rate, slag control, etc … determine the productivity and cost of the welding process. Welding flux design therefore seeks to maximize the contribution of the welding flux to the society while minimizing its cost to the manufacturer, user and the environment. Each lifecycle stage of the flux is taken into consideration during the design stage. Health and safety of the welder and other workers at the welding environment are also important.

The flux is therefore expected to produce minimum fume, no or minimum noxious odours and minimum amount of toxic materials in the fume. Some of the commonly encountered requirements are presented in figure 1. Most of the requirements are bundles of other requirements and can be broken down to secondary and tertiary requirements. For instance, weld-metal quality depends on mechanical property, microstructure, bead morphology etc … all of which are also determined by other requirements (Figure 1). The requirements presented in Figure 1 are not exhaustive; depending on the situation more requirements may be added. The requirements the WFD selects for a particular flux depend on the welding method, the particular metal to be welded and the service requirement of the weldment.

These requirements are incompatible because it is not possible to improve one quality characteristic without decreasing the achievement or satisfaction of one or more of the other quality characteristics. The problem of flux design therefore, is that of determining the flux ingredients levels that will achieve the best compromise between the various requirements. Studies have shown that the types and levels of flux ingredients and process parameters are key factors that determine these requirements.[11–17] Application of optimization models to welding process parameter optimization has received much attention while so far application of such models to welding flux formulation is scanty in the literature.[8–10, 18, 19] As mentioned earlier, the traditional approach of achieving compromises and balances is by lengthy trial and error experiments. The flux so designed can not be guaranteed to be the best compromise flux because it is not possible to explore all possible combinations of flux levels because of cost and time limitations.

An integration of Kanjilal and co-workers method with the MODM approach will mitigate the problems of the WFD. As the WFD can not face testing all possible combinations of flux levels and measure the quality of resulting flux, a model capturing the relationship between each quality characteristics and flux levels should be assumed over the domain of interest through regression equations. The proven method a WFD may use to capture such relationship is the mixture experiment approach. The details of the mixture experiment approach abound in the literature.[20-27] Various model forms that may be used to fit regression models of the responses are presented in the paper of ADEYEYE & OYAWALE.[1] A key assumption is that each of the responses defining the quality of the flux is related to the same set of varying factors. The objective is to find factor setting that will achieve the best compromise flux formulation.

The specific steps a WFD may follow are presented as follows: (i) Determination of the welding process for which the flux will be used and its specific requirements. For instance, extrudability, strong and tough coating are not requirements for SAW where as they are very important requirements for SMAW. (ii) Determination of the type of metal the flux will be used for and its specific characteristics and requirements. (iii) Determination of the service requirement of the weldment. This will assist the WFD to establish the mechanical properties, weld-metal chemistry and metallurgical features which the welding flux should achieve when used to weld. (iv) Preparation of a list of requirements with the preferences of the WFD. Typical preferences of WFD may be: a welding flux that will maximize penetration, minimize diffusible hydrogen content and achieve a target of say 300ppm oxygen content in the weld-metal. (v) Laying out the experiment using the mixture experiment design procedure.[27–30] (vi) Performing the experiment as prescribed by the algorithm in step v above. (vii) Using the data from the experiment to develop response models that capture the relationship between each of the requirements and flux component levels over the domain of interest. [1] (viii) Using the appropriate MODM method that suits the particular welding flux design situation to find the factor setting that achieves the best compromises and balances.

Steps i to vii above have been addressed in the literature. [1–7, 18, 19] Step (viii) is our focus in this paper. Some of the common well tested and validated MODM methods the WFD can couple with the mixture experiment to achieve the best compromise welding flux formulation are discussed in the following section.

## Description of various MODM approaches applicable to welding flux design

This section presents brief discussions of the most widely used MODM methods that can be integrated with the mixture experiment methodology to mitigate the problems associated with the traditional welding flux design approach. The methods are scalarization techniques, goal programming and compromise programming. These MODM methods were selected for discussion because they are suitable for welding flux design problems and also sufficiently flexible for incorporating the flux formulators preferences concerning the relative importance of each objective or quality characteristic.

- Flux requirement
  - Weld - metal requirement
    - Composition
      - *Chromium*
      - *Manganese*
      - *Carbon*
      - *Difussible – hydrogen*
    - Microstructure
      - Ferrite number
      - Acicular ferrite
      - Bainite e.t.c...
      - Inclusion volume fraction
      - Inclusion size
      - Inclusion number density
    - Mechanical property
      - Yield strength
      - Tensile strength
      - Charpy impact strength
      - Hardness
      - Elongation
    - Weld bead
      - Penetration
      - Reinforcement
      - Bead width
      - Dilution
  - Environmental requirement
    - Fume
      - Generation rate
      - Particle number
      - Mass distridution
    - Noxious odour
    - Toxic materials
      - $Cr^{6+}$
      - $Mn$
      - $Ni$, *etc.*.
  - Manufacturability requirement
    - Extrudability
    - Good bonding
    - Uniform mixing
  - Storage requirement
    - Durability of coating
    - Moisture pick - up
    - Shelf - life
  - Operational requirement
    - Arc striking
    - Arc stability
    - Penetration control
    - Spatter
    - Slag control
    - Slag detachabilty
    - Deposition rate
    - Electrode overheating

**Figure 1.** Typical welding flux requirements

**Notations**

$a$: Achievement or satisfaction function

$D$: Overall, global or composite desirability index

$I$: Set of responses, quality characteristics or objectives

$J$: Set of terms in the response functions/equations

$p$: A topological metric i.e. a real number belonging to the closed interval $[0,\infty]$

$Q$: Set of priority levels

$x$: *n*-dimensional decision/predictor variables

$C_s$: Set of feasible constraints

$d_i$: Desirability of response $i$, for each $i \in I$:

$DL_i$: Absolute distance between the value of response $i$ and its ideal value, for each $i \in I$

$DL_{ni}$: Normalized distance between the value of response $i$ and its ideal value, for each $i \in I$

$DL_p$: Composite/overall distance function for all normalized distances for metric $p$

$f_i(x)$: Regression equation/function for response $i$, for each $i \in I$:

$f_{qi}(x)$: Regression equation/function for response $i$, at priority level $q$, for each $i \in I$ and $q \in Q$

$f_i^*(x)$: Best, ideal or anchor value for response $i$, for each $i \in I$

$f_i^{**}(x)$: Worst, anti-ideal or nadir value for response $i$, for each $i \in I$

$L_i$: Lower limit for the value of response $i$, for each $i \in I$:

$L_{n\infty}$: Largest distance for $p = \infty$

$n_i$: Negative deviation/underachievement for response $i$, for each $i \in I$:

$n_{qi}$: Negative deviation/underachievement for response $i$, at priority level $q$ for each $i \in I$ and $q \in Q$

$p_i$: Positive deviation/overachievement of response $i$, for each $i \in I$:

$p_{qi}$: Positive deviation/overachievement for response $i$, at priority level $q$, for each $i \in I$ and $q \in Q$

$s_i$: Is an exponent chosen to reflect how rapidly the deviation from the target value of response $i$ towards its lower limit becomes undesirable, for each $i \in I$

$t_i$: Is an exponent chosen to reflect how rapidly the deviation from the target value of response $i$ becomes undesirable, for each $i \in I$

$T_i$: Target value/aspiration level for response $i$, for each $i \in I$:

$U_i$: Upper limit for response $i$, for each $i \in I$:

$u_i$ : Weight assigned to the negative deviation of response $i$, for each $i \in I$ :

$u_{qi}$ : Weight assigned to the negative deviation of response $i$, for priority level $q$ for each $i \in I$ and $q \in Q$

$v_i$ : Weight assigned to the positive deviation of response $i$, for each $i \in I$ :

$v_{qi}$ : Weight assigned to the positive deviation of response $i$, for priority level $q$ , for each $i \in I$ and $q \in Q$

$w_i$ : Weight assigned to response/objective $i$, for each $i \in I$ :

$Z_q$ : Achievement/satisfaction function for priority level $q$ , for each $q \in Q$

$Z_q^*$ : Optimal value of the satisfaction/achievement function for priority level $q$, for each $q \in Q$

$\beta_{ij}$ : Coefficient of term $j$ in response function $i$ , for each $j \in J$ and $i \in I$

$\gamma_i$ : Is an exponent chosen to reflect how rapidly the deviation from the target value of response $i$ towards its upper limit becomes undesirable, for each $i \in I$

**Scalarization Techniques**
We shall discuss two types of scalarization techniques, namely;

- Linear Aggregation/ Weighted Sum Scalarization (WSS)
- Nonlinear Aggregation (Desirability indices)

**Linear aggregation/weighted sum scalarization (WSS)**
The WSS approach consists of adding all the response equations together using a weighting coefficient, $w_i$ for each response. The weighting coefficient denotes the relative importance of the responses. Since a minimizing objective can be converted to a maximizing objective by multiplying it by -1, the multi-objective optimization problem can be transformed into a single/combinational problem of the form below without any loss of generality.

$$\max imize, WSS = \sum_{i \in I} w_i f_i(x)$$

Subject to

$$x \in C_s \tag{1}$$

Where $w_i > 0, \forall i$ and $\sum_{i \in I} w_i = 1$

Consider a case where the WFD wants to decide the flux ingredient levels that will give the best compromise flux formulation given the following objectives;

a. Maximize acicular ferrite (AF) content, $f_1(x)$

b. Maximize charpy impact toughness, $f_2(x)$

c. Minimize diffusible hydrogen content, $f_3(x)$

Once the response equations have been established according to steps i to vii in section 2 above, the WSS may be used to achieve the desired flux component levels as follows;

**Step 1:** Convert the minimizing objective, $f_3(x)$ to maximizing objective by multiplying it by –1 (i.e. minimize $f_3(x) = \text{maximize} - f_3(x)$).

**Step 2:** Normalize the objectives. This is necessary because the objective/response functions have different units. For instance the unit of AF in the microstructure is in fractions (%), diffusible hydrogen is in mL per 100 g of weld-metal, while that of charpy impact toughness is in joules. In such cases the WFD must first convert all objectives into the same dimensions or dimensionless before combining them into one. Also the values of different functions or the coefficients of the terms in the functions may have different order of magnitude. Consider the hypothetical response/objective functions

$$f_1(x) = 0.5x_1 + 0.2x_2 + 0.8x_1x_2$$
$$f_2(x) = 16.5x_1 + 25.0x_2 + 20.8x_1x_2$$

Using the WSS approach without normalization may lead to a situation where $f_2(x)$ dominates $f_1(x)$. Therefore, if we want $w_i$ to closely reflect the relative importance of the functions, all functions must be expressed in units of approximately the same numerical value. The objective functions may be converted to their normal forms as follows; [31, 32]

Normal form of:

$$f_i(x) = \left( w_i \Big/ \sqrt{\sum_{j \in J} \beta_{ij}^{\,2}} \right) f_i(x) \; ; \qquad (2)$$

for each $i \in I$ and $j \in J$

**Step 3:** Aggregate the objective functions into a single function as follows and add the structural constraints;

$$Maximize, WSS = \sum_{i \in I} \left( w_i \Big/ \sqrt{\sum_{j \in J} \beta_{ij}^{\,2}} \right) f_i(x)$$

Subject to; (3)

$x \in C_s$

Note that each minimizing objective must be converted to maximizing objective before combining them into one.

**Step 4:** Solve the resulting model using the appropriate software or algorithm.

The WSS method is suitable for flux design situations in which the WFD is interested in determining flux ingredient levels that maximizes desirable quality characteristics while at the same it minimizes undesirable characteristics. Trade-off options may be explored by the WFD by using various weight structures.

**Nonlinear aggregation (desirability indices)**

Instead of linear aggregation the WFD can use nonlinear aggregation methods such as computing the product of the objective functions values which is a modelling approach based on the theory of utility functions. A utility function assigns to each combination of values that may occur in the response space a scalar value- the so called utility. We discuss the commonest of the nonlinear aggregation method and how it can be applied in welding flux design. The desirability function (DF) approach is very common among the nonlinear aggregation methods. It was first proposed by Harrington[33] and further modified by Derringer and SUICH[34] and Kim and LIN[35]. In the DF approach, the quality of a compromise/balance between the responses can be measured by the desirability concept. The adequacy of each of the responses, $f_i(x)$ are first quantified by a value $d_i$ between 0 and 1. A desirability of zero (i.e. $d_i = 0$) represents a property level that is expected to render the welding flux unacceptable for use. A desirability of 1(i.e. $d_i = 1$) represents a property level at which the specifications of the WFD is perfectly satisfied. The procedure a WFD may follow to determine the factor setting that give the best compromise flux formulation are presented below:

**Step 1:** Transform each response $f_i(x)$ to the same scale using a desirability function denoted by $d_i$, such that $d_i \in [0,1]$. If $d_i = 0$, the welding flux is not at all acceptable according to the specifications of i[th] response and if $d_i = 1$, the welding flux satisfies the specifications completely. There are many forms of desirability function which the WFD may use depending on the goal of optimization. Generally, the goal of optimization is to maximize desirable responses, minimize undesirable responses and hit the target level of some. Derringer and Suich[34] desirability functions are the most widely used and are presented below.

***(i) The Larger-the-best (LTB) Case:*** In the LTB case the WFD is interested in maximizing the response. For instance, studies have shown that the larger the amount of AF in the microstructure the better for low alloy C-Mn steels, deep penetration is also desirable, etc … For such cases the individual desirability function is given by;

$$d_i = \begin{cases} 0, & f_i(x) < L_i \\ \left( \dfrac{f_i(x) - L_i}{T_i - L_i} \right)^{t_i}, & L_i \le f_i(x) \le T_i \\ 1, & f_i(x) > T_i \end{cases},$$

for each $i \in I$ (4)

With $T_i$ in this case denoting large enough value for the i$^{th}$ response. That is a property level at which a small increase will not further improve the flux. It may be fixed based on previous experience, preliminary experiment, literature, etc ...

***(ii) The Smaller-the-best (STB) Case:*** For responses such as diffusible hydrogen, fume generation, toxic content of fume, spatter, etc…the smaller their amount the better. WFDs usually aim at welding fluxes that minimizes such responses. The desirability function for such responses is given by;

$$d_i = \begin{cases} 1, & f_i(x) < T_i \\ \left( \dfrac{f_i(x) - U_i}{T_i - U_i} \right)^{t_i}, & T_i \le f_i(x) \le U_i \\ 0, & f_i(x) > U_i \end{cases}$$

for each $i \in I$ (5)

With $T_i$ in this case representing small enough value for the response at which a small decrease will not further improve the welding flux. $t_i$ is suitably chosen to reflect rapidly the deviation from the target becomes undesirable.

***(iii)Nominal-the-best (NTB):*** In the case of NTB, the specifications consist of a target value $T_i$ and the deviations around it are minimized. $d_i$ takes the value of 1 if the quality characteristic attains the target value and decreases if it deviates from the target. If $T_i$ lies on the midpoint i.e. $\dfrac{U_i + L_i}{2}$ of the speci

fication interval, the specification is called a two-sided symmetric specification, otherwise a two-sided asymmetric specification. The desirability function is expressed as;

$$d_i = \begin{cases} \left( \dfrac{f_i(x) - L_i}{T_i - L_i} \right)^{s_i}, & L_i \le f_i(x) \le T_i \\ \left( \dfrac{f_i(x) - U_i}{T_i - U_i} \right)^{r_i}, & T_i \le f_i(x) \le U_i \\ 0, & otherwise \end{cases}$$

for each $i \in I$ (6)

$s_i$ and $\gamma_i$ are suitably chosen to reflect how rapidly a deviation from the target becomes undesirable.

**Step 2:** Construct the overall (i.e. global/composite) desirability index D. This can be done by aggregating the individual $d_i$ in a single value, D, still in the $[0,1]$ interval representing the overall desirability of the welding flux. The most widely used composite desirability is the weighted geometric mean given by;

$$D = \left[ \prod_{i \in I} d_i^{w_i} \right]^{1 / \sum_{i \in I} w_i} \tag{7}$$

Where, $w_i$ is a weighting coefficient indicating the relative importance of the $i^{th}$ response and $\sum_{i\in I} w_i = 1$

**Step 3:** Find the flux ingredient levels that maximizes the overall desirability D, in the domain of interest, that is;

$$\max imize, D = \left[\prod_{i\in I} d_i^{\,w_i}\right]^{1/\sum_{i\in I} w_i} \qquad (8)$$

Subject to;

$x \in C_s$

**Step 4:** Use the flux ingredient levels of step 3 to formulate the welding flux. If the WFD wants to explore the available trade-off options, then various values of $w_i$, $s_i$ and $\gamma_i$ are used and the WFD selects the solution that best suits his needs.

## Goal Programming (GP)

The GP approach is suitable for welding flux design situation where the WFD has some specific numeric values (target values) established for the quality characteristics/responses and wants a welding flux formulation that minimizes the weighted some of the deviations of the quality characteristics from their respective target values. There are two cases of GP, namely; (i) Non pre-emptive Goal Programming (NGP) (ii) Pre-emptive Goal Programming (PGP).

**(i) Nonpre-emptive goal programming (NGP):**

In NGP, the quality characteristics/responses are presumed to be of roughly comparable importance. Since it is not possible to achieve all the goals because of their conflicting nature, there will be deviations from their target values for all or some of the responses. These deviations are unwanted and therefore, they should be minimized. The unwanted deviations are assigned weights according to their relative importance to the WFD and minimized as an Archimedian sum. The specific steps the WFD may follow are as follows:

**Step 1:** Establish the desired target levels ($T_i, L_i \,\&\, U_i$) for each of the responses/quality characteristics, (e.g. acicular ferrite ≥50 %, oxygen content is 240 μL/L and diffusible hydrogen content $\leq 8$ mL per 100 g).

**Step 2:** Assign weights to each response and their respective negative ($n_i$) and positive ($p_i$) deviations

**Step 3:** Construct the goal constraints of the problem. The goal constraint is usually given by;

$$f_i(x) + n_i - p_i = T_i, L_i, or U_i$$

for each $i \in I$ (9)

**Step 4:** Construct the achievement function of each response as illustrated in the table below.

**Table 1.** Construction of achievement function

| Objective | Description | Achievement Function |
|---|---|---|
| $f_i(x) \geq L_i$ | Under-achievement or negative ($n_i$) deviation (i.e. values below $L_i$) is unwanted and must be minimised. | Minimize $n_i$ |
| $f_i(x) \leq U_i$ | Over-achievement or positive deviation ($p_i$) (i.e. values above $U_i$) is unwanted and must be minimised. | Minimize $p_i$ |
| $f_i(x) = T_i$ | Both negative ($n_i$) and positive ($p_i$) deviations are unwanted and must be minimised | Minimize($n_i + p_i$) |

**Step 5:** Construct the overall achievement function and add the goal constraints to the structural constraints of the problem. The complete NGP model of the problem may be stated as;

$$\min imize, a = \sum_{i \in I} (u_i n_i + v_i p_i)$$

Subject to;

$$f_i(x) + n_i - p_i = T_i, L_i, or U_i$$

$$\text{for each } \; i \in I \qquad (10)$$

$$x \in C_s$$

$$n_i \times p_i = 0 \; \text{ for each } \; i \in I$$

(It is not possible to have both $p_i$ and $n_i$ together for any response $i$). The weights $u_i$, $v_i$ take the value zero if the minimization of the corresponding deviational variable is not important to the WFD.

**Step 6:** Solve the model in step 5 to find the flux ingredient levels that minimizes the weighted sum of the deviations.

**Step 7:** Use the values obtained to develop the needed welding flux. Trade-off exploration may be achieved by using different weight structures.

**(ii) Pre-emptive goal programming (PGP)**

The PGP method is suitable for welding flux formulation situation in which some quality characteristics/responses are of overwhelming importance when compared to others. There is a hierarchy of priority levels for the responses, so that the responses of primary importance receive first priority attention, those of secondary importance receive second priority attention and so forth.

The achievement function is minimized in a lexicographic sense. A lexicographic minimization may be defined as a sequential minimization of each priority while maintaining the minimal value $Z_q^*$ reached by all higher priority level minimization. The steps the WFD may follow are the same as that of NGP except that in step 5, a hierarchy of priority levels are established and the solution is in sequential order.

**Step 5:** Establish the priorities in hierarchical order and construct the achievement or satisfaction function, $Z_q$ for each priority level as below;

$$Z_q = \sum_{i \in I} (u_{qi} n_i + v_{qi} p_i) \tag{11}$$

for each $q \in Q$ and $Q \leq I$

The weights $u_{qi}$ and $v_{qi}$ take the value zero if the minimization of the corresponding deviational variable is not important to the WFD at that priority level.

**Step 6:** Minimize the achievement/ satisfaction function in lexicographic order i.e.

$$lex \min \lfloor z_1, z_2, ......z_Q \rfloor$$

Subject to;

$x \in C_s$ (Structural constraints) (12)

$f_{qi}(x) + n_{qi} - p_{qi} = T_{qi}, L_{qi}, or U_{qi}$ (Goals on the $q^{th}$ priority level) for each $i \in I$ and $q \in Q$

$z_j = z_j{}^*$ for j=1 to q-1(Solutions of higher level priorities).

Where, $z_1 >>> z_2 ... >>> z_Q$ and $z_j{}^*$ is the optimal level that was achieved for the achievement function $z_j$ of any priority level $j < q$.

When we deal with goals on the same priority level, the approach is just like the one described for NGP. The solution methodology ensures that the optimal solution of a higher priority goal is not sacrificed in order to achieve a lower priority goal. For each priority level, $z_q$ is minimized while requiring that all higher priority satisfaction or achievement levels are maintained as hard constraints.

**Step 7:** use the values obtained from the solution of the last priority level to develop the needed welding flux. Trade-off options or sensitivity analysis are done by using different weight structures within priority levels and different priority structures for the responses.

**Compromise Programming (CP)**

Compromise Programming (CP) was first proposed by ZELENY[36, 37] and subsequently used by many researchers.[38, 39] CP identifies the best compromise solution as the one that has the shortest distance to an ideal point where the multiple objectives/ responses simultaneously reach their optimum values. The ideal point is not practically achievable but may be used as a base point. The operative structure of CP may be summarised in the following way;

**Step 1:** For each response function, determine the ideal (best or anchor) value $f_i^*(x)$ and the anti-ideal (worst or nadir) value $f_i^{**}(x)$ within the solution space for each $i \in I$ .

**Step 2:** Define the distance or degree of closeness $DL_i$ between the $i^{th}$ response and its ideal value. The distance is defined by $DL_i = f_i^*(x) - f_i(x)$ when the $i^{th}$ response is maximized or as $DL_i = f_i(x) - f_i^*(x)$ when the $i^{th}$ response is minimized. When the units used to measure the responses are different (e.g. acicular ferrite (%), toughness (joules), yield strength (kN/mm$^2$), diffusible hydrogen (mL per 100 g)…) normalised distances rather than the absolute deviations must be used (ROMERO et al, 1987). Thus the normalised degree of closeness is given by;

$$DL_{ni} = \frac{f_i^*(x) - f_i(x)}{f_i^*(x) - f_i^{**}(x)}, \text{ for each } i \in I \tag{13}$$

**Step 3:** Construct the composite function of the normalized distances. The corresponding composite distance functions are introduced through a family of p-metrics. The basic structure of the composite function is given by;

$$DL_p = \left[ \sum_{i \in I} \left( w_i^p \left( \frac{f_i^*(x) - f_i(x)}{f_i^*(x) - f_i^{**}(x)} \right)^p \right) \right]^{1/p} \tag{14}$$

P= a topological metric i.e. a real number belonging to the closed interval $[0, \infty]$

**Step 4:** Seek the solution that minimizes $DL_p$. The problem may be stated as;

$$Minimize, DL_p = \left[ \sum_{i \in I} \left( w_i^p \left( \frac{f_i^*(x) - f_i(x)}{f_i^*(x) - f_i^{**}(x)} \right)^p \right) \right]^{1/p} \tag{15}$$

Subject to,

$x \in C_s$

***$L_1$ metric (p = 1)***: The equation (15) above is the general model. If the WFD considers all distances from the ideal point to be of equal importance, then $p = 1$ and the best compromise flux formulation is obtained by solving;

$$\min imize, DL_1 = \sum_{i \in I} w_i \left( \frac{f_i^*(x) - f_i(x)}{f_i^*(x) - f_i^{**}(x)} \right) \quad (16)$$

Subject to,

$x \in C_s$

***$DL_\infty$ metric ($p$=∞):*** If only the largest deviation counts to the WFD, then the problem becomes a min-max problem and $p = \infty$. The WFD determines the best compromise flux formulation by solving;

$$\min imize, D_\infty = L_{n\infty}$$

Subject to;

$$w_1 \left( \frac{f_i^*(x) - f_i(x)}{f_i^*(x) - f_i^{**}(x)} \right) \le L_{n\infty} \quad (17)$$

$$w_I \left( \frac{f_I^*(x) - f_I(x)}{f_I^*(x) - f_I^{**}(x)} \right) \le L_{n\infty}$$

$x \in C_s$

The other best compromise solutions fall between the solutions corresponding to $L_1$ and $L_\infty$. For instance if the WFD weighs each deviation in proportion to its magnitude, then $p = 2$ and equation (15) is solved to obtained the needed flux ingredient levels. The parameter p represents the concern of the WFD over the maximum deviation. The larger the value of $p$, the greater the concern becomes. As $p \to \infty$, the alternative with the largest deviation completely dominates the distance measure. Sensitivity analysis or trade-off exploration may be done by the WFD by using different values of $w_i$ and $p$.

## CONCLUSION

MODM methods that a WFD can integrate with mixture experiments to mitigate the limitations of the traditional welding flux design approach has been discussed. The following conclusions can be drawn from the study:

- If all the responses defining the quality of a welding flux are related to the same set of predictor variables and regression equations that capture the relationship between the predictor variables and response variables can be established, then the MODM method can be used to determine the best compromise welding flux formulation and also to explore various trade-off options.
- The WSS method is suitable for situations where the WFD is interested in minimizing undesirable responses while at the same time he wants to maximise desirable responses.
- Desirability indices method is suitable when the WFD wants to minimise some responses, maximise some and achieve target values for some simultaneously.

- NGP is suitable for cases where the WFD wants to achieve target values for the responses and the responses are of comparable importance.
- PGP is useful when the responses are in hierarchical order of importance and the WFD wants to achieve lower priority response(s) without sacrificing the achievement of higher priority response.
- CP is useful when the WFD wants a welding flux formulation that is closest to the ideal formulation.

This paper has not exhausted the MODM methods. Many other multi-objective methods such as reference point method and heuristics such as genetic algorithm, particle swarm optimization, tabu search, etc… may also be useful for welding flux formulation.

## Acknowledgement

This work was supported by MacArthur Foundation Grant University of Ibadan under the Staff Training and Research Capacity Building Programme.

## References

[1] Adeyeye, Ademola David & Festus A. Oyawale (2008): Mixture Experiments And Their Applications In Welding Flux Design. *Journal of the Brazilian Society of Mechanical Sciences and Engineering;* Vol. 30, No 4, pp. 319–326.

[2] Kanjilal, P., Majumder, S. K. & Pal, T. K. (2004): Prediction of Submerged Arc Weld-Metal Composition from Flux Ingredients with the Help of Statistical Design of Mixture Experiment. *Scandinavian Journal of Metallurgy*; Vol. 33, pp. 146–159.

[3] Kanjilal, P., Majumdar, S. K. & Pal, T. K. (2005): Prediction of Acicular Ferrite from Flux Ingredients in Submerged Arc Weld Metal of C-Mn Steel. *ISIJ International;* Vol.45, No. 6, pp. 876–885.

[4] Kanjilal, P., Pal, T. K. & Majumdar, S. K. (2006): Weld metal microstructure prediction in submerged arc weld metal of C-Mn steel. *Steel Researchinternational;* Vol. 77, No. 7, pp. 512–523.

[5] Kanjilal, P., Pal, T. K. & Majumdar, S. K. (2007): Prediction of Mechanical Properties in Submerged Arc Weld Metal of C-Mn Steel. *Materials and Manufacturing Processes;* Vol. 22, pp. 114–127.

[6] Kanjilal, P., Pal, T. K. & Majumdar, S. K. (2007): Prediction of Element Transfer in Submerged Arc Welding. *Welding Journal*; Vol.86, No. 5, pp. 135s–148s.

[7] Adeyeye, Ademola David & Festus Adekunle Oyawale (2009): Weld-metal Property Optimization from Flux Ingredients through Mixture Experiments and Mathematical Programming Approach. *Materials Research*; Vol. 12, No. 3, pp.

339–343.

[8] BENYOUNIS, K. Y. A. G. OLABI, M. S. J. HASHMI (2009): Mechanical Properties, Weld Bead And Cost Universal Approach For $CO_2$ Laser Welding Process Optimization. *International Journal of Computational Materials Science and Surface Engineering*. Vol. 2, No. 1–2, pp. 99–109.[9] ESME, U., A. KOKANGUL, M. BAYRAMOGLU, N. GEREN (2009): Mathematical Modeling for Prediction and Optimization of Tig Welding Pool Geometry. *Metalurgija*; Vol. 48, No. 2, pp. 109–112.

[10] GIRIDHARAN, P. K. & N. MURUGAN **(**2009**):** Optimization of Pulsed GTA Welding Process Parameters for The Welding of AISI 304L Stainless Steel Sheets. *The International Journal of Advanced Manufacturing Technology;* Vol. 40, No. 5–6, pp. 478–489.

[11] BRACARENSE, A. Q. & S. LIU (1993): Chemical Composition Variations in Shielded Metal Arc Welds. *Welding Journal*; Vol. 72, No. 12, pp. 529s–536s.

[12] BRACARENSE, A. Q & S. LIU (1994): Control of Covered Electrode Hearting by Flux Ingredients Substitution. *Welding and Metal Fabrication*; May, pp. 224–229.

[13] BRACARENSE, A. Q. & S. LIU (1997): Chemical Composition and Hardness Control by Endothermic Reactions in the Coating of Covered Electrodes. *Welding Journal*; Vol. 76, No. 13, pp. 509–515s.

[14] FLEMING, D. A., BRACARENSE, A. Q., LIU, S., OLSON, D. L. (1996): Toward developing a SMA welding electrode for HSLA-100 grade steel. *Welding Journal;* Vol. 75, No. 6, pp. 171s–183s.

[15] DE RISSONE, R. N. M., SURIAN, E. S., CONDE, R. H., DE VEDIA, L. A. (2001): Effect of Slag Variations on ANSI/AWS A5.1–91 E6013 Electrode Properties: Replacement of TiO2 in Electrode Coating with MnO, FeO, CaO**,** MgO, $K_2O$, or $Na_2O$. *Science and Technology of Welding & Joining;* Vol. 6, No. 5, pp. 323–329.

[16] DE RISSONE, N. M. R.; J. P. FARIAS, I. DE SOUZA BOTT & E. S. SURIAN (2002): ANSI/AWS A5.1-91 E6013 Rutile Electrodes: The Effect of Calcite. *Welding Journal;* Vol. 81, No. 7, pp 113s–124s.

[17] ZINIGRAD, MICHAEL (2006): Computational Methods for Development of New Welding Materials. *Coputational Materials Science;*Vol. 37, No. 4, pp. 417–424.

[18] GUNARAJ, V. & MURUGAN, N (2000): Prediction and Optimization of Weld Bead Volume for the Submerged Arc Process – Part 1. *Welding Journal;* Vol. 79, No. 10, pp. 286s–294s.

[19] GUNARAJ, V. & MURUGAN, N. (2000): Prediction and Optimization of Weld Bead Volume for the Submerged Arc Process – Part 2. *Welding Journal;* Vol. 79, No. 11, pp. 331s–338s.

[20] MAGE, I. & TORMAD NAES (2005):

Split-Plot Design for Mixture Experiments with Process Variables: A Comparison of Design Strategies. *Chemometrics and Intelligent Laboratory Systems;* Vol. 78, No. 1-2, pp. 81–95.

[21] Scheffe, H. (1958): Experiments with Mixtures. *Journal of the RoyalStatistical Society;* B20, pp. 344–360.

[22] Scheffe, H. (1963): The Simple-Centroid Design for Experiments with Mixtures. *Journal of the Royal Statistical Society;* B25, No. 2, pp. 235–263.

[23] Snee, R. D. E., & Marquardt, D. W. (1974): Extreme Vertices Designs for Linear Mixture Models. *Technometrics;* Vol. 16, No. 3, pp. 399–408.

[24] Piepel, G. F., & Cornell, J. A. (1987): Designs for Mixture-Amount Experiments. *Journal of Quality Technology;* Vol. 19, No. 1, pp. 11–28.

[25] Goldfarb, H. B., Borroo, C. M., & Montgomery, D. C. (2003): Mixture-Process Variable Experiments with Noise Variables. *Journal of Quality Technology*; Vol. 35, No. 4, pp. 393–405.

[26] Goldfarb, H. B., Borroo, C. M., Montgomery, D. C. & Anderson-Cook, C. M. (2004): Evaluating Mixture-Process Designs with Control and Noise Variables. *Journal of Quality Technology;* Vol. 36, No 3, pp. 245–262.

[27] Mclean, R. A. & Anderson, V. l. (1966): Extreme Vertices Design of Mixture Experiments. *Technometrics;* Vol. 8, pp. 447–456.

[28] Pepelyshev Andrey, Irene Poli & Viatcheslav Melas (2009): Uniform Coverage Designs for Mixture Experiments. *Journal of Statistical Planning and Inference*; Vol. 139, No. 10, pp. 3442–3452.

[29] Martin, R. J. , M. C. Bursnall & E. C. Stillman (1999): Efficient Designs for Constrained Mixture Experiments. *Statistics and Computing*; Vol. 9, No. 3, pp. 229–237.

[30] Ding, Jian-Tong., Yan, Pei-Yu., Liu, shu-Lin., & Zhu, Jin-Quan (1999): Extreme Vertices Design of Concrete with Combined Mineral Admixtures. *Cement and Concrete Research;* Vol. 29, No 6, pp. 957–960.

[31] Adulbhan P. & Tabucanon M. T. (1977): Bicriterion Linear Programming. *International Journal of Computer and Operations Research;* Vol. 4, No. 2, pp. 141–153.

[32] Adulbhan P. & Tabucanon M. T. (1979):A Biobjective Model for Production Planning in a Cement Factory. Vol 3, pp. 41–51.

[33] Harrington, E. C. (1965): The Desirability Function. *Industrial Quality Control;* Vol. 21, No. 10, pp. 494–498.

[34] Derringer, G. & Suich, R. (1980): Simultaneous Optimization of Several Response Variables. *Journal of Quality Technology*; Vol. 12, No. 4, pp. 214–219.

[35] Kim, K. J. & D. K. J., Lin (2000): Simultaneous Optimization of Mechanical Properties of Steel by Maxi-

mizing Exponential Desirability Functions. *Applied Statistics;* Vol. 49, No. 3, pp. 311–325.

[36] ZELENY, M. (1973): *Compromise Programming, Multiple-Criteria Decision Making*. Edited by J.L. Cochrane & M. Zeleny, University of South Carolina Press, Columbia, South Carolina, pp. 262–301.

[37] ZELENY, M. (1974): A Concept of Compromise Solution and the Method of the Displaced Ideal", *Computer & Operations Research;* Vol. 1, pp. 479–496.

[38] ALLOUCHE, MOHAMED ANIS BELAÏD AOUNI, JEAN-MARC MARTEL, TAÏCIR LOUKIL, & ABDELWAHEB REBAÏ (2009): Solving Multi-Criteria Scheduling Flow Shop Problem through Compromise Programming and Satisfaction Functions. *European Journal of Operational Research;* Vol. 192, No. 2, pp. 460–467.

[39] BALLESTERO, ENRIQUE (2007): Compromise Programming: A Utility-Based Linear-Quadratic Composite Metric from the Trade-Off between Achievement and Balanced (Non-Corner) Solutions. *European Journal of Operational Research*; Vol. 182, No. 3, pp. 1369–1382.

[40] ROMERO, CARLOS, FRANCISCO AMADOR & ANTONIO BARCO (1987): Multiple Objectives in Agricultural Planning: A Compromise Programming Application. *American Journal of Agricultural Economics;* Vol. 69, No. 1, pp. 78–86.

# The drilling and casing program for $CO_2$ storage

# Načrtovanje in izvedba globokih vrtin pri skladiščenju $CO_2$

Željko Vukelić[1,] *

[1]University of Ljubljana, Faculty of natural science, Aškerčeva cesta 12, SI-1000 Ljubljana, Slovenia

*Corresponding author. E-mail: zeljko.vukelic@ntf.uni-lj.si

**Received:** May 20, 2009 **Accepted:** November 6, 2009

**Abstract:** This paper deals with the design and construction of boreholes, with respect to geologic feasibilities of $CO_2$ injection into boreholes and rocks capable of taking in carbon dioxide. The boreholes have to be carried out by following appropriate technologic standards which only will ensure adequate and economic storing of $CO_2$. The objective is to reach the foreseen depth and 100 % air tight of the borehole. The design and construction of the boreholes for the underground $CO_2$ repository is extremely demanding. Each single phase has therefore to be accurately planned, this process requiring thorough work and high-expertise engineering solutions.

**Izvleček:** V članku obravnavam načrtovanje in izvedbo globokih vrtin glede na geološke pogoje za vtiskovanje $CO_2$ v vrtine oziroma v hribine, ki sprejemajo ogljikov dioksid. Vrtine je treba izdelati tehnološko korektno, kajti le tako je mogoče zagotoviti ustrezno in ekonomično skladiščenje $CO_2$. Z vrtinami je treba doseči predvideno globino in stoodstotno tesnitev vrtine. Projektiranje in izvedba vrtin za podzemno skladiščenju $CO_2$ je izjemno zahtevna. Zato je treba posamezno fazo izvedbe vrtine skrbno načrtovati, kar pa zahteva poglobljeno delo in kakovostne inženirske rešitve.

**Key words:** $CO_2$, borehole, construction, underground repository
**Ključne besede:** $CO_2$, vrtina, načrtovanje, podzemno skladišče

*Professional Paper*

## Introduction

This paper deals with the design and construction of boreholes, with respect to geologic feasibilities of $CO_2$ injection into boreholes and rocks capable of taking in carbon dioxide. The boreholes have to be carried out by following appropriate technologic standards which only will ensure adequate and economic storing of $CO_2$. The objective is to reach the foreseen depth and 100 % air tight of the borehole. The design and execution of boreholes have been limited to rotary drilling technique, suitable for the performance of deep boreholes.

## Principle of rotary drilling of deep boreholes

As a curiosity I should like to mention a case in Titusville, Pennsylvania, back in 1859, when oil flushed upon the surface from a 21 m deep borehole. Since then we have experienced huge development in the field of drilling, as oil deposits have been discovered at depths exceeding 1000 m. With rotary drilling technique a roller cone bit is being employed. When roller cone bit rotates, a force is applied to it by a weight. During drilling into rock, the roller cone bit is being cooled by mud, running continually through roller cone bit nozzles and flushing rock cuttings upon the surface. Special devices enable drilled rock cuttings to be removed from the mud, to be then returned purified into the borehole. As a rule, mud is being injected into the borehole by high-pressure piston pumps (Figure 2).

## Deep boreholes design and construction

When designing and executing deep boreholes for $CO_2$ repository, the foreseen depth into which $CO_2$ shall be injected, must be achieved. The main objectives of the borehole are:

- to install communication between surface and geologic structure (rock) underground
- to enable the injection of $CO_2$ into underground rock
- to ensure 100 % air tight of the borehole
- to enable monitoring

### Design of borehole performance

The depth of the borehole for $CO_2$ repository depends on the location of the underground repository, appearing at a certain depth below the surface. The average borehole depth is up to 2000 m, whereas boreholes from 3500 m to 4500 m are defined as very deep and boreholes exceeding 4500 m as extremely deep. A deep borehole design has to comprise the following aspects:

- general data of the borehole

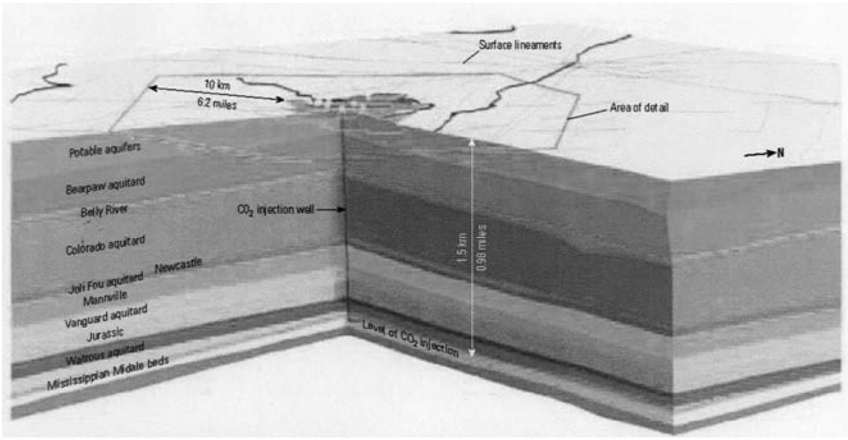


**Figure 1.** The principle of storing $CO_2$ through deep boreholes[2]

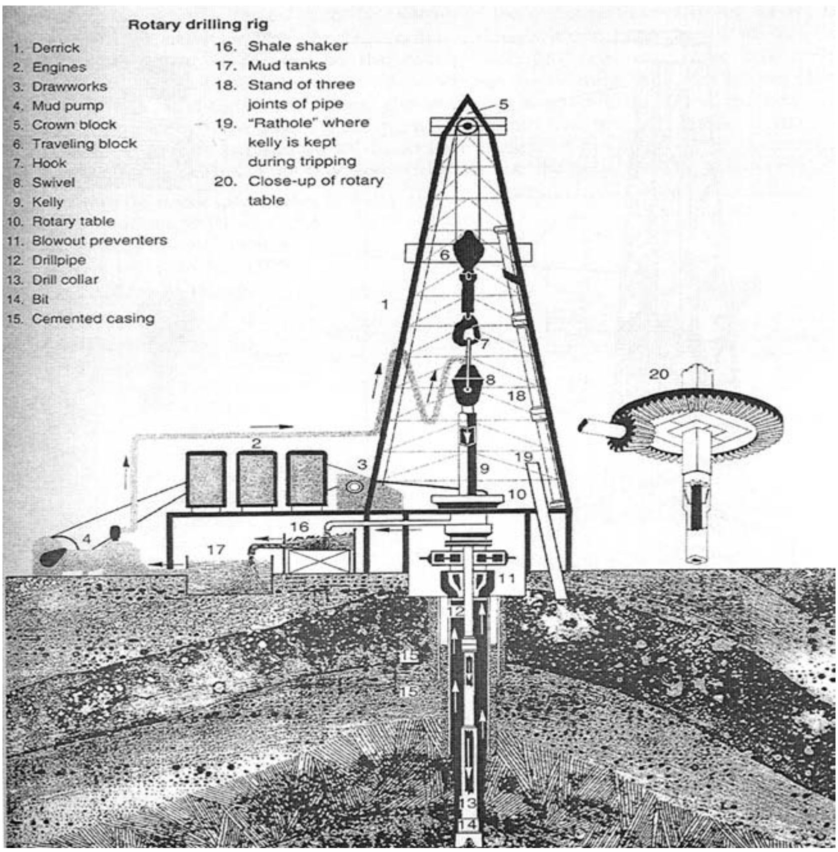


**Figure 2.** Drilling equipment for rotary drilling[1]

- program of the borehole performance
- method of drilling and borehole casing

***General data of boreholes***

The general data of the borehole have to be presented immediately after determining the location of the borehole performance. General data will help to define:

- borehole coordinates and location (place, country, etc.)
- purpose and scope of boring
- geology
- geophysics
- information on adjacent boreholes, if existing
- cost and time frame of the borehole construction

It is important, however, to make distinction between the boreholes with respect to their function, defining them as exploratory, monitoring or productive (boreholes with $CO_2$ injection) boreholes. Productive and monitoring boreholes must comprise precise geologic data and determine the method of construction, since all essential underground repository parameters have to be known. In the case of exploratory boreholes, however, frame parameters are adequate, as these will suffice for confirming or eliminating the location of the underground $CO_2$ repository.

***Program of the borehole performance***

This document is to be prepared after the investor has reached the decision on the borehole performance, this being already a constituent part of the contract between the investor and the client. This document shall be prepared by experts in the following fields:

- engineers who will determine the size of underground $CO_2$ storage
- engineers who will establish the functioning features of the underground $CO_2$ storage
- geologists
- engineers in charge of the boreholes construction

The main elements of the borehole design program are:

- micro location of the borehole mouth
- definition and purpose of the boring: exploratory, monitoring, productive
- precise geologic forecast
- precise description of geophysical data
- well logging measurements program (Gamma ray, resistivity, density, sonic, caliper)
- precise description of drilling and casing
- program of sampling and testing in the borehole
- borehole construction cost (cost

of preparing, transportation, daily operating cost, well casing cost, well cementing cost, well logging cost, etc.)
- timetable for the implementation of single phases of the borehole construction
- manpower
- drilling equipment and supplementary equipment for the borehole construction

***Drilling and borehole casing program***

The program of drilling and borehole casing program is the most important document for the construction of the borehole underground repository of $CO_2$. The construction of the borehole has to make possible the reaching of foreseen depths of the underground $CO_2$ repository. An efficient program of the drilling and borehole casing program is essential for a competent, safe and economic borehole construction. The borehole design and construction must consider the following technical feasibilities:
- choice of the roller cone bit diameter for drilling and drilling pipes
- number of different diameters of borehole casing
- method of cementing the annulus between pipes and borehole

Depending on the final depth of the boreholes, consideration needs to be given to optimum ratio between the borehole diameter and pipes in the borehole, where the following graph (Figure 3) can be of assistance:

In practice, however, when designing deep boreholes, either for oil and gas exploration or for underground $CO_2$ storing, we usually encounter the following performance technique, as shown in Figure 4.

It has to be pointed out that along with applying of high quality steel casing, the cementing of interspaces between pipes and borehole-wall has to be thoroughly planned, as perfect setting must be ensured, since $CO_2$ is injected with pressures exceeding several 100 bar. The cementing is being carried out applying cement slurry of a density of up to 1800 kg/m$^3$, respectively by water: cement ratio between 0.35 and 0.5 (1000 kg cement/500 L water). With deep boreholes, chemicals are added into cement slurry against its hardening due to increased temperatures in the borehole, and against increasing of its density. By applying these admixtures, the appropriate rheological parameters of the cement slurry are achieved, assuring satisfactory cementing of casing and consequently satisfactory borehole performance (Figure 5).

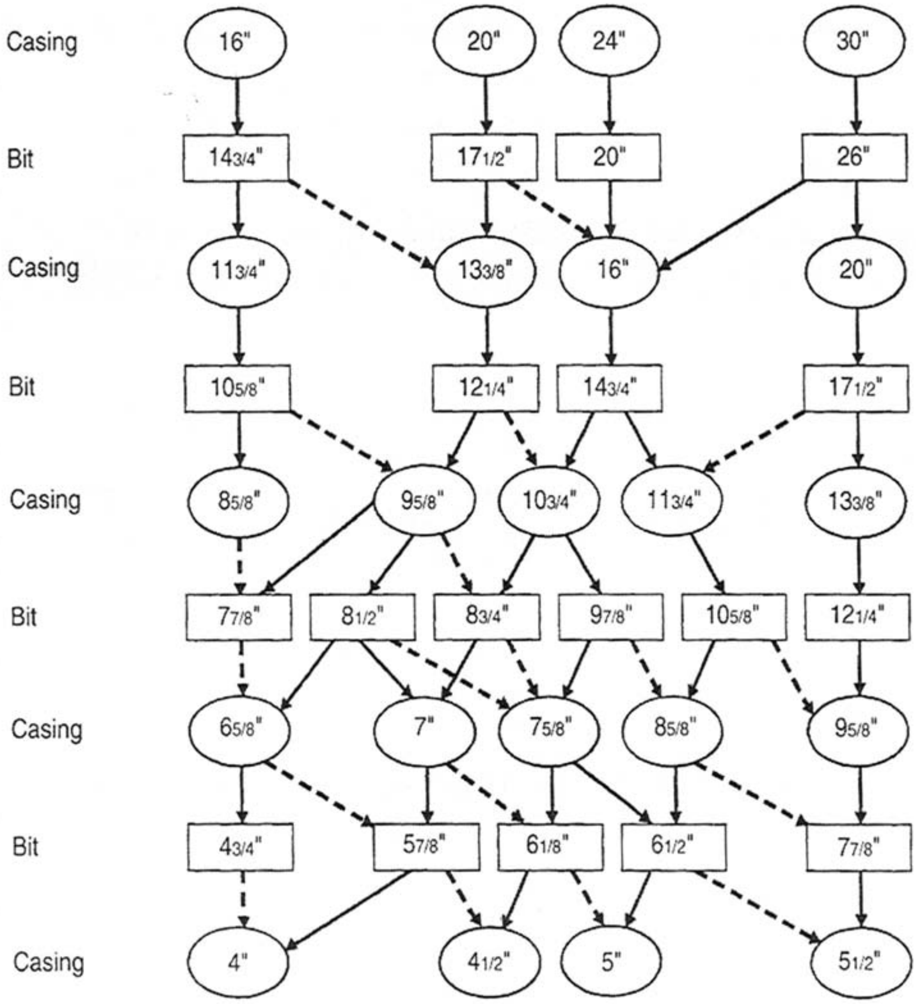


**Figure 3.** Optimum ratio between the drilling diameter and casing[1]

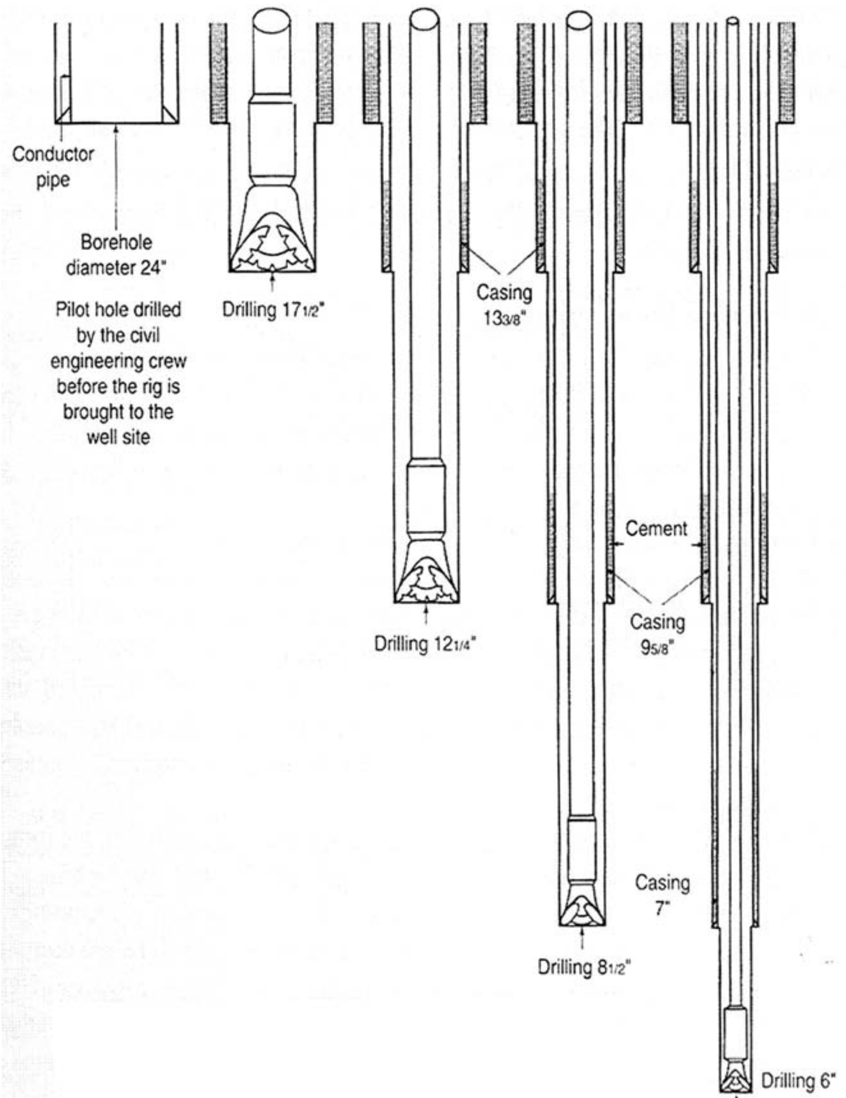


**Figure 4.** The construction of the borehole for underground storage of $CO_2$[1]

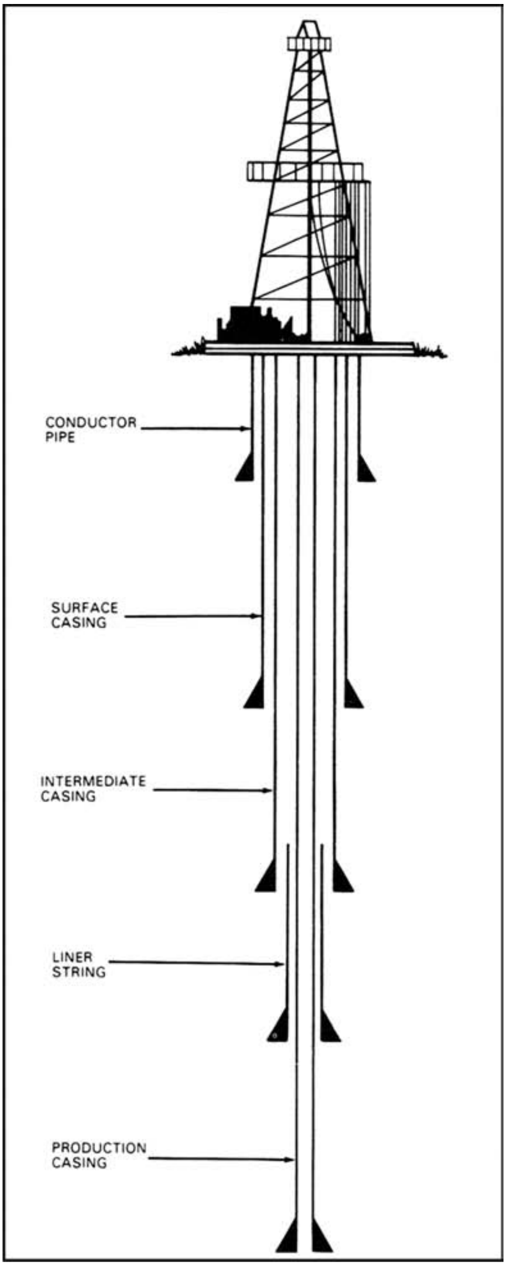


**Figure 5.** Final performance of the borehole for underground storage of $CO_2$[3]

## CONCLUSION

This paper presents an overview of the design and construction of deep boreholes for the underground storage of $CO_2$. I have presented the principles of designing the boreholes and the way of their implementation in practice. The design and construction of the boreholes for the underground $CO_2$ repository is extremely demanding. Each single phase has therefore to be accurately planned, this process requiring thorough work and high-expertise engineering solutions.

## REFERENCES

[1] J. P. NGUYEN: Drilling, Editions TECHNIP, 1996, Paris.

[2] www.greenfacts.org: $CO_2$ Capture and Storage, 2005.

[3] VUKELIČ, Ž., ŠPORIN, J.: *Rešene naloge iz vrtalne tehnike in projekt vrtine*, Ljubljana: Naravoslovnotehniška fakulteta, Oddelek za geotehnologijo in rudarstvo, 2007.

# Author`s Index, Vol. 57, No. 2


| | |
|---|---|
| Adeyeye Ademola David | ademola.adeyeye@mail.ui.edu.ng |
| Bombač David | david.bombac@ntf.uni-lj.si |
| Choubey V. K. | |
| Dervarič Evgen | evgen.dervaric@ntf.uni-lj.si |
| Fajfar Peter | peter.fajfar@ntf.uni-lj.si |
| Kovačič Miha | miha.kovacic@store-steel.si |
| Lajlar Bojan | bojan.lajlar@rlv.si |
| Likar Jakob | jakob.likar@ntf.uni-lj.si |
| Malenković Vladimir | vladimir.malenkovic@rlv.si |
| Malina Jadranka | |
| Markoli Boštjan | bostjan.markoli@ntf.uni-lj.s |
| Medved Milan | milan.medved@rlv.si |
| Oyawale Festus Adekunle | |
| Purandara B. K. | purandarabk@yahoo.com |
| Rađenović Ankica | |
| Šmuc Andrej | andrej.smuc@ntf.uni-lj.si |
| Štrkalj Anita | strkalj@simet.hr |
| Venkatesh B. | |
| Vukelić Željko | zeljko.vukelic@ntf.uni-lj.si |

# INSTRUCTIONS TO AUTHORS

**RMZ-MATERIALS & GEOENVIRONMENT** (RMZ- Materiali in geookolje) is a periodical publication with four issues per year (established 1952 and renamed to RMZ-M&G in 1998). The main topics of contents are Mining and Geotechnology, Metallurgy and Materials, Geology and Geoenvironment.

**RMZ-M&G** publishes original Scientific articles, Review papers, Preliminary notes, Professional papers **in English**. In addition, evaluations of other publications (books, monographs,...), In memoriam, Professional remarks and reviews are welcome. The Title, Abstract and Key words in Slovene will be included by the author(s) or will be provided by the referee or the Editorial Office.

**** Additional information and remarks for Slovenian authors:***
*Only Professional papers, Publications notes, Events notes, Discussion of papers and In memoriam, will be exceptionally published in the Slovenian language.*

**Authorship and originality** of the contributions. Authors are responsible for originality of presented data, ideas and conclusions as well as for correct citation of data adopted from other sources. The publication in RMZ-M&G obligate authors that the article will not be published anywhere else in the same form.

## Specification of Contributions

*RMZ-M&G will publish papers of the following categories:*

*<u>Full papers</u> (optimal number of pages is 7 to 15, longer articles should be discussed with Editor prior to submission). An abstract is required.*

- **Original scientific papers** represent unpublished results of original research.
- **Review papers** summarize previously published scientific, research and/or expertise articles on the new scientific level and can contain also other cited sources, which are not mainly result of author(s).

- **Preliminary notes** represent preliminary research findings, which should be published rapidly.
- **Professional papers** are the result of technological research achievements, application research results and information about achievements in practice and industry.

*Short papers (the number of pages is limited to 1 for Discussion of papers and 2 pages for Publication note, Event note and In Memoriam). No abstract is required for short papers.*

- **Publication notes** contain author's opinion on new published books, monographs, textbooks, or other published material. A figure of cover page is expected.
- **Event notes** in which descriptions of a scientific or professional event are given.
- **Discussion of papers (Comments)** where only professional disagreements can be discussed. Normally the source author(s) reply the remarks in the same issue.
- **In memoriam** (a photo is expected).

**Supervision and review of manuscripts.** All manuscripts will be supervised. The referees evaluate manuscripts and can ask authors to change particular segments, and propose to the Editor the acceptability of submitted articles. Authors can suggest the referee but Editor has a right to choose another. **The name of the referee remains anonymous.** The technical corrections will be done too and authors can be asked to correct missing items. The final decision whether the manuscript will be published is made by the Editor in Chief.

## The Form of the Manuscript

The manuscript should be submitted as a complete hard copy including figures and tables. The figures should also be enclosed separately, both charts and photos in the original version. In addition, all material should also be provided in electronic form on a diskette or a CD. The necessary information can conveniently also be delivered by E-mail.

## Composition of manuscript is defined in the attached Template

The original file of Template is available on RMZ-Materials and Geoenvironment Home page address:

**http://www.rmz-mg.com**

**References** - can be arranged in two ways:
- first possibility: alphabetic arrangement of first authors - in text: (Borgne, 1955), or
- second possibility: [1] numerated in the same order as cited in the text: example[1]

Format of papers in journals:

Le Borgne, E. (1955): Susceptibilite magnetic anomale du sol superficiel. *Annales de Geophysique*, 11, pp. 399–419.

Format of books:

Roberts, J. L. (1989): Geological structures, *MacMillan*, *London*, 250 p.

**Text** on the hard print copy can be prepared with any text-processor. The electronic version on the diskette, CD or E-mail transfer should be in MS Word or ASCII format.
**Captions of figures and tables** should be enclosed separately.
**Figures (graphs and photos)** and tables should be original and sent separately in addition to text. They can be prepared on paper or computer designed (MSExcel, Corel, Acad).
**Format.** Electronic figures are recommended to be in CDR, Al, EPS, TIF or JPG formats. Resolution of bitmap graphics (TIF, JPG) should be at least 300 dpi. Text in vector graphics (CDR, Al, EPS) must be in MSWord Times typography or converted in curves.
**Color prints.** Authors will be charged for color prints of figures and photos.
**Labeling** of the additionally provided material for the manuscript should be very clear and must contain at least the lead author's name, address, the beginning of the title and the date of delivery of the manuscript. In case of an E-mail transfer the exact message with above asked data must accompany the attachment with the file containing the manuscript.

**Information** about RMZ-M&G:
Editor in Chief prof. dr. Peter Fajfar (phone: ++386 1 4250-316) or
Secretary Barbara Bohar Bobnar, univ. dipl. ing. geol. (phone: ++386 1 4704-630),
Aškerčeva 12, 1000 Ljubljana, Slovenia
or at E-mail addresses:
peter.fajfar@ntf.uni-lj.si,
barbara.bohar@ntf.uni-lj.si

**Sending of manuscripts.** Manuscripts can be sent by mail to the **Editorial Office** address:

- RMZ-Materials & Geoenvironment
  Aškerčeva 12,
  1000 Ljubljana, Slovenia

or delivered to:

- **Reception** of the Faculty of Natural Science and Engineering (for RMZ-M&G)
  Aškerčeva 12,
  1000 Ljubljana, Slovenia
- E-mail - addresses of Editor and Secretary
- You can also contact them on their phone numbers.

*These instructions are valid from August 2009*

# NAVODILA AVTORJEM

**RMZ-MATERIALS AND GEOENVIRONMENT** (RMZ- Materiali in geookolje) – kratica RMZ-M&G - je revija (ustanovljena kot zbornik 1952 in preimenovana v revijo RMZ-M&G 1998), ki izhaja vsako leto v štirih zvezkih. V reviji objavljamo prispevke s področja rudarstva, geotehnologije, materialov, metalurgije, geologije in geookolja.

**RMZ- M&G objavlja izvirne znanstvene, pregledne in strokovne članke ter predhodne objave samo v angleškem jeziku. Strokovni članki so lahko izjemoma napisani v slovenskem jeziku.** Kot dodatek so zaželene recenzije drugih publikacij (knjig, monografij …), nekrologi In Memoriam, predstavitve znanstvenih in strokovnih dogodkov, kratke objave in strokovne replike na članke objavljene v RMZ-M&G v slovenskem ali angleškem jeziku. Prispevki naj bodo kratki in jasni.

**Avtorstvo in izvirnost** prispevkov. Avtorji so odgovorni za izvirnost podatkov, idej in sklepov v predloženem prispevku oziroma za pravilno citiranje privzetih podatkov. Z objavo v RMZ-M&G se tudi obvežejo, da ne bodo nikjer drugje objavili enakega prispevka.

## Vrste prispevkov

*Optimalno število strani je 7 do 15, za daljše članke je potrebno soglasje glavnega urednika.*

**Izvirni znanstveni članki** opisujejo še neobjavljene rezultate lastnih raziskav.

**Pregledni članki** povzemajo že objavljene znanstvene, raziskovalne ali strokovne dosežke na novem znanstvenem nivoju in lahko vsebujejo tudi druge (citirane) vire, ki niso večinsko rezultat dela avtorjev.

**Predhodna objava** povzema izsledke raziskave, ki je v teku in zahteva hitro objavo.

**Strokovni članki** vsebujejo rezultate tehnoloških dosežkov, razvojnih projektov in druge informacije iz prakse.

**Recenzije** publikacij zajemajo ocene novih knjig, monografij, učbenikov, razstav …(do dve strani; zaželena slika naslovnice in kratka navedba osnovnih podatkov - izkaznica).

**In memoriam** (do dve strani, zaželena slika).
**Strokovne pripombe** na objavljene članke ne smejo presegati ene strani in opozarjajo izključno na strokovne nedoslednosti objavljenih člankov v prejšnjih številkah RMZ-M&G. Praviloma že v isti številki avtorji prvotnega članka napišejo odgovor na pripombe.
**Poljudni članki**, ki povzemajo znanstvene in strokovne dogodke (do dve strani).

**Recenzije.** Vsi prispevki bodo predloženi v recenzijo. Recenzent oceni primernost prispevka za objavo in lahko predlaga kot pogoj za objavo dopolnilo k prispevku. Recenzenta izbere Uredništvo med strokovnjaki, ki so dejavni na sorodnih področjih, kot jih obravnava prispevek. Avtorji lahko sami predlagajo recenzenta, vendar si uredništvo pridržuje pravico, da izbere drugega recenzenta. **Recenzent ostane anonimen**. Prispevki bodo tudi tehnično ocenjeni in avtorji so dolžni popraviti pomanjkljivosti. Končno odločitev za objavo da glavni in odgovorni urednik.

## Oblika prispevka

Prispevek predložite v tiskanem oštevilčenem izvodu (po možnosti z vključenimi slikami in tabelami) ter na disketi ali CD, lahko pa ga pošljete tudi prek E-maila. Slike in grafe je možno poslati tudi risane na papirju, fotografije naj bodo originalne.

## Razčlenitev prispevka:

Predloga za pisanje članka se nahaja na spletni strani:

http://www.rmz-mg.com/predloga.htm

**Seznam literature** je lahko urejen na dva načina:
-po abecednem zaporedju prvih avtorjev ali
-po [1]vrstnem zaporedju citiranosti v prispevku.

Oblika je za oba načina enaka:
Članki:

Le Borgne, E. (1955): Susceptibilite magnetic anomale du sol superficiel. *Annales de Geophysique*; Vol. 11, pp. 399–419.

Knjige:

ROBERTS, J. L. (1989): Geological structures, *MacMillan*, *London*, 250 p.

**Tekst** izpisanega izvoda je lahko pripravljen v kateremkoli urejevalniku. Na disketi, CD ali v elektronskem prenosu pa mora biti v MS Word ali v ASCII obliki.
**Naslovi slik in tabel** naj bodo priloženi posebej. Naslove slik, tabel in celotno besedilo, ki se pojavlja na slikah in tabelah, je potrebno navesti v angleškem in slovenskem jeziku.
**Slike** (ilustracije in fotografije) in tabele morajo biti izvirne in priložene posebej. Njihov položaj v besedilu mora biti jasen iz priloženega kompletnega izvoda. Narejene so lahko na papirju ali pa v računalniški obliki (MS Excel, Corel, Acad).
**Format** elektronskih slik naj bo v EPS, TIF ali JPG obliki z ločljivostjo okrog 300 dpi. Tekst v grafiki naj bo v Times tipografiji.
**Barvne slike.** Objavo barvnih slik sofinancirajo avtorji
**Označenost** poslanega materiala. Izpisan izvod, disketa ali CD morajo biti jasno označeni – vsaj z imenom prvega avtorja, začetkom naslova in datumom izročitve uredništvu RMZ-M&G. Elektronski prenos mora biti pospremljen z jasnim sporočilom in z enakimi podatki kot velja za ostale načine posredovanja.

**Informacije** o RMZ-M&G: urednik prof. dr. Peter Fajfar, univ. dipl. ing. metal. (tel. ++386 1 4250316) ali tajnica Barbara Bohar Bobnar, univ. dipl. ing. geol. (tel. ++386 1 4704630), Aškerčeva 12, 1000 Ljubljana
ali na E-mail naslovih:
peter.fajfar@ntf.uni-lj.si
barbara.bohar@ntf.uni-lj.si

**Pošiljanje prispevkov**. Prispevke pošljite priporočeno na naslov **Uredništva:**

- RMZ-Materials and Geoenvironment
  Aškerčeva 12,
  1000 Ljubljana, Slovenija

oziroma jih oddajte v

- **Recepciji** Naravoslovnotehniške fakultete (pritličje) (za RMZ-M&G)
  Aškerčeva 12,
  1000 Ljubljana, Slovenija
- Možna je tudi oddaja pri uredniku oziroma pri tajnici.

*Navodila veljajo od avgusta 2009.*

# TEMPLATE

## The title of the manuscript should be written in bold letters (Times New Roman, 14, Center)

## Naslov članka (Times New Roman, 14, Center)

Name Surname[1], …. , & Name Surname[X] (Times New Roman, 12, Center)

[x] University of ..., Faculty of ..., Address…, Country ... (Times New Roman, 11, Center)

*Corresponding author. E-mail: ... (Times New Roman, 11, Center)

**Abstract** (Times New Roman, Normal, 11): The abstract should be concise and should present the aim of the work, essential results and conclusion. It should be typed in font size 11, single-spaced. Except for the first line, the text should be indented from the left margin by 10 mm. The length should not exceed fifteen (15) lines (10 are recommended).

**Izvleček** (Times New Roman, navadno, 11): Kratek izvleček namena članka ter ključnih rezultatov in ugotovitev. Razen prve vrstice naj bo tekst zamaknjen z levega roba za 10 mm. Dolžina naj ne presega petnajst (15) vrstic (10 je priporočeno).

**Key words:** a list of up to 5 key words (3 to 5) that will be useful for indexing or searching. Use the same styling as for abstract.
**Ključne besede:** seznam največ 5 ključnih besed (3–5) za pomoč pri indeksiranju ali iskanju. Uporabite enako obliko kot za izvleček.

### Introduction (Times New Roman, Bold, 12)

Two lines below the keywords begin the introduction. Use Times New Roman, font size 12, Justify alignment.

There are two (2) admissible methods of citing references in text:

1. by stating the first author and the year of publication of the reference in the parenthesis at the appropriate place in the text and arranging the reference list in the alphabetic order of first authors; e.g.:
   "Detailed information about geohistorical development of this zone can be found in: Antonijević (1957), Grubić (1962), ..."
   "… the method was described previously (Hoefs, 1996)"
2. by consecutive Arabic numerals in square brackets, superscripted at the appropriate place in the text and arranging the reference list at the end of the text in the like manner; e.g.:
   "... while the portal was made in Zope environment. [3]"

## Materials and methods (Times New Roman, Bold, 12)

This section describes the available data and procedure of work and therefore provides enough information to allow the interpretation of the results, obtained by the used methods.

## Results and discussion (Times New Roman, Bold, 12)

Tables, figures, pictures, and schemes should be incorporated in the text at the appropriate place and should fit on one page. Break larger schemes and tables into smaller parts to prevent extending over more than one page.

## Conclusions (Times New Roman, Bold, 12)

This paragraph summarizes the results and draws conclusions.

**Acknowledgements (Times New Roman, Bold, 12, Center - optional)**

This work was supported by the ****.

## References (Times New Roman, Bold, 12)

In regard to the method used in the text, the styling, punctuation and capitalization should conform to the following:

FIRST OPTION - in alphabetical order

Casati, P., Jadoul, F., Nicora, A., Marinelli, M., Fantini-Sestini, N. & Fois, E. (1981): Geologia della Valle del'Anisici e dei gruppi M. Popera - Tre Cime di Lavaredo (Dolomiti Orientali). *Riv. Ital. Paleont.*; Vol. 87, No. 3, pp. 391–400, Milano.

Folk, R. L. (1959): Practical petrographic classification of limestones. *Amer. Ass. Petrol. Geol. Bull.;* Vol. 43, No. 1, pp. 1–38, Tulsa.

SECOND OPTION - in numerical order

[1] Trček, B. (2001): *Solute transport monitoring in the unsaturated zone of the karst aquifer by natural tracers.* Ph. D. Thesis. Ljubljana: University of Ljubljana 2001; 125 p.

[2] Higashitani, K., Iseri, H., Okuhara, K., Hatade, S. (1995): Magnetic Effects on Zeta Potential and Diffusivity of Nonmagnetic Particles. *Journal of Colloid and Interface Science, 172*, pp. 383–388.

Citing the Internet site:

CASREACT-Chemical reactions database [online]. Chemical Abstracts Service, 2000, updated 2. 2. 2000 [cited 3. 2. 2000]. Accessible on Internet: http://www.cas.org/CASFILES/casreact.html.

**Texts in Slovene (title, abstract and key words) can be written by the author(s) or will be provided by the referee or by the Editorial Board.**

# PREDLOGA ZA SLOVENSKE ČLANKE

## Naslov članka (Times New Roman, 14, Na sredino)

## The title of the manuscript should be written in bold letters (Times New Roman, 14, Center)

Ime Priimek[1], …, Ime Priimek[X] (Times New Roman, 12, Na sredino)

[X]Univerza…, Fakulteta…, Naslov…, Država… (Times New Roman, 11, Center)

*Korespondenčni avtor. E-mail: ... (Times New Roman, 11, Center)

**Izvleček** (Times New Roman, Navadno, 11): Kratek izvleček namena članka ter ključnih rezultatov in ugotovitev. Razen prve j bo tekst zamaknjen z levega roba za 10 mm. Dolžina naj ne presega petnajst (15) vrstic (10 je priporočeno).

**Abstract** (Times New Roman, Normal, 11): The abstract should be concise and should present the aim of the work, essential results and conclusion. It should be typed in font size 11, single-spaced. Except for the first line, the text should be indented from the left margin by 10 mm. The length should not exceed fifteen (15) lines (10 are recommended).

**Ključne besede:** seznam največ 5 ključnih besed (3–5) za pomoč pri indeksiranju ali iskanju. Uporabite enako obliko kot za izvleček.
**Key words:** a list of up to 5 key words (3 to 5) that will be useful for indexing or searching. Use the same styling as for abstract.

### Uvod (Times New Roman, Krepko, 12)

Dve vrstici pod ključnimi besedami se začne Uvod. Uporabite pisavo Times New Roman, velikost črk 12, z obojestransko poravnavo. Naslovi slik in tabel (vključno z besedilom v slikah) morajo biti v slovenskem jeziku.

**Slika (Tabela) X.** Pripadajoče besedilo k sliki (tabeli)

Obstajata dve sprejemljivi metodi navajanja referenc:

1. z navedbo prvega avtorja in letnice objave reference v oklepaju na ustreznem mestu v tekstu in z ureditvijo seznama referenc po abecednem zaporedju prvih avtorjev; npr.:

   "Detailed information about geohistorical development of this zone can be found in: Antonijević (1957), Grubić (1962), ..."

   "… the method was described previously (Hoefs, 1996)"

ali

2. z zaporednimi arabskimi številkami v oglatih oklepajih na ustreznem mestu v tekstu in z ureditvijo seznama referenc v številčnem zaporedju navajanja; npr.;

   "... while the portal was made in Zope[3] environment."

## Materiali in metode (Times New Roman, Krepko, 12)

Ta del opisuje razpoložljive podatke, metode in način dela ter omogoča zadostno količino informacij, da lahko z opisanimi metodami delo ponovimo.

## Rezultati in razprava (Times New Roman, Krepko, 12)

Tabele, sheme in slike je treba vnesti (z ukazom Insert, ne Paste) v tekst na ustreznem mestu. Večje sheme in tabele je po treba ločiti na manjše dele, da ne presegajo ene strani.

## Sklepi (Times New Roman, Krepko, 12)

Povzetek rezultatov in sklepi.

**Zahvale (Times New Roman, Krepko, 12, Na sredino - opcija)**

Izvedbo tega dela je omogočilo ………

**Viri (Times New Roman, Krepko, 12)**

Glede na uporabljeno metodo citiranja referenc v tekstu upoštevajte eno od naslednjih oblik:

PRVA MOŽNOST (priporočena) - v abecednem zaporedju

Casati, P., Jadoul, F., Nicora, A., Marinelli, M., Fantini-Sestini, N. & Fois, E. (1981): Geologia della Valle del'Anisici e dei gruppi M. Popera – Tre Cime di Lavaredo (Dolomiti Orientali). *Riv. Ital. Paleont.*; Vol. 87, No. 3, pp. 391–400, Milano.

Folk, R. L. (1959): Practical petrographic classification of limestones. *Amer. Ass. Petrol. Geol. Bull.;* Vol. 43, No. 1, pp. 1–38, Tulsa.

DRUGA MOŽNOST - v numeričnem zaporedju

[1] Trček, B. (2001): *Solute transport monitoring in the unsaturated zone of the karst aquifer by natural tracers.* Ph. D. Thesis. Ljubljana: University of Ljubljana 2001; 125 p.

[2] Higashitani, K., Iseri, H., Okuhara, K., Hatade, S. (1995): Magnetic Effects on Zeta Potential and Diffusivity of Nonmagnetic Particles. *Journal of Colloid and Interface Science, 172*, pp. 383–388.

Citiranje spletne strani:

CASREACT-Chemical reactions database [online]. Chemical Abstracts Service, 2000, obnovljeno 2. 2. 2000 [citirano 3. 2. 2000]. Dostopno na svetovnem spletu: http://www.cas.org/CASFILES/casreact.html.

**Znanstveni, pregledni in strokovni članki ter predhodne objave se objavijo v angleškem jeziku. Izjemoma se strokovni članek objavi v slovenskem jeziku.**

RTH